The cellular epitranscriptome:

analysis of N6-methyladenosine (m⁶A) in

Arabidopsis thaliana RNAs upon acclimation

Dissertation

Zur Erlangung des Doktorgrades der Naturwissenschaften

(Dr. rer. nat.)

der Fakultät für Biologie

der Ludwig-Maximilians-Universität München

vorgelegt von

Alexandre Magno Vicente

aus Varginha, Brasilien

München, July 2022

Diese Dissertation wurde angefertigt

unter der Leitung von PD Dr. Jörg Meurer

in der Fakultät für Biologie

der Ludwig-Maximilians-Universität München

Erstgutachter: PD Dr. Jörg Meurer

Zweitgutachter: Prof. Dr. Hans Henning Kunz

Tag der Abgabe: 11. July 2022

Tag der mündlichen Prüfung: 04. October 2022

To my grandparents and parents,
who taught me the values of knowledge and most important
values of honesty
Dedicated to Terezinha Sarto Vicente, in memorium

Eidesstattliche Erklärung

Ich versichere hiermit an Eides statt, dass die vorgelegte Dissertation von mir selbstständig und ohne unerlaubte Hilfe angefertigt wurde. Des Weiteren erkläre ich, dass ich nicht anderweitig ohne Erfolg versucht habe, eine Dissertation einzureichen oder mich der Doktorprüfung zu unterziehen. Die folgende Dissertation liegt weder ganz noch in wesentlichen Teilen einer anderen Prüfungskommission vor.

I declare that I have authored this thesis independently and that I have not used other than the declared (re)sources. As well I declare that I have not submitted a dissertation without success and not passed the oral exam. The present dissertation (neither the entire dissertation nor parts) has not been presented to another examination board.

München, 11.07.2022

………………………………………
Alexandre Magno Vicente

Contents

Manuscripts and Collaboration Work

Manuscripts published:

Manavski, N.*; **Vicente, A**.*; Chi, W.; Meurer, J. (2021) The Chloroplast Epitranscriptome: Factors, Sites, Regulation, and Detection Methods. *Genes 12*, 1121. https://doi.org/10.3390/genes12081121 **(* these author contributed equality to this work).**

Bellin, L.; Scherer, V.; Dörfer, E.; Lau, A.; **Vicente, A**.; Meurer, J.; Hickl, D.; Möhlmann, T. (2021) Cytosolic CTP Production Limits the Establishment of Photosynthesis in *Arabidopsis*. Frontiers in Plant Science, https://doi.org/10.3389/fpls.2021.789189

Manuscripts in preparation:

Vicente *et al*., (2022**)** FIP37-mediated methylation of nucleus-derived mRNAs ensures efficient photosynthetic performance during cold acclimation in *Arabidopsis thaliana.*

Schmid, L-M.; Möhlmann, T.; John, A.; **Vicente, A.**.; Marino, G.; Lehmann, M.; Manavski, N.; Leister, D.; Meurer, J. (2022) PUMPKIN and its Importance in the Plastid Pyrimidine Salvage Pathway.

Schmid, L-M.; **Vicente, A**.; Manavski, N.; Meurer, J. (2022) Chloroplast Ribosome Biogenesis Factors. Review Article.

Manavski, N.; Torabi S.; Schmid, L-M.; **Vicente, A.**; Zoschke R.; Meurer, J. (2022) The chloroplast HCF145 protein is a member of a new RNA-binding family with multiple conserved motifs in photosynthetic organisms.

Summary

Several chemical modifications in cellular RNAs have been identified to date. The most common internal modification of eukaryotic RNAs is known as m^{6}A. This modification is able to configure the outcome of gene expression by adjusting RNA decay, translation efficiency, RNA structure and alternative splicing. Although thousands of m^{6}A sites were found in RNAs of several plant species, nearly nothing is known about the impact of m^{6}A on plant acclimation. Here, we showed that mRNAs encoding writers, erasers and readers - proteins capable of installing, removing and recognizing/interpreting RNA modifications, respectively, - are responsive to cold, heat and high light conditions in *Arabidopsis thaliana*. Quantification of m^{6}A by mass spectrometric analysis showed that m^{6}A-modified poly(A)-enriched mRNAs are more abundant under cold acclimation. Under this condition, knockdown lines for components of the major m^{6}A writer complex showed a decrease in photosynthetic performance, especially in the *fip37-4* mutant. Immunological analysis of photosynthetic proteins and blue native gels has shown that under cold specific proteins and supercomplexes are downregulated in *fip37-4*. Interestingly, *fip37-4* has a further role in thylakoid organization under cold as revealed by chloroplast ultrastructure analysis. In addition, ROS formation was increased while the expression of cold acclimation-related genes was reduced in *fip37-4* at low temperatures. Plant development regarding leaf area, weight, chlorophyll/anthocyanin content and root development was impaired under control, but a much stronger deficiency especially in photosynthesis was clear under cold acclimation. Altogether, these results indicate that FIP37-based RNA methylations play crucial roles in plastid functions under cold and several other aspects of plant development.

Zusammenfassung

Bislang wurden mehrere chemische Modifikationen in zellulären RNAs identifiziert. Die m^6A Modifikation ist die häufigste interne RNA-Modifikation von Eukaryoten. m^6A Modifikationen beeinflussen die Genexpression durch die Regulierung von RNA-Abbau, Translationseffizienz, RNA-Struktur und alternativem Spleißen. Obwohl Tausende m^6A-Markierungen in RNAs verschiedener Pflanzenarten identifiziert wurden, ist noch sehr wenig über die Auswirkungen von m^6A auf die Akklimatisierung von Pflanzen bekannt. Hier konnten wir zeigen, dass mRNAs, die für "Writer", "Eraser" und "Reader" kodieren - Proteine, die RNA-Modifikationen einbauen, entfernen und erkennen/interpretieren - in *Arabidopsis thaliana* auf Kälte, Hitze und hohe Lichtverhältnisse reagieren. Die Quantifizierung von m^6A mittels Massenspektrometrie zeigte, dass m^6A-modifizierte poly(A)-angereicherte mRNAs unter Kälteakklimatisierung gehäuft vorkommen. Unter dieser Bedingung zeigten Knockdown-Linien für Komponenten des maßgeblichen nukleären m^6A-Methylltransferasekomplexes eine deutliche Verringerung der photosynthetischen Leistung, insbesondere bei *fip37-4*. Immunologische Analysen photosynthetischer Proteine und Untersuchungen mit nativen Gelanalysen haben gezeigt, dass in der Kälte spezifische plastidäre Proteine und Superkomplexe in *fip37-4* herunterreguliert werden. Interessanterweise spielt *fip37-4* eine weitere Rolle bei der Thylakoidmembrananordnung in der Kälte, was durch die Ultrastruktur der Chloroplasten bestätigt wurde. Zusätzlich war die ROS-Bildung erhöht, während die Expression von Genen, die generell mit Kälteakklimatisierung zusammenhängen, in *fip37-4* bei niedrigen Temperaturen reduziert war. Unter Kontrollbedingungen war die Pflanzenentwicklung in Bezug auf Blattfläche, Gewicht, Chlorophyll-/Anthocyanin-Gehalt und Wurzelentwicklung beeinträchtigt, jedoch wurden starke Defekte der Photosynthese erst unter Kälteakklimatisierung besonders deutlich. Insgesamt deuten diese Ergebnisse darauf hin, dass die FIP37-vermittelte RNA Methylierung eine entscheidende Rolle in Plastidenfunktionen in der Kälte und in anderen Aspekten der Pflanzenentwicklung spielt.

1. Introduction

1.1 Plant Acclimation to Environmental Conditions

Extreme environmental conditions are major factors that reduce plant development, quality and productivity. In both agricultural and natural environments, plants are commonly exposed to adverse conditions, such as extreme temperatures, soil salinity and water limitation. Plants need to develop mechanisms to recognize and overcome these environmental challenges.

In contrast to plant adaptation, which involves the gaining of genetic traits that improve performance/survival over multiple plant generations, plant acclimation includes morpho-physiological adjustments within the lifetime of a single organism that are beneficial in response to rapid environmental fluctuations and, consequently, improve plant performance/survival. Plastids, such as chloroplasts, are protagonists in acclimation responses (Kleine *et al.*, 2021) and, because photosynthesis reacts quite sensitive to environmental changes (light, water and temperature), function as important sensors and are responsible to activate plant acclimation responses on different levels and tissues (Schwenkert *et al.*, 2021, Crosatti *et al.*, 2013).

1.1.2 *Arabidopsis thaliana* as a Plant Model Organism to Study Plant Acclimation

Arabidopsis thaliana belongs to the Brassicaceae family within the dicotyledonous group of angiosperm vascular plants. This rosette plant is considered to be an extraordinary model for many aspects of plant biology, genetics, biochemistry and physiology. Its small size, diploid genetics and self-fertilization are traits that allowed its development as a model organism. Due to the high seed yield of Arabidopsis and its low basal requirement for growth, significant advances were rapidly made in tools and methods that stimulated plant biology research in the 1980s (Somerville and Koornneef, 2002). Moreover, the discovery that developing floral tissue of *Arabidopsis* in contacts with *Agrobacterium tumefaciens* result in transformed progeny plants (Feldmann and David Marks, 1987) and the

development of transfer DNA insertion (T-DNA) mutant collections were crucial examples of the scientific innovations during this period. Its genome consisting of two sets of five chromosomes was sequenced and published in 2000 as the first genome of a flowering plant, a landmark achievement for plant biology (Somerville and Koornneef, 2002, The Arabidopsis Genome Initiative, 2000).

Despite its identity as native to Europe and central Asia, Arabidopsis has extended its geographic territories worldwide (Figure 1). By now more than 1135 different accessions have been described and more than 1000 have been sequenced (https://1001genomes.org/about.html). *A. thaliana* is described not only as a pioneer of rocky, nutrient-poor and disturbed soils but also commonly found in forests and meadow environments (Mitchell-Olds and Schmitt, 2006, Krämer, 2015). Particularly, as a widespread plant around the globe, it must face different climates and environmental conditions. Therefore, *A. thaliana* can considerably adapt and acclimate to these environments, and the comprehension of how it works is an important research question nowadays.


Figure 1: Distribution map of *Arabidopsis thaliana* worldwide. Areas dark-colored correspond to the continuous distribution of A. thaliana. Adapted from (Krämer, 2015)

1.1.3 Plant Acclimation to Heat, Salt and Light Changes

Plants are able to sense abiotic conditions through different mechanisms that transform the physical and chemical information present in a certain environment into a biological signal recognized by the cells (Zhu, 2016). High temperatures, for example, lead to improper folding and denaturation of proteins. As a consequence, proteins form aggregates under this condition. The environment is then perceived by the plants at the molecular level. Later, heat shock proteins (HSPs) interact with such aggregated complexes of proteins creating a cellular response to high temperatures. Transcription factors are stimulated and their binding to heat shock elements (HSEs) triggers the transcription of heat stress response genes (Al-Whaibi, 2011, Lamers *et al*., 2020). Salt stress is commonly connected to the production of reactive oxygen species (ROS) in plant cells, which serve as a signal that is sensed by the ROS sensor/receptor and, consequently, transduced via the mitogen-activated protein kinase (MAPK) cascade to regulate plant response, development and growth under salt stress (Yang and Guo, 2018). Moreover, rapid light fluctuations require cellular responses to avoid photodamage and sustain photosynthetic efficiency. Thus, plant cells activate the production of anthocyanins to reduce light intensity within plant tissues, adjust the size of light-harvesting antennae, enhance mechanisms for thermal dissipation of excess absorbed light energy and scavenge reactive oxygen species that often form under these conditions (Niyogi, 1999).

1.1.4 Coping with Low Temperatures – Plant Cold Acclimation

At low and non-freezing temperatures (0-15°C), plants activate a cascade of cellular events that lead to the regulation of gene expression at different levels, triggering physiological changes that enable cold tolerance, a phenomenon known as cold acclimation. For example, increased content of unsaturated fatty acid in plant cell membranes, accumulation of cytosolic Ca^{2+}, increased levels of reactive oxygen species (ROS), changes in the expression of genes and transcription factors, proline accumulation, changes in sugar levels and in photosynthetic output are common cellular responses to how plants cope with low temperatures (Figure 2) (Theocharis *et al*., 2012).
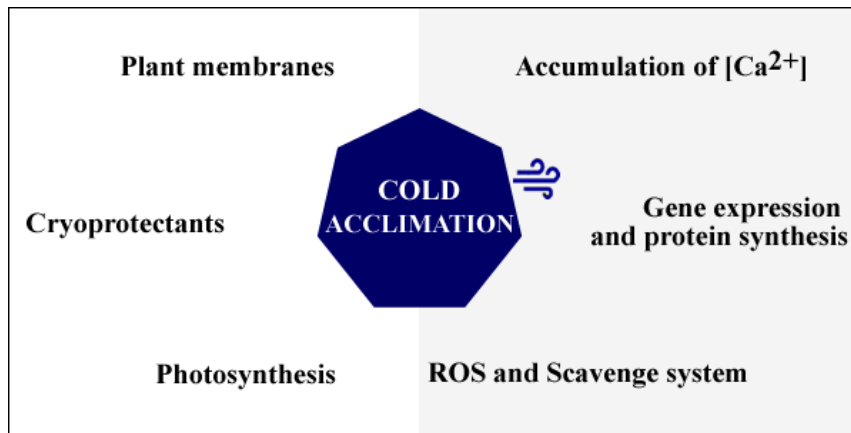
Figure 2: Plant cold acclimation. Cellular responses triggered as a result of cold acclimation. Adapted from Theocharis *et al.*, (2012).

Cold acclimation of plants is highly dependent on the expression of specific genes encoding factors that facilitate metabolic changes that confer cold tolerance. A variety of cold-responsive genes have been described to date in Arabidopsis. Transcription factors, such as the cold-responsive C-repeat-binding factors (CBFs), including CBF1, CBF2 and CBF3, play essential roles in plant acclimation (Liu *et al.*, 2019). These factors are able to bind to the C-repeat responsive element motif (CRT) commonly found in promoters of cold-responsive (COR) genes, such as COR15a and RD29a. In turn, CBF genes can also be tightly regulated by another set of transcription factors, including ICE1 (Inducer of CBF expression I) and the zinc-finger protein ZAT12, which controls the transcription activation of CBFs at low temperatures (Zhao *et al.*, 2015)

Several transcriptomic studies have contributed significantly to the understanding of the cold response of Arabidopsis (Kreps *et al.*, 2002, Tiwari *et al.*, 2020, Garcia-Molina *et al.*, 2020). Importantly, however, the accumulation of mRNAs does not always correspond to the amounts of proteins. Thus, the involvement of post-transcriptional regulation must also be considered an important step in controlling plant acclimation to environmental conditions.

1.2 RNA Modifications: Roles in Plant Post-transcriptional Regulation

The 'Central Dogma of Life' explains how the genetic information from DNA is converted to proteins through RNA molecules. Chemical modifications are known to influence the central dogma, controlling gene expression via DNA modifications and RNA

modifications. To date, more than 170 different modifications have been identified in different RNA classes (Boccaletto *et al.*, 2018). These regulatory marks can control the RNA fate in a very dynamic and specific way, influencing several aspects of gene control and, therefore, cellular development and functions (Frye *et al.*, 2018). While the role of only a few specific RNA modifications is known, the occurrence and detailed function of most others are not yet clear. Indeed, the known RNA modifications probably only represent the tip of an iceberg, especially in plant cells and organelles, such as chloroplasts.

1.2.1 Deciphering Plant m^{6}A Modification

RNA modifications are present in all three domains of life. Collectively termed epitranscriptome, these modifications are dynamic and involve key factors able to deposit (writers), remove (erasers) and interpret (readers) these chemical modifications (Figure 3). Among all RNA marks, m^{6}A is the most common internal modification in eukaryotic RNAs. m^{6}A can control RNA metabolism through RNA decay, folding, localization, transport and processing. In plants, m^{6}A has been shown to play important roles in a wide range of biological processes, such as stress response, organ development, floral transition and viral infection (Yue *et al.*, 2019). Recent transcriptome-wide analysis revealed dynamic m^{6}A modifications not only in plant nuclear and cytoplasmic RNAs but especially in chloroplast RNAs, indicating an essential and yet unexplored role in chloroplast and photosynthesis performance (Wang *et al.*, 2017, Manavski *et al.* 2021).

1.2.2 Short History of m^{6}A in Plants

m^{6}A in plant RNAs was first described in 1979 through analysis of maize (*Zea mays*) embryos using ^{32}P-labeled poly(A)-containing RNAs. During that time it was already possible to not only detect but also quantify the m^{6}A modification in plant RNAs (J. L. Nichols, 1979). Two years later, the major sequence containing N6-methyladenosine was found to be Pu(Purine)-m^{6}A-C (Nichols and Welder, 1981). So far, this sequence was validated several times in different studies and organisms and it is commonly written as RRm^{6}ACH (where R=G/A, H=A/C/U). Despite this rapid progress in plant research regarding the m^{6}A modification in the 80s, it did not gain real attention until 29 years after its discovery in *Arabidopsis thaliana* (Zhong *et al.*, 2008).
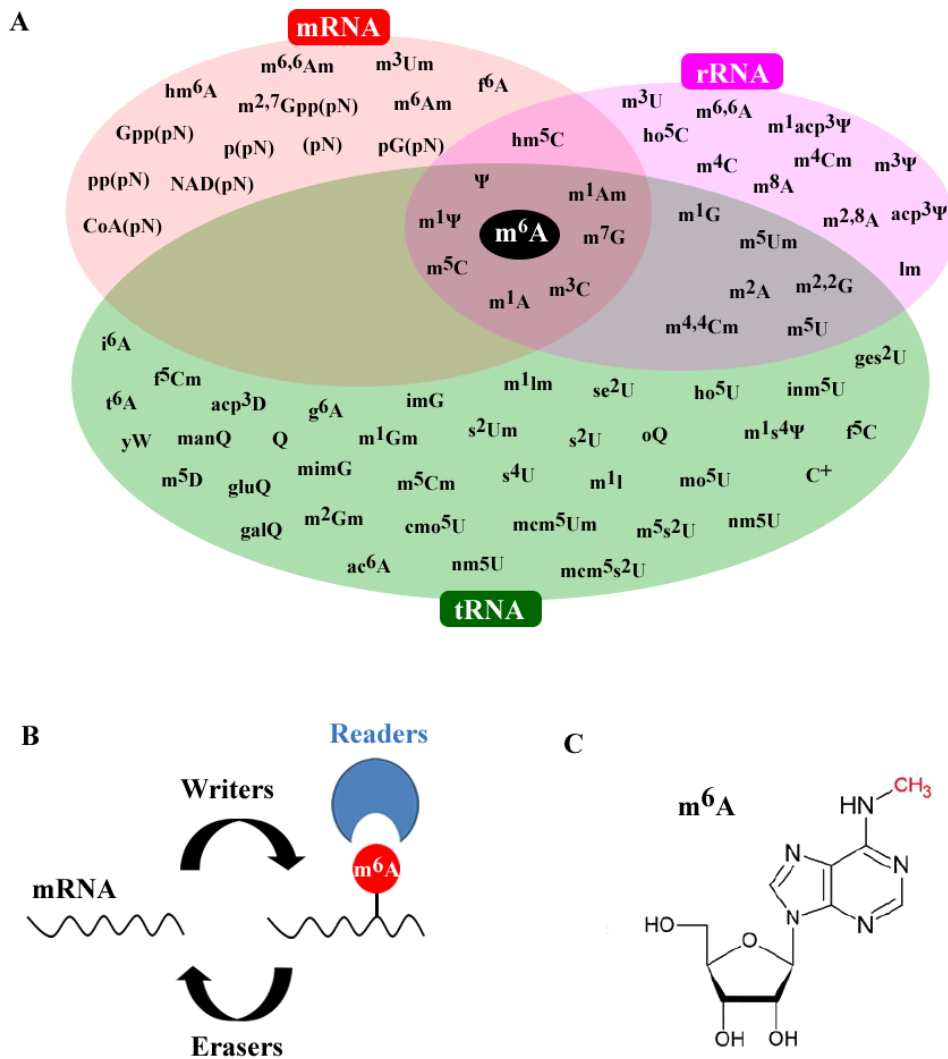
Figure 3: Post-transcriptional chemical modifications in different classes of RNAs. (A) Common RNA modifications found in mRNA, rRNA and tRNAs. (B) m^6A modification is dynamically regulated by writers, erasers and readers, key factors responsible to install, remove and interpret m^6A, respectively. (C) Chemical structure of the N6-methyladenosine (m^6A) present in different classes of RNAs. Adapted from Oerum *et al.,* (2021).

1.2.3 Methylation of Nucleus-Derived RNAs

1.2.3.1 Writing m^6A

The N6-methyladenosine methyltransferases or also called m^6A writers are regulatory proteins responsible to transfer a methyl group from SAM (S-adenosylmethionine) to the adenosine located at the sixth N-position in RNAs (Figure 4A) (Lence *et al.*, 2019). The major writer forms a very organized complex comprised mainly of two proteins, METTL3

and METTL14 (homolog MTA and MTB in Arabidopsis, respectively), which is commonly termed the m^{6}A–methyltransferase complex (MAC). While METTL3 contains the SAM binding methyltransferase domain and comprises the catalytic subunit, METTL14 stabilizes the complex and promotes binding to RNA (Huang *et al.*, 2019). METTL3 and METTL14 interact with each other via the methyltransferase domains (MTD) forming a heterodimer (Figure 4B). The SAM-binding site from METTL3 contains two loops named active site loop1 (ASL1) and active site loop 2 (ASL2). ALS1 presents a conserved DPPW motif known to be involved in recruiting the adenine group of the acceptor RNA. In addition, the two zinc fingers in METTL3, ZFD1 and ZFD2, are responsible for the RRACH sequence motif identification, whereas the C-terminal arginine−glycine (RGG) repeats from the METTL14 allow the binding of the target-RNA in a sequence-independent manner (Figure 4B) (Morales and Reyes, 2021).

The MAC complex, however, associates with auxiliary proteins, such as WTAP, RBM15, VIRMA and HAKAI, to form the m^{6}A-Methyltransferase-associated complex (MACOM). The functions of each component of the MAC and MACOM and their homologs in Arabidopsis are summarized in Table 1. WTAP or WILMS' TUMOR 1-ASSOCIATING PROTEIN (homolog FIP37 in Arabidopsis) acts as an adaptor subunit and stabilizes the interaction between METTL3 and METTL14 (Liu *et al.*, 2014, Schwartz *et al.*, 2014). Moreover, VIRMA (homolog VIRILIZER in Arabidopsis) and HAKAI (homolog HAKAI in Arabidopsis) interacts with the WTAP protein in Hela cells (Yu *et al.*, 2018). Therefore, WTAP/FIP37 plays a role as a central subunit within the m^{6}A writer complex interconnecting most of the components of the MAC and MACOM (Figure 4C). The FIP37 protein will be further discussed below in section 1.2.3.2 and in Chapters 3 and 4.

In Arabidopsis, MTA was the first m^{6}A methyltransferase to be discovered (Zhong *et al.*, 2008). Complete depletion of MTA led to embryo lethality, in agreement with previous studies focused on METTL3 in animals (Geula, *et al.*, 2015). Reduced levels of MTA using a *MTA* knockout mutant complemented with MTA under the control of the ABI3 promoter lead to altered growth patterns, reduced apical dominance, abnormal flower architecture (number and size) and trichomes with a higher number of branches (Bodi *et al.*, 2012). Moreover, a recent study comparing WT and an *MTA* knockdown line has shown that m^{6}A stabilizes transcripts encoding proteins required for osmotic and salt stress responses. m^{6}A

acted as a protecting mark inhibiting site-specific cleavage in Arabidopsis mRNAs, controlling essentially the salt-stress-responsive transcriptome (Anderson *et al.*, 2018).
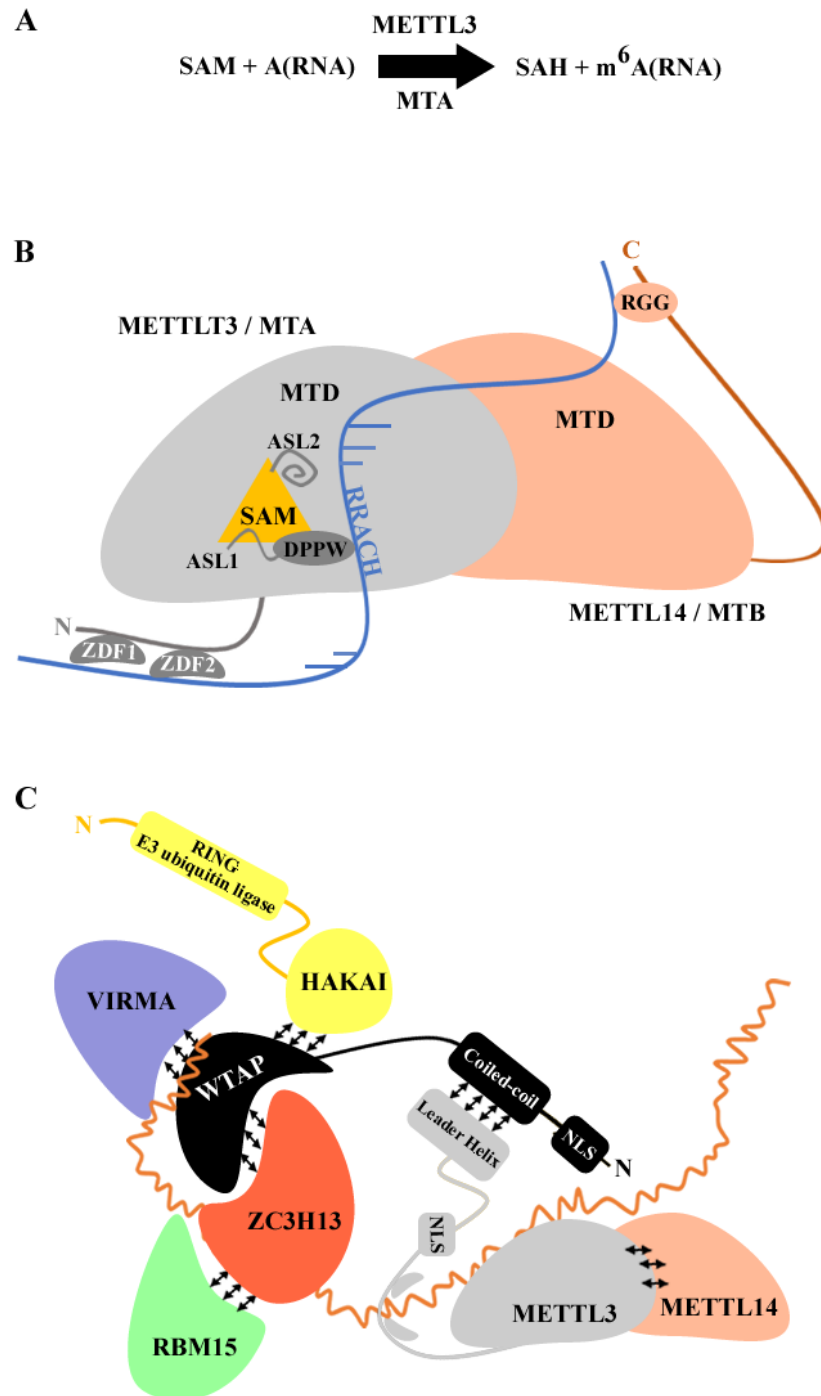
Figure 4: The human m⁶A MAC and MACOM complex. (A) Reaction performed by m⁶A writer proteins shows a methyl group from SAM (S-adenosylmethionine) being transferred to the adenosine located at the sixth position in RNA molecules. (B) The m⁶A MAC and (C) the MACOM complex illustrate important domains and interaction sites depicted by arrows among all individual components. The RNA is shown in blue and orange in (B) and (C), respectively. Adapted from Morales and Reyes (2021).

Null mutants of Arabidopsis *mtb*, *fip37* and *virilizer* (*vir*) are also embryonic lethal (Tzafrir *et al.*, 2004) (Vespa et al., 2004). Yet, for *fip37*, a viable hypomorphic allele, produced by a T-DNA insertion in its 7th intron was identified. For *hakai*, CRISPR/Cas9 was used to remove a single nucleotide of the first exon in its allele. In addition, inducible RNAi lines to knock down the expression of *MTB* and an EMS-induced point mutation in *VIR* were also created (Růžička *et al.*, 2017). Thus, a set of viable lines that partially disrupt the expression of genes coding for each of the m^{6}A writer components is available allowing the analysis of the functional role of each of these proteins.

Table 1: Components and functions of the methyltransferase complex.

		Arabidopsis	Human homologues	Function
MACOM	MAC	MTA	METTL3	Catalytic subunit
		MTB	METTL14	RNA binding
		FIP	WTAP	Adaptor subunit
		FPA	RBM15	?
		VIRILIZER	VIRMA	Methylation specificity
		HAKAI	HAKAI	?
		-	ZC3H13	Important for nuclear localization

RNA sequencing using *vir-1* root tips has revealed that the *vir-1* mutation affects a range of processes which include response to environmental signals, plant growth and development (Růžička *et al.*, 2017). Using tandem affinity purification (TAP) followed by proteolysis and mass spectrometry, VIR-GS bait-associated proteins were identified in Arabidopsis. Similar to mammalian cells, FIP37 and HAKAI co-purified with VIR and MTB. To examine the relationship of these proteins to MTA, several pairwise interactions were tested using a two-hybrid system. As a result, not only the MTA-FIP37 was confirmed (Zhong *et al.*, 2008), but also heterodimerization between MTA and MTB, consistent with what occurred between the mammalian orthologs METLL3 and METLL14. Moreover, FIP37 interacts with itself and a steady interaction between MTB and HAKAI was also observed. Thus, in addition to MTA and FIP37, MTB, HAKAI and VIR are also members of the m^{6}A writer complex in Arabidopsis (Figure 4C).

While the characterization of MTA and VIR progressed in the past, studies focusing on the role of MTB are still under investigation. Recently, it has been shown that all mutants of m^{6}A writer components, including MTB, have exhibited salt-sensitive phenotypes in an m^{6}A-dependent way (Hu *et al.*, 2021). HAKAI, the orthologue of an E3 ubiquitin ligase, is another component of the Arabidopsis m^{6}A writer complex (Ruzicka *et al.*, 2017). Although m^{6}A levels are reduced to 65% of the WT level in both *hakai* mutants (*hakai-1* and *hakai-2*), these plants are viable and no obvious growth defects were found compared to WT plants. FPA is the homolog of RBM15 in plants. Although its role in controlling *FLC (FLOWERING LOCUS C)* transcription by alternative polyadenylation has been demonstrated (Hornyik *et al.*, 2010), neither its function in m^{6}A RNA methylation nor its contribution to the MACOM has been verified. All the components of the Arabidopsis m^{6}A writer complex MTA, MTB, VIR, FIP37 and HAKAI are nucleus localized proteins (Růžička *et al.*, 2017). Whether m^{6}A can influence organelles' function, such as chloroplasts, still remains to be determined.

1.2.3.2 FIP37 and its Central Role in the m^{6}A Writer Complex

FIP37 was first identified in 1998 in a two-hybrid screen for proteins interacting with the Arabidopsis FKBP12 (Faure *et al.*, 1998). The FKBP12 is part of a family of proteins called immunophilins that are receptors for immunosuppressive drugs. Among this family, FK506-binding proteins (FKBPs) are intracellular drug receptors for FK506 and rapamycin. As they differ in size, FKBP12 (12 kDa) characterizes the minimal amino acid sequence containing the two main functions of FKBPs, PPiase (peptidyl-prolyl cis-trans isomerase) activity and drug binding.

After its identification, the FKBP12-Interacting Protein of 37 kDa (here FIP37) was first functionally characterized in 2004 (Vespa *et al.*, 2004). Three T-DNA mutant alleles (*atfip37-1*, *atfip37-2* and *atfip37-3*) were analyzed but no homozygous plants were isolated in the progeny of any of these *atfip37* lines. Seed development in siliques of heterozygous *atfip37-1* plants was further characterized and it could be shown that endosperm growth was already limited during the early syncytial phase. Endosperm cellularization was delayed until the midtorpedo stage in *fip37-1* while many cell layers were present in the WT endosperm. Embryo development in *fip37-1* was also strongly impaired in early

embryogenesis. *fip37-1* embryos could reach the midglobular stage but no further development was observed. Embryonic cells collapsed and the resulted embryos seemed to die during seed maturation. Therefore, loss of *fip37* caused sporophytic recessive seed-lethal phenotype providing evidence for an essential function of AtFIP37 during endosperm development and embryogenesis (Vespa *et al.*, 2004). Later, a viable line produced by a T-DNA insertion in its 7th intron (*fip37-4*) was identified (Růžička *et al.*, 2017).

Several studies investigated the function of FIP37 in plant development. The same research group demonstrated that FIP37 is involved in trichome development (Vespa *et al.*, 2004). The *AtFIP37* cDNA was placed under the control of the constitutive *35S* promoter and transgenic lines overexpressing *FIP37* displayed the phenotype of numerous and vastly branched trichomes on the adaxial leaf epidermis. Later, researchers found that FIP37 interacts *in vivo* and *in vitro* with MTA using yeast two-hybrid and coimmunoprecipitation experiments, respectively (Zhong *et al.*, 2008). When co-expression of MTA-YFP and FIP37-CFP was performed, YFP-tagged MTA proteins colocalize to the same spots previously described by FIP37, further supporting the *in vivo* interaction.

Mutants lacking *FIP37* have also been shown to influence the overproliferation of shoot apical meristem (SAM) (Shen *et al.*, 2016). m^{6}A-seq has revealed that FIP37 mediates methylation of the key shoot meristem regulators, such as *WUSCHEL (WUS)* and *SHOOTMERISTEMLESS (STM)* transcripts, controlling their RNA stability and preventing overproliferation of the shoot apical meristem responsible to produce aerial organs. On the other hand, downregulation of *FIP37* expression displays a massive overproliferation of SAMs, with an 85% reduction of m^{6}A levels (Shen *et al.*, 2016). In particular, loss of m^{6}A significantly increases the mRNA stability of *WUS* and *STM* transcripts, which directly leads to an inappropriate control of SAM proliferation in Arabidopsis. Thus, dynamic regulation of both *WUS* and *STM* is controlled by FIP37-mediated m^{6}A modification (Shen *et al.*, 2016).

Recently, an m^{6}A network called DENA (Deeplearning Explore Nanopore m^{6}A) was developed using direct RNA-sequencing data of *in vivo* transcribed RNAs from wild-type and m^{6}A-deficient Arabidopsis lines (Qin *et al.*, 2022). DENA accomplished a high accuracy of m^{6}A detection (90%) in the m^{6}A sites identified by miCLIP in Arabidopsis. m^{6}A profiles of *fip37-4* and *mtb* mutants at single-nucleotide resolution were evaluated and

an overlapping function between the two mutants was found. Over 55,000 RRACH sites were predicted and, among them, 19,672 (32.88%), 14,068 (25.52%) and 18,606 (26.77%) m^6A sites were identified in WT, *mtb* and *fip37-4*, respectively. Moreover, m^6A sites were commonly present near stop codon and within 3`UTR in mRNAs. Interestingly, Gene Ontology (GO) analysis on all m^6A-altered genes clearly shows an overrepresentation of processes associated with abiotic (salt, cold and light conditions) and biotic stress responses. In addition, mRNAs encoding factors for photosynthesis, electron transport chain and light reactions were highly enriched, in agreement with the high methylation pattern found in chloroplast RNAs and nuclear-encoded transcripts associated with chloroplasts (Manavski *et al.*, 2021). Thus, recent characterization indicated that FIP37 is involved in several important biological processes in Arabidopsis (Qin *et al.*, 2022, Shen *et al.*, 2016) but no specific studies on plant acclimation or a relationship to photosynthesis have been performed (Chapter 3).

1.2.3.3 Reading and Erasing m^6A

Besides m^6A writer proteins, RNA binding proteins capable of identifying m^6A marks have been identified (Figure 3B). The YT521-B homology domain family of proteins (YTHDF) is a common example of factors that have been shown to recognize and bind to m^6A modification (Zhang *et al.*, 2010, Scutenaire *et al.*, 2018, Arribas-Hernández *et al.*, 2018). m^6A does not alter base pairing between nucleotides, but it alters secondary structures present within RNA molecules and consequently plays an important role in protein-RNA interactions (Liu *et al.*, 2015). Therefore, reduced or increased levels of m^6A result in distinct RNA secondary structures that aid or prevent the binding of factors that further regulate the fate of RNAs related to several biological processes in plants.

Among 13 YTH family proteins in plants, 11 have been classified as "Evolutionarily Conserved C-Terminal Region Proteins" 1–11 (ECT 1–11). These proteins are classified into two clades, the nuclear YTHDC proteins and YTHDF proteins that are mainly located in the cytoplasm. ECT2 is very well characterized in Arabidopsis (Scutenaire *et al.*, 2018) (Wei *et al.*, 2018). ECT2 binds to m^6A-containing RNAs *in vivo* via a tri-tryptophan binding pocket carried by its YTH domain, and mutations in these amino acids result in loss of its m^6A binding capability. ECT2 is localized in the cytoplasm but it relocates to stress

granules upon heat exposure, indicating an important role in mRNAs related to heat stress response (Scutenaire *et al.*, 2018). Moreover, using formaldehyde crosslinking and immunoprecipitation (FA-CLIP), more than 3000 transcripts with ECT2 binding sites that were enriched within the 3´UTRs were identified (Wei *et al.*, 2018). Interestingly, the expression of ECT2 targets was lower in comparison to non-target transcripts, indicating that ECT2 triggers m^6A-dependent stability of mRNAs (Wei *et al.*, 2018). Besides the YTH proteins, additional proteins have been suggested to function as m^6A readers. In mammals, for example, the writer protein METTL3 was shown to bind m^6A marks via interaction with the eukaryotic initiation factor 3h (eiF3h) to promote translation (Choe *et al.*, 2018). Whether the same mechanism occurs in plants is still unknown.

Eraser proteins capable of removing m^6A have been characterized in the past years (Duan *et al.*, 2017, Martínez-Pérez *et al.*, 2017) (Figure 3B). In animals, the Fat Mass and Obesity-associated Factor (FTO) and ALKBH family of proteins act as m^6A demethylases. FTO is conserved among eukaryotes but not present in Arabidopsis (Balacco and Soller, 2019). Arabidopsis, however, contains 13 predicted ALKBH proteins showing different sublocalization patterns (Mielecki *et al.*, 2012). Among them, two m^6A eraser proteins (ALKBH9B and ALKBH10B) have been well studied regarding plant metabolism and development. Martínez-Pérez and colleges first described ALKBH9B in 2017 as m^6A demethylase in plants (Martínez-Pérez *et al.*, 2017). The research group working on the alfalfa mosaic virus (AMV) has demonstrated that ALKBH9B affects viral single-strand RNA methylation. The observations that (1) the depletion of the *ALKBH9B* gene leads to viral RNA hypermethylation and, consequently, RNA degradation and (2) the lack of ALKBH9B leads to lower viral infection, indicates that m^6A methylation plays an important role in viral infection in Arabidopsis (Martínez-Pérez *et al.*, 2017). On the other hand, the role of ALKBH10B in the control of floral transition in Arabidopsis via RNAs was also reported (Duan *et al.*, 2017). ALKBH10B removes m^6A from transcripts, such as *Flowering Locus T (FT)* and from the transcripts of *SPL3* and *SPL9* (*SQUAMOSA PROMOTER BINDING PROTEINLIKES*), two transcriptional activators of *FT* expression. Interestingly, m^6A demethylation enhances the stability of these transcripts and, consequently, produces normal floral phase transition in WT plants. In cells lacking ALKBH10B, however, the same transcripts are hypermethylated leading to enhanced RNA decay and therefore the flowering transition is drastically delayed (Duan *et al.*, 2017).

1.2.3.4 Roles of m^{6}A in Nucleus-derived Transcripts Related to Photosynthesis

A surprisingly high number of nucleus-derived transcripts encoding chloroplast proteins contain m^{6}A modifications, indicating important roles in photosynthesis and chloroplast function. The m^{6}A methylome in plants was first identified in two accessions of *A. thaliana*, Can-0 and Hen-16, two wild-collected lines from areas that vary drastically in photosynthetically active radiation. m^{6}A was shown to be remarkably conserved across these two lines. Surprisingly, m^{6}A was enriched not only within the 3' UTR and stop codon but also around the start codon (Luo *et al.*, 2014), a feature observed only in plant RNAs. Interestingly, new conserved motifs in addition to the RRm^{6}ACH were found (Luo *et al.*, 2014, Parker *et al.*, 2020), suggesting the possibility of distinct sequence motifs for m^{6}A target-methylation. Indeed, Wei and colleagues identified a new URUAY (R=G>A,Y=U>A) motif specific to plants that is involved in RNA stabilization (Wei *et al.*, 2018). In both, Can-0 and Hen-16, gene ontology unveiled many biological pathways related to chloroplast functions. Particularly, more than 60% of transcripts containing m^{6}A in both start and stop codons were associated with chloroplast functions (Luo *et al.*, 2014).

Differential m^{6}A patterns using specific plant organs were also examined in *Arabidopsis* (Wan *et al.*, 2015). 70.6%, 73.7% and 76.7% of the transcripts were chemically modified by m^{6}A in the leaves, flowers and roots, respectively. The consensus sequence RRm^{6}ACH was again described in over 75% of the transcripts, but only one dominant peak of m^{6}A enrichment was identified around the 3' UTR and stop codon in the *Arabidopsis* transcriptome. 290 extensively m^{6}A methylated transcripts were shared in all of the three analyzed organs and many of them encode chloroplast localized proteins. Most interestingly, differential m^{6}A methylation among leaves, flowers and roots showed that the leaves had the highest extent of m^{6}A methylation among the three organs. These transcripts were mainly related to photosynthesis, regulation of transcription and stress response. The m^{6}A methylation level was also compared to the gene expression using the three organs of Arabidopsis. Highly expressed transcripts were less modified by m^{6}A. On the other hand, most of the transcripts presenting a low level of expression were more methylated. This observation implies an important function of m^{6}A in plant cells regarding RNA stability. Genes lower expressed may require a higher level of m^{6}A to maintain RNA stability, and vice versa (Wan *et al.*, 2015). The role of m^{6}A in the decay of mRNAs under

salt stress has been described in Arabidopsis. In this case, m^{6}A is added to salt-stress-related transcripts to protect RNAs from degradation (Anderson *et al.*, 2018). Interestingly, an opposite situation where m^{6}A marks lead to RNA degradations is described in Arabidopsis floral transition (Duan *et al.*, 2017). Why under certain conditions m^{6}A stabilizes or destabilizes a specific set of transcripts may be due to its localization within RNAs (5' UTR, CDS or 3' UTR) and the diversity in loops of secondary structures in RNAs (Liu and Pan, 2016). Whether and how m^{6}A methylation in the nucleus impacts gene expression in the chloroplast and vice-versa via retrograde signaling remains unclear.

To date, many of the epitranscriptomes of Arabidopsis were studied using antibody-based approaches, such as MeRIP/m^{6}A-seq for the chloroplast epitranscriptome. This technique involves immunoprecipitation of ~100 nucleotide-long RNA fragments using m^{6}A-specific antibodies, followed by sequencing of the immunoprecipitated fragments (Manavski *et al.,* 2021). m^{6}A-containing fragments then generate overlapping sequencing reads that produce a peak that reveals the m^{6}A residues (Meyer *et al.*, 2012). However, this approach presents several limitations. For example, antibodies for m^{6}A can also detect a second base modification, N6,2′-O-dimethyladenosine (m^{6}Am), which is located at the 5′ ends of transcripts. In addition, the mandatory fragmentation of RNAs for library constructions may result in the underrepresentation of m^{6}A sites (McIntyre *et al.*, 2020). As a consequence, new approaches adopting or not the use of antibodies have been developed (Garcia-Campos *et al.*, 2019, Linder *et al.*, 2015, Liu *et al.*, 2019, Meyer, 2019, Parker *et al.*, 2020). For example, m^{6}A individual-nucleotide-resolution cross-linking and immunoprecipitation (miCLIP) can be used to induce specific mutational signatures that allow precise identification of m^{6}A residues in RNA molecules. Anti-m^{6}A antibodies are crosslinked to RNA using UV and reverse transcription of crosslinked RNA results in a precise pattern of mutations or truncations in the cDNA. These signatures are computationally identified and mapping of m^{6}A residues at single-nucleotide resolution is achieved (Grozhik *et al.*, 2017).

Nanopore direct RNA sequencing (DRS) and miCLIP were recently applied to examine the epitranscriptome of a mutant defective in m^{6}A (*vir-1*) and *VIR*-complemented lines in Arabidopsis (Parker *et al.*, 2020). This technology relies on a protein pore that sits in a membrane through which an electrical current is created. In a simple way, the RNA sequence can be identified by the magnitude of signals transmitted when intact RNAs pass through the nanopore by a motor protein (Garalde *et al.*, 2018). Researchers have shown

the use of nanopore in revealing full-length mRNAs and poly(A) tails, mapping 5' cap position, alternative splicing and RNA cleavage sites in Arabidopsis. Interesting, novel examples of intronic alternative polyadenylation that potentially modulates gene expression were identified. For instance, frequent cleavage and polyadenylation at the PTM homeodomain transcription factor mRNA (AT5G35210) were found. PTM is involved in retrograde signaling upon cleavage of a C-terminal transmembrane domain that sequesters it to the chloroplast (Feng *et al.*, 2016). Cleavage and polyadenylation within the PTM intron 10 terminate transcripts prior to a sequence encoding the transmembrane domain, consequently bypassing established retrograde control (Parker *et al.*, 2020).

Up to now many chloroplast-related transcripts that carry m^6A were identified. Appendix Table 2 shows a list of representative photosynthetic transcripts containing m^6A extracted from three epitranscriptomes of different accessions of Arabidopsis. Regardless of whether nucleus- or chloroplast-encoded genes are targeted, a compelling link between RNA modifications and photosynthesis in plants is likely (Figure 7). In addition to all the indications described here, it remains to be clarified how exactly m^6A regulates nuclear-encoded RNAs associated with chloroplast functions as well as chloroplast-encoded RNAs and how acclimation conditions may affect the compartmentalized m^6A methylomes within the plant cell (Figure 7).

1.3 Chloroplast RNA Methylation

### 1.3.1 Origin and Genome Information of Chloroplasts

Chloroplasts are semi-autonomous organelles found in plants, cyanobacteria and algae. As they perform essential processes, such as photosynthesis - the biological process that allowed and still preserves life on Earth – it is of utter importance to understand the functions and regulations of these photosynthetic machineries.

Chloroplasts are believed to have evolved from endosymbiotic bacteria over billion years ago (Margulis, 1993). A free-living cyanobacterium coexisted with its eukaryotic host cell and during coevolution, the chloroplast DNA (cpDNA) from the ancestral organism (or ancestor) suffered a significant reduction. As a result, many genes have been transferred from the cpDNA into the eukaryotic nuclear genome, a process called endosymbiotic gene

transfer (Ku *et al.*, 2015). Therefore, the majority of the chloroplast proteins are, indeed, encoded by the nucleus, synthesized in the cytosol and transported to the organelle. Since then a close relationship and dependence between chloroplast and the nucleus exist (Dobrogojski *et al.*, 2020).

The chloroplast genome of *Arabidopsis thaliana* is circular DNA composed of over 150 thousand base pairs containing a total of 129 protein-coding and non-coding genes. In its arrangement, the cpDNA contains two identical fragments called inverted repeats (IR). IRs are particularly separated by two other DNA fragments, the long single copy section (LSC) and the short single copy section (SSC) (Mower and Vickrey, 2018) (Figure 5). Similar to bacteria, many chloroplast genes within the cpDNA are organized in operons (Börner *et al.*, 2015), and only a few genes contain introns in their sequences. Notably, 45 coding genes of the cpDNA encode photosynthesis-related proteins, including five representative proteins of the photosystem I (PSI), 15 proteins of the photosystem II (PSII), six genes coding for ATP synthase subunits, six proteins being part of the cytochrome b_6f complex, 12 genes coding for NADH dehydrogenase subunits and one single gene coding for the large subunit of RuBisCo (Dobrogojski *et al.*, 2020).

Interestingly, the chloroplast undergoes several restructurings when the plant is exposed to different environmental conditions, mainly affecting proteins related to photosynthesis (Watson, *et al.,* 2018, Schwenkert *et al.*, 2021). The expression of cpDNA genes relies on several nuclear-encoded protein factors, such as the T3/T7 phage-type RNA polymerase (NEP) and sigma factors, which commonly control plastid gene expression in response to environmental signals (Barkan and Goldschmidt-Clermont, 2000). Moreover, many of the readjustments in chloroplast protein levels under abiotic stresses occur due to post-transcriptional modifications (Woodson and Chory, 2008), which encouraged us to study the influence of RNA modifications in chloroplast functions upon plant acclimation.
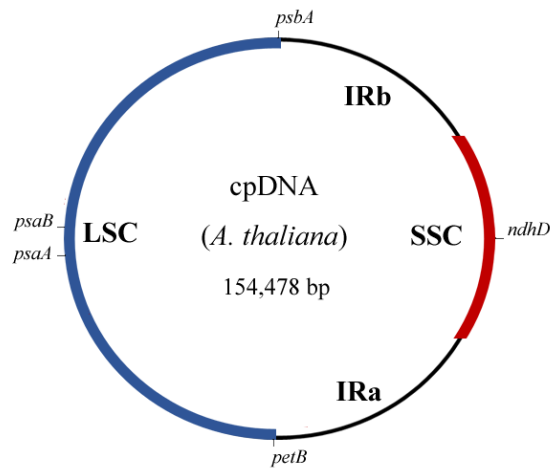
Figure 5: The chloroplast genome. cpDNA map showing the two inverted repeats (IRa and IRb), the long unique sequence (LSC) and the short unique sequence (SSC). Representative genes from the photosynthetic apparatus (PSI and PSII), cytochrome b6/f complex and NADH-plastoquinone oxidoreductase are depicted. Adapted from Dobrogojski *et al.*, (2020).

1.3.2 How Chloroplasts Sustain Life on Earth – Photosynthesis

Plants use the energy from the sun to produce the oxygen we breathe and the food we eat. Oxygenic photosynthesis comprises the conversion of H_2O and CO_2 into organic compounds such as carbohydrates. It can be divided into the 'light' and 'dark' reactions. In the presence of light, water is split into oxygen, protons and electrons, while in the dark, the protons and electrons are used to reduce CO_2 to carbohydrate ($C_6H_{12}O_6$) (Johnson, 2016). These two processes can be explained by the following formulas:

- **Light reactions:** $2\ H_2O + light \rightarrow O_2 + 4\ H^+ + 4\ e^-$

- **Dark reactions:** $CO_2 + 4\ H^+ + 4\ e^- \rightarrow carbohydrate + H_2O$

- **Overall:** $H_2O + light + CO_2 \rightarrow carbohydrate + O_2$

While the light reactions occur in the thylakoid membrane of chloroplasts, the dark reactions take place in the stroma, through the Calvin–Benson cycle. The energy from light is transformed into chemical energy by two chlorophyll complexes of proteins termed photosystems I and II (PSI and PSII). This light energy is used as a source of power to transfer electrons through different membrane compounds that act as electron donors or acceptors. The electron reduces $NADP^+$ to produce $NADPH + H^+$ and oxidizes H_2O to O_2.

In addition, light energy creates a proton motive force used to synthesize ATP from adenosine diphosphate (ADP) and inorganic phosphate (Pi). Finally, the Calvin–Benson cycle uses ATP and NADPH previously formed to convert CO_2 into carbohydrates, restoring ADP and $NADP^+$. Therefore, both light and dark reactions are mutually dependent (Figure 6).

The cyclic electron flow, an alternative electron transfer pathway, is also described in plants and algae. It comprises the recycling of electrons from ferredoxin (Fd) back to plastoquinone (PQ). In this way, NADPH is not produced and water oxidation does not occur. Nonetheless, since protons are transferred into the lumen by the oxidation of plastoquinone, ATP can still be formed (Figure 6). Therefore, the cyclic electron flow is especially important as an ATP source. In this way, photosynthetic organisms can control the proportion of NADPH/ATP needed for their metabolism (Johnson, 2016). Indeed, among the two cyclic electron flow described in angiosperms: the NDH- and the PROTON GRADIENT REGULATION5/1 (PGR5/PGRL1)-dependent pathways, the latter is quite important to protect PSI from photoinhibition. Upon a sudden increase in light, the PGR5/PGRL1 dependent pathway backflows electrons from PSI to the PQ and generates a ΔpH across the thylakoid membrane via Cyt *b6f* complex, which drives ATP synthesis and increases the ATP/NADPH ratio. Thus, by increasing the electron sink downstream of PSI, these alternative electron flows protect the PSI complex through improvements in PSI acceptor-side limitation (Yamamoto and Shikanai, 2019).

Both photosystems contain light-harvesting complexes (LHCs) forming an antenna consisting of hundreds of pigments. PSII, for example, is a water–plastoquinone oxidoreductase that uses light energy to stimulate a special pair of chlorophylls, known as P680. On the other hand, PSI is a light-driven plastocyanin–ferredoxin oxidoreductase and contains a special pair of chlorophylls known as P700 (Johnson, 2016). Both, PSI and PSII are composed of several proteins that are encoded not only in the chloroplast genome but also in the nucleus.
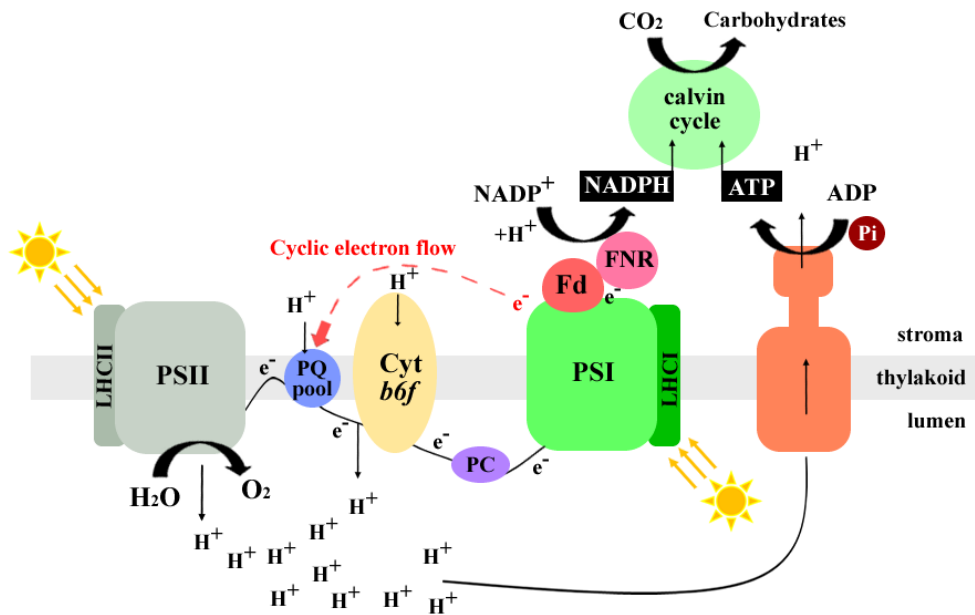
Figure 6: The photosynthetic electron and proton transfer chain. The electron transfer reactions start with the splitting of water by PSII. PSII uses light to oxidize water to oxygen and reduces the electron acceptor plastoquinone (PQ pool). Plastoquinone, in turn, carries the electrons derived from water to another protein complex called cytochrome b_6f (cytb_6f). cytb_6f oxidizes plastoquinone and reduces plastocyanin, a small water-soluble electron carrier protein. A second light-driven reaction is then performed by PSI. PSI oxidizes plastocyanin and reduces another soluble electron carrier protein ferredoxin (Fd). Finally, ferredoxin can then be used by the FNR (ferredoxin–NADP$^+$ reductase) enzyme to reduce NADP$^+$ to NADPH. The ATP synthase allows the protons to move from the lumen to the stroma and this exergonic reaction forms ATP. This scheme illustrates the linear electron transfer flow or Z-scheme of photosynthesis. Adapted from (Johnson, 2016) and (Lima-Melo *et al.*, 2021).

Here, we hypothesize that post-transcriptional modifications of nucleus-derived RNAs associated with chloroplasts, such as m^{6}A methylations, might affect photosynthetic performance.

1.3.3 The Chloroplast Epitranscriptome

The m^{6}A methylome was also investigated in *Arabidopsis thaliana* with a special focus on chloroplast-derived transcripts (Wang *et al.*, 2017). In this study, over 86% of the chloroplast transcripts were methylated by m^{6}A. Strikingly, the overall m^{6}A methylation extent in plastids was higher than that in the nucleus (~4,6 to ~5.8 m^{6}A sites per transcript in the chloroplast and ~1,4 to ~2,0 m^{6}A sites per transcript in the nucleus), implying that m^{6}A potentially plays a yet unexplored important role in regulating the fate and function of chloroplast RNAs. The previously dominant m^{6}A enrichment observed within the 3´ UTR

and near stop codon in nuclear mRNAs was not observed in the chloroplast transcriptome. Instead, m^{6}A peaks were found evenly distributed in chloroplast transcripts with higher methylation marks in exons when compared to introns, suggesting that the mechanism of regulation involving m^{6}A may differ between the nucleus and chloroplast. The two most common m^{6}A consensus sequences were GGm^{6}ACC and GGm^{6}ACU in the Arabidopsis chloroplast transcriptome. In addition, features of the methylation extent compared to gene expression in the chloroplast were similar to those found in the nuclear RNA in Arabidopsis. Most of the highly expressed transcripts were less modified by m^{6}A, and vice versa. The most modified transcripts found in this analysis were associated with chloroplast-encoded rRNAs as well as ribosomal and photosynthetic proteins (Wang *et al.*, 2017).

Recently, an rRNA methyltransferase, called CMAL (Chloroplast MraW-Like) was identified in Arabidopsis. This writer protein performs the N$_4$-methylation of C$_{1352}$ in chloroplast 16S rRNAs (Zou *et al.*, 2020) (Figure 7). CMAL-mediated methylation was shown to be important for efficient plastid translation. Specifically, this modification may support the structural rearrangements of the helix 44 creating an ideal conformation during 30S ribosome assembly. Interestingly, the loss of CMAL leads not only to defects in plastid functions but also to abnormal leaf, root and overall plant development. Further investigations showed that CMAL's involvement in plant development is possibly also due to its ability to modulate auxin-derived signalling pathways (Zou *et al.*, 2020).

In *E.coli*, the *ksgA* gene encodes an rRNA adenine di-methyltransferase responsible for di-methylation of two adjacent adenosines at the N6 position, A1518 and A1519 (m$_2^6$A$_{1518}$m$_2^6$A$_{1519}$) (Buul and Knippenberg, 1985). The homolog of KsgA in Arabidopsis, Paleface1 (PFC1), was identified in a screen for cold-sensitive mutants (Tokuhisa *et al.*, 1998) (Figure 7). The *pfc1* mutant showed chlorosis and impaired chloroplast development only when exposed to low temperatures (5°C). Moreover, primer extension assays indeed showed the absence of methylation in the two adenosines (A1518 and A1519) in *pfc1* mutant lines at the 3' end of chloroplast 16S rRNAs. Whether m^{6}A di-methylases, such as PFC1, act alone or in a complex together with other factors in the chloroplast is still to be determined.
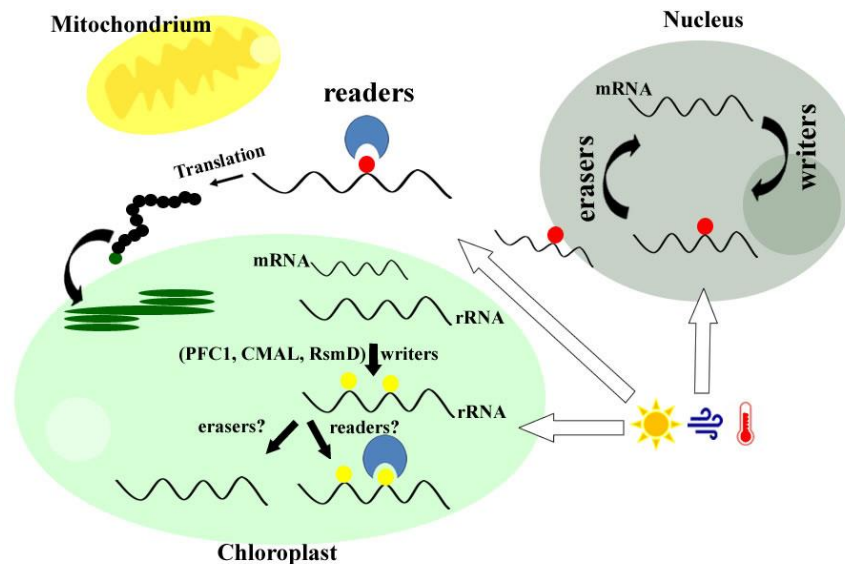
Figure 7: The RNA methylome in plants. m^6A methylation and demethylation of nuclear-derived RNAs mainly take place in the nucleus and participate in the processing, stability, and localization of RNAs whereas m^6A readers function mostly in the cytoplasm. m^6A methylated transcripts predominantly encode chloroplast proteins important for gene expression, photosynthesis, and other plastid functions. Only three 16S rRNA writers – PFC1 for m^6A, CMAL for m^4Cm and RsmD for m^2G methylations - have been described in chloroplasts but writers for mRNAs, as well as erasers and readers are entirely unknown. These modifiers and interpreters are presumably crucial for the fate of transcripts important for the regulation of gene expression to ensure photosynthesis, stress responses and acclimation processes upon environmental changes. Red and yellow circles: RNA methylation marks in mRNAs and rRNAs, respectively. Adapted from (Manavski *et al.*, 2021).

RsmD, another 16S rRNA methyltransferase, is responsible to install the m^2G methylation in *E. coli* (Lesnyak *et al.*, 2007). In Arabidopsis, the orthologous chloroplast RsmD has been shown to play a role in cold stress adaptation (Figure 7). In the cold, lack of RsmD resulted in retarded growth, shorter roots and pale-green leaves compared to WT plants. These phenotypes were not detected in response to other stresses such as drought and salt stress. Remarkably, the *rsmd* mutant was hypersensitive to erythromycin or lincomycin and showed less accumulation of chloroplast proteins, indicating that RsmD influences plastid translation in Arabidopsis (Ngoc *et al.*, 2021). More recently, RsmD was further studied and its function in chloroplast development and photosynthesis was also analysed. The loss of function in *rsmd* mutant showed impaired photosynthetic efficiency already under normal growth conditions.

Taken together, different RNA modifications generally play critical roles in many aspects of plant development, phytopathogenic attack and stress responses. Elucidation the function

of these RNA marks is a challenging and growing field in plant research. Thus, how the nuclear and chloroplast m^{6}A epitranscriptomes regulate chloroplast functions and how they can impact photosynthesis under acclimation conditions are central questions of this thesis.

1.3.4 Plant Mitochondrial RNA Methylation

The m^{6}A methylome was also studied in plant mitochondria and it shares a lot of similarities to the chloroplast epitranscriptome. Over 86% of the transcripts are modified by m^{6}A in the mitochondria with an estimation of ~4.6 to ~4.9 m^{6}A sites per mtRNAs (Wang *et al.*, 2017). The two most observed consensus motifs were GGm^{6}ACA and GGm^{6}ACU in the Arabidopsis mitochondria. About 45%, 20% and 34% of the m^{6}A-modified transcripts were highly methylated by m^{6}A in roots, leaves and flowers, respectively. ~400 m^{6}A sites from the roots, ~280 sites from the leaves, and ~340 sites from the flowers were mapped to the mitochondrial genome (mtDNA). Among these transcripts, mitochondria-encoded ribosomal RNAs (rRNAs), ribosomal proteins, NADH dehydrogenase subunits, and redox proteins were highly methylated by m^{6}A. Regarding m^{6}A methylation levels and gene expression in mitochondria, most of the highly expressed transcripts were also less methylated, and those transcripts with lower expression were highly modified by m^{6}A marks. Similar to chloroplasts, the dominant m^{6}A peak near the stop codon and in the 3´ UTR commonly observed for nuclear mRNA was not observed for mitochondria RNAs. Instead, m^{6}A peaks were found evenly distributed in plastid transcripts with higher methylations in exons when compared to introns, indicating that gene regulation by m^{6}A may be different between nucleus and organelles (Wang *et al.*, 2017). Recently, another study showed that mtRNAs in both cauliflower and Arabidopsis carry N6-adenosine methylation. Several m^{6}A modifications were injurious to translation, whereas a single m^{6}A modification located in the start codon suggested an enhancement in the translatability of the mitochondrial transcripts (Murik *et al.*, 2020).

1.4 Aims of the Thesis

In plants, the nuclear/cytoplasmic epitranscriptome plays important roles in a wide range of biological processes, such as organ development, viral infection and stress response. Recent transcriptome-wide analyses have unveiled m^{6}A modifications in plant

nuclear/cytoplasmic RNAs related to photosynthesis and in chloroplast RNAs, suggesting an important and so far undefined function in plastids. Here we characterize and investigate the influence of m^{6}A in photosynthetic performance mainly by using a knockdown line of FIP37, an essential member of the major nucleus-localized m^{6}A writer complex (Manavski *et al.,* 2021).

General Goal: Investigation of the effects of m^{6}A methylation labels on cytoplasmic RNAs in photosynthetic performance of *Arabidopsis thaliana* under acclimation conditions.

Specific Goals:
- Inspect the expression of writer, readers and erasers under cold, heat and high light conditions;
- Quantify m^{6}A levels in Arabidopsis mRNAs when plants are exposed to cold, heat and high light;
- Investigate photosynthetic performance (Photosystem I and II) in knockdown lines for components of the m^{6}A writer complex under acclimation conditions;
- Characterize a representative knockdown line for the m^{6}A writer complex under cold acclimation regarding the following:
  1) Accumulation of photosynthetic proteins
  2) Chloroplast ultrastructure
  3) ROS formation
  4) Plant development
  5) Expression of cold acclimation genes
  6) Production of pigments

2. Methods

2.1 Plant Cultivation

The *Arabidopsis thaliana* ecotype Col-0 was used as the wild-type (WT) control strain. Knockdown lines for *FIP37*, FIP37-4HA (FIPc), *MTA*, *HAKAI*, *VIRILIZER* and its complemented versions have been previously described and kindly donated by the authors (Růžička *et al.*, 2017, Parker *et al.*, 2020, Shen *et al.*, 2016). Plants were cultivated on half-strength MS medium (Murashige and Skoog) supplemented with sucrose (1,5%) under long-day standard conditions (16 h at 22°C and 80 µmol photons m^{-2} s^{-1}/8 h at 18°C in the dark) using LED (Light-Emitting Diode) cabinets - LED-41 HIL2 (Percival Scientific, Perry, Iowa, USA). Surface-sterilized seeds were stratified (4°C for two days) and cultivated normally for 10 days under standard conditions or for more days when described. For high light (HL) acclimation the light intensity was increased to 450 µmol photons m^{-2} s^{-1} (corresponding to 80% of the white and red LED light intensities). For cold and heat treatments, plants were grown at a constant temperature of 4°C or 32°C, respectively. Acclimation treatments were applied after standard conditions for up to 4 days. To test de-acclimation samples plants were reincubated at standard conditions for four additional days after heat, cold and HL treatments (Figure 8). Sampling was performed by harvesting leaves followed by immersion in liquid nitrogen. Samples were then ground and stored at -80°C prior to usage.
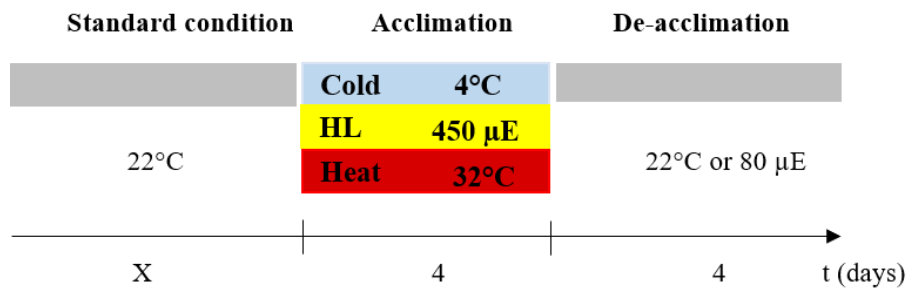
Figure 8: Details of acclimation, de-acclimation and standard conditions used. Time periods of plant growth, temperatures and light intensities are demonstrated. X varies between 10 and 14 days depending on the experiment.

2.2 Transcript and Protein Analysis

Heatmaps representing changes in transcripts of the genes encoding different RNA modifiers (writers, erasers and readers) in WT plants under acclimation conditions were obtained from previous data sets (Garcia-Molina *et al.*, 2020). Gene expression analysis using 10-day-old seedlings (total RNA isolation, electrophoresis, blotting and hybridization with radioactive $[^{32}P]$-dCTP-labeled probes) were performed as previously described (Manavski *et al.*, 2015). Primers for PCR-probes are listed in Appendix Table 3.

Immunoblot analysis was carried out with total proteins extracted from 10-day-old WT and *fip37-4* seedlings lysed in extraction buffer [100 mM NaCl, 50 mM Tris-HCl pH 7.5; 0.5% (v/v) Triton X-100; 1 mM DTT]. 30 µg of total proteins were loaded onto 10% acrylamide (w/v) SDS-PAGE gels, fractionated by electrophoresis (100V) and blotted onto PVDF membranes. Then, membranes were blocked for 1 hour in a cold room using 5% (w/v) milk powder in TBS-T [50 mM Tris, 150 mM NaCl, 0.1% (v/v) Tween 20; pH 7.5] and incubated overnight with primary and subsequently secondary antibodies (Appendix Table 4). Immunoblots were developed with the SuperSignal West Pico PLUS Chemiluminescent Substrate (Thermo Scientific) using the Fusion FX7 GelDoc (PeqLab).

2.3 Colorimetric Assay

Quantification of m^6A methylation level in total RNAs was first performed using the colorimetric m^6A RNA Methylation Assay Kit (Abcam, Cambridge, UK) according to the manufacturer´s protocol. Briefly, positive control, negative control and total RNAs were incubated with the binding solution at 37°C for 90 minutes. Three washing steps using the diluted wash buffer were performed and the diluted capture antibody was added to each well. After 1 hour of incubation at room temperature, the samples were incubated with the m^6A detection antibody for more 30 minutes. Next, the diluted enhancer solution was added followed by five washing steps. Finally, the developer solution was combined with each sample. After 10 minutes under dark, the Stop Solution was added in order to stop enzymatic reactions and the absorbance was measured at 450 nm. The m^6A% in total RNAs was calculated using the following formula: m^6A% = (Sample OD − NC OD) ÷ S)/(PC OD

$-$ NC OD) $\div p) \times 100\%$. NC and PC: negative and positive control; S: the amount of RNA used as input (ng); p: the amount of positive control used as input (ng).

2.4 Liquid Chromatography - Mass Spectrometry (LC-MS)

For m^6A quantification, total RNA was extracted from 14-day-old seedlings of WT before and after 4 days of cold, heat or HL treatment. DNase treatment was performed using 10 µg of the total RNA (Zymo kit – Check details). For poly(A)-enriched RNAs the NEBNext® Poly(A) mRNA Magnetic Isolation kit was used and the integrity of RNAs was confirmed by Bioanalyzer (Agilent RNA 6000 Pico). RNAs were then concentrated in a Speedvacuum centrifuge and precipitated overnight using 5 µl of 5 M ammonium acetate and 125 µl of cold 100 % ethanol. Prior to LC-MS, samples were centrifugated for 1 hour at 4°C and the pellet resuspended in RNase-free water. RNA was digested to single nucleosides by using 2 U alkaline phosphatase, 0.2 U phosphodiesterase I (VWR, Radnor, Pennsylvania, USA), and 2 U benzonase in Tris buffer pH 8 (5 mM) and $MgCl_2$ (1 mM). Furthermore, 0,5 µg tetrahydrouridine (Merck, Darmstadt, Germany), 1 µM butylated hydroxytoluene, and 0,1 µg pentostatin were also added in order to avoid deamination and oxidation of the nucleosides. Followed by incubation for 2 h at 37°C, 10 µl of LC-MS buffer A (5 mM NH_4OAc, pH 5,3) was then added to each sample and LC-MS was finally performed.

2.5 Physiological and Photosynthetic Measurements

Fiji software was used to measure leaf area and root development from pictures of horizontally and vertically grown seedlings (Schindelin *et al.*, 2012). Photosynthetic measurements were conducted with dark-adapted (30 min) seedlings with an IMAGING PAM and Dual-PAM-100 Measuring System (Heinz Walz GmbH) using an induction-recovery protocol. The maximal quantum yield of PSII (F_v/F_m) was calculated as (F_m– F_o)/Fm; the effective quantum yield of PSII (YII) as ($F_m´$ - F´)/Fm´ and the NPQ as ($F_m´$- $F_m´$)/$F_m´$.

2.6 Transmission Electron Microscopy Analysis

For transmission electron microscopy, 10-day-old seedlings of WT and *fip37-4* cultivated on MS medium supplemented with sucrose were analyzed before and after four days of cold treatment. Plants were stored in the dark for 16 h before fixation to avoid starch accumulation. Then primary leaves were cut into 1 mm^2 piece and fixed for 1-3 days at 4°C in cacodylate buffer (75 mM cacodylate, 2 mM MgCl$_2$, pH 7, supplemented with 2.5% glutaraldehyde) as described previously (Espinoza-Corral *et al.*, 2019). After postfixation with 1% (w/v) OsO$_4$ for 1 h, en bloc staining with 1% (w/v) uranyl acetate in 20% (v/v) acetone and dehydration in a graded acetone series was carried out. The plant material was then embedded in Spurr's resin. Ultrathin sections were contrasted with lead citrate and examined with a Zeiss EM 912 transmission electron microscope (Zeiss, Oberkochen, Germany), operating at 80 kV in the zero-loss mode. Images were acquired with a Tröndle 2k x2k slow-scan CCD camera (TRS Tröndle Restlichtverstärkersysteme, Moorenweis, Germany). Image processing was carried out with FIJI, version 2.1 (Schindelin *et al.*, 2012).

2.7 ROS Measurements and Quantitative Reverse Transcription PCR (RT-qPCR)

Superoxide and H$_2$O$_2$ staining were detected with nitro blue tetrazolium (NBT) and 3,3'-diaminobenzidine (DAB), respectively. In situ detection of O$_2^-$ was performed by treating plants with NBT as previously described by (Wohlgemuth *et al.*, 2002). Arabidopsi*s* plants were vacuum-infiltrated with 0.1% NBT 50 mM potassium phosphate buffer (pH 7.8) and 10 mM sodium-azide for 20 minutes followed by an incubation step for one hour at room temperature. Plants were then boiled in 95% Ethanol for 15 minutes to remove chlorophyll. Detection of H$_2$O$_2$ was performed by treating plants with DAB-HCl as previously described by (Fryer *et al.*, 2002). Plants were vacuum-infiltrated with 5 mM DAB-HCl, pH 3, for 20 min, and incubated in the same solution for at least 8 hours overnight. Plants were then boiled in an ethanol:acetic acid:glycerol (3:1:1) solution under the hood until they turned transparent and were later photographed. For RT-qPCR 10- and 14-day-old plant rosettes were harvested and homogenized in liquid nitrogen. Each biological replicate consists of five plants pooled from the same genotype grown on ½ MS-media plates. The RNA extraction was performed with help of the Nucleospin RNA Plant Kit (Macherey-Nagel, Düren, Germany) according to the manufacturer's protocol. RNA purity and concentration

were quantified using a Nanodrop spectrophotometer. Total RNA was transcribed into cDNA using the qScript cDNA Synthesis Kit (Quantabio, USA). The qPCR was performed using the quantabio SYBR green quantification kit (Quantabio) on the PFX96 system (BioRad, Hercules, CA, USA) using the specific primers listed in Appendix Table 3. Actin (At2g3760) was used as a reference gene for transcript normalization. Mean values and standard deviations were calculated from at least three biological replicates.

2.8 Blue Native Gel and Thylakoid Extraction

For native electrophoretic separation of thylakoid complexes, Arabidopsis thylakoid fractions were extracted at 4°C in the dark. For this, leaves were harvested and blended in 30 mL of buffer T1 (0.4 M Sorbitol, 0.1 M Tricine pH 7.8) containing protease inhibitor (Roche). The solution was then filtered with miracloth and centrifugated (4 min, 4000 rpm at 4°C). Next, the pellet was resuspended in 30 mL T2 buffer (20 mM HEPES pH 7.5, 10 mM EDTA), for 10 minutes on ice to break up the chloroplasts followed by another centrifugation step (10 min, 10000 rpm, 4°C). The thylakoid fractions were then resuspended in 100 µl of T2 buffer and chlorophyll content was accessed. For it, 1 µl of each sample was diluted in acetone (80%) and incubated on ice for 10 minutes under dark conditions. After another step of centrifugation (10 min, 13000 rpm, 4°C), the absorbance at 646, 663 and 750 nm was measured in a spectrophotometer (Amersham Biosciences, USA) and the chlorophyll measurements were performed by calculations previously described (Porra, 1989). 50 µg of chlorophyll for each sample was washed and resuspended in thylakoid buffer containing 1% DM (n-dodecyl-β-D-maltoside) and 1/10 volume of BN sample buffer (100 mM BisTris/ HCl pH 7, 6-ACA 750 mM, 5% Comassie-G, 30% Sucrose) was added. Thylakoid protein complexes were then separated on a blue-native PAGE (gradient gel 4-12% polyacrylamide) (Schägger *et al.*, 1988) with a blue cathode buffer (50 mM Tricine, 15 mM Bis-Tris pH 7.0, 0.02% Coomassie-G) and an anode buffer (50 mM Bis-Tris, pH 7.0). After running at 50 V overnight (~16 hours), the blue cathode buffer was replaced with the same buffer without Coomassie-G. Finally, a scan of the gel was made after an additional run at 80 V for 3 hours.

2.9 Chlorophyll and Anthocyanin Content Measurements

For chlorophyll measurements 50 mg leaves of WT, *fip37-4* and FIPc plants were grounded in liquid nitrogen, incubated in 80% acetone mixing overnight under cold (4°C) and dark conditions. Samples were centrifugated for 5 min and the absorbance of the supernatant at A646, A663 and A750 nm was measured in a spectrophotometer (Amersham Biosciences, USA). The chlorophyll content was calculated as previously described (Porra, 1989). Measurement of anthocyanin content was performed according to Neff and Chory (Neff and Chory, 1998). Shortly, 50-mg samples of seedlings of WT, *fip37-4* and FIPc exposed to cold treatment were incubated with 300 µL of 1% (v/v HCl in methanol at 4°C overnight shaking). Next, 200 µL of distilled water and 500 µL of chloroform were added, vortexed, and briefly centrifuged to separate anthocyanins and chlorophylls. The anthocyanin content was then determined by measuring A530 and A657 of the aqueous phase using a spectrophotometer (Amersham Biosciences, USA). For the calculus, the equation (A530-0.25 x A657) x TV / (FW x 1000) was used, where TV = total volume of the extract (in milliliters) and FW = fresh weight of seedlings (in grams).

3. Results

FIP37-Mediated Methylation of Nucleus-Derived mRNAs Ensures Efficient Photosynthetic Performance During Cold Acclimation in *Arabidopsis thaliana*

Parts of the results presented in this chapter were performed in collaboration with the following researchers:

- PD Dr. Jörg Meurer (supervision)

- Dr. Kayo Manavsky (general support and advises)

- Dr. Lisa-Marie Schmid (introduction to basic methods)

- MSc. Paul Rohn (immunological analysis)

- Dr. Antoni Garcia (University of Valencia) (generation of the heatmap)

- Prof. Stefanie Kaiser and MSc. Gregor Ammann (Goethe-Universität Frankfurt) (m^6A mass spectrometry)

- Prof. Andreas Kingl and MSc. Charlotte Seydel (LMU) (electron micrographs)

- Dr. Torsten Möhlmann and MSc. Leo Bellin (University of Kaiserslautern) (ROS detection)

Data presented in this thesis are destined for publication or have been published already.

3.1 Expression of Genes Encoding RNA Modifiers Is Responsive to Cold, Heat and High light

Previous transcriptome-wide maps of N6-Methyladenosine (m^{6}A) have revealed the involvement of highly methylated RNAs in plant stress response and development (Anderson *et al.*, 2018, Shen *et al.*, 2016, Hu *et al.*, 2021, Qin *et al.*, 2022). However, the involvement of m^{6}A methylation in plant acclimation has so far not been addressed. Therefore, gene expression patterns of several epitranscriptomic players, presumably functionally linked to chloroplasts, were first determined under cold, heat and high light (HL). For this, expression data from previous global transcriptome analyses under these conditions were retrieved and subjected to heatmap analysis (Garcia-Molina *et al*., 2020). The data showed that the expression of several of these modifier genes is differentially regulated under acclimation and de-acclimation conditions. Interestingly, many of these genes were differentially expressed exclusively to one or rarely two particular conditions, either cold, heat or HL (Figure 9A), suggesting that these genes potentially have specific roles under certain acclimation conditions. The expression of genes encoding representative members of the m^{6}A writer complex (MAC and MACOM) was determined by RNA gel blot analysis (Figure 9B) and, strikingly, the expression of these genes was strongly responsive to acclimation, especially under cold. These results suggest that factors responsible for the installation, removal, and recognition of RNA modifications may play an important role in plant acclimation.

3.2 m^{6}A Is Enriched in Arabidopsis Poly(A) RNAs Under Cold Acclimation

Our heatmap results and expression analyses have shown that epitranscriptomic players related to chloroplasts are differentially expressed under acclimation conditions. Therefore, it is possible that the m^{6}A mark varies quantitatively in plant transcripts upon cold, heat and HL treatment. To test this hypothesis, we first performed colorimetric assays (Abcam, Cambridge) using total RNAs extracted from plants under standard and cold conditions. No significant differences in m^{6}A percentage were found using total RNA samples (data not shown). Next, poly(A)-enriched RNAs as input were used followed by LC-MS.
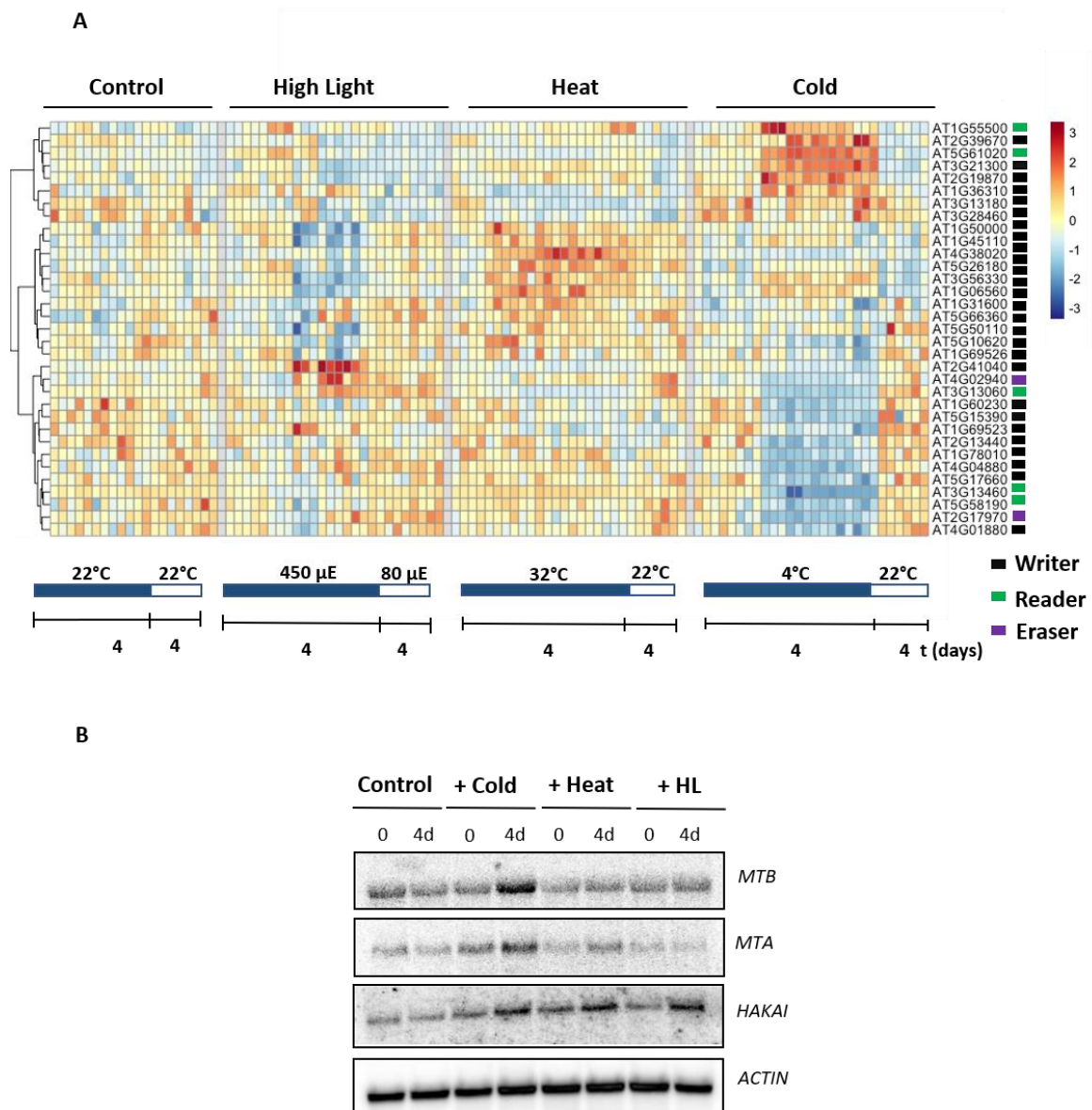
Figure 9: Changes in transcript levels of RNA writers, readers and erasers during acclimation to high light, heat, and cold. (A) Heatmaps based on Z-means of fold changes of differentially expressed genes extracted from (Garcia-Molina *et al.*, 2020). Hierarchical clustering was generated according to Ward d2. (B) RNA-gel-blot analysis of selected components of the m[6]A MAC (*MTA* and *MTB*) and MACOM (*HAKAI*) complex in wild-type plants before and after 4 days of cold, heat and HL treatment using 8 µg of total RNAs from Arabidopsis leaves. *ACTIN* probe was used as a loading control (lower panel).

The electropherogram obtained by Bioanalyzer (Agilent, California) shows a representative sample of the poly(A)-enriched RNA used for m[6]A quantification and the successful removal of most rRNAs is shown (Figure 10A). Interestingly, the m[6]A levels were significantly enriched in poly(A)-RNAs when plants were acclimated to cold (Figure 10B). This result is congruent with the upregulation of the components of the major m[6]A writer complex in Arabidopsis (Figure 9).
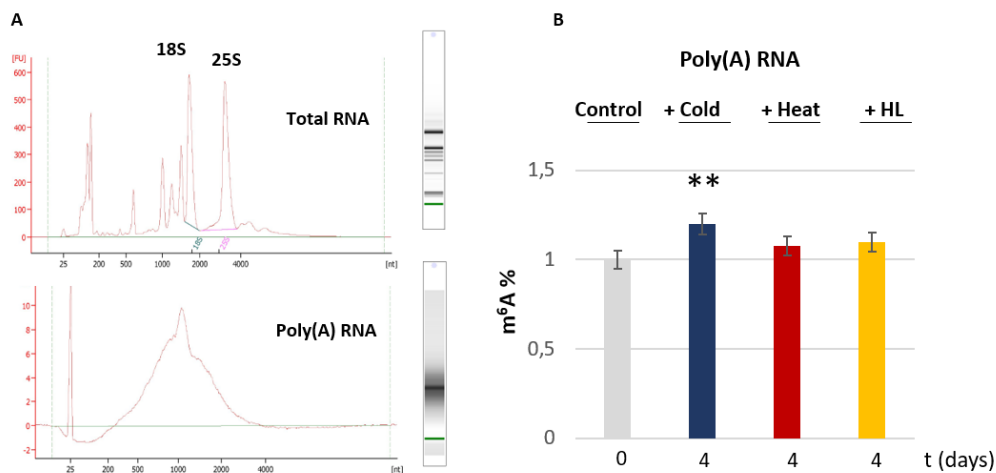
Figure 10: The percentage of m⁶A varies in Arabidopsis poly(A)-enriched RNAs upon acclimation. (A) Electropherogram from Bioanalyzer (RNA Pico 6.000) analysis shows a representative sample of total and poly(A)-enriched RNA samples used for m^6A quantification. 16S and 23S rRNAs in total RNAs and their depletion in poly(A)-enriched RNA samples are shown. (B) Quantification of poly(A)-enriched RNA samples using LC-MS. At least three replicates for each condition were measured. Statistical significance was determined using Tukey HSD. ** corresponds to a p-value ≤ 0.01. Normalization to control was performed for each sample.

3.3 Decreased Photosynthetic Capacity in Mutant Lines of the m⁶A Writer Components Under Acclimation Conditions

Because m^6A was considerably enriched in Arabidopsis transcripts under cold, we further explored how plants lacking individual m^6A writers would behave under this condition. Photosynthesis is the biological process of capturing light energy to form carbohydrates and is strongly affected by exposure to cold (Theocharis *et al*., 2012, Hüner *et al*., 2006). Therefore, we primarily measured the photosynthetic performance of mutant lines of the m^6A writer complex under cold acclimation. Single mutant and knockdown lines defective in these factors have reduced m^6A levels and certain developmental deficiencies in plants (Parker *et al.*, 2020, Růžička *et al.*, 2017). To monitor the effects of low m^6A levels on photosynthetic performance under cold acclimation, we first measured the maximal photochemical efficiency of PSII (F_v/F_m) before and after different times of cold treatments in writer mutants (from 0 to 4 days) (Figure 11). The Fv/Fm value was comparable to the WT in all tested mutant lines within 4 days of growth under standard conditions (at 22°C).

Under cold, however, *fip37-4* already showed a clear reduction in photosynthesis performance only within a few hours of treatment when compared to the WT (Figure 11C). This impairment in photosynthesis gradually increased during longer cold treatment (Figures 11B and C). After 4 days of cold treatment, all mutant lines showed a reduction of F_v/F_m below 0.65, which was most prominent in *fip37-4* (0,58) and *vir-1* (0,60) as compared to the WT (0,69). Thus, the reduced m^{6}A levels in Arabidopsis in these single mutant lines caused reduced photosynthetic performance under cold acclimation.
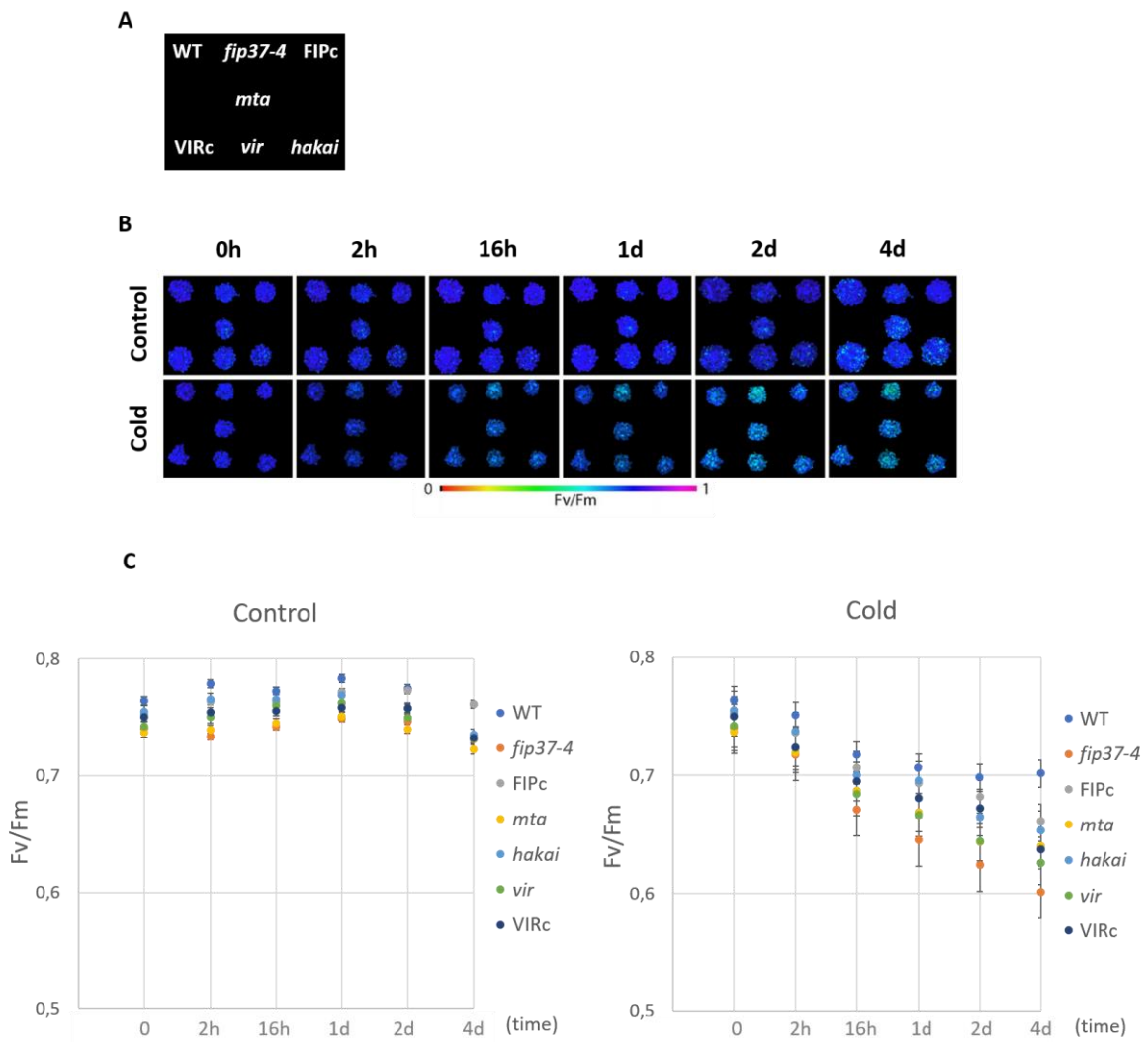
Figure 11: Photosynthetic performance of mutants in genes encoding members of the m^{6}A writer complex is reduced under cold acclimation. (A) Orientation of the knockdown and complemented lines for different members of the m^{6}A MAC and MACOM used. (B) Chlorophyll fluorescence images for Fv/Fm are shown in a false-color scale ranging from 0 to 1 with the bar as a scale shown underneath. (C) F_v/F_m was calculated from the PAM Chlorophyll Fluorescence Imaging devise of different members of the m^{6}A writer complex under several time points (0, 2 hours, 16 hours, 1 day, 2 days and 4 days) of cold treatment (4°C).

As the most affected mutant line, FIP37 may play an important and distinct role in photosynthesis under cold acclimation. Thus, we decided to further focus on this factor. To obtain a comprehensive picture of FIP37, the T-DNA insertion line SALK_018636 and its complemented version (both already shown in Figure 11) were further investigated under cold and de-acclimation conditions.

The genotyping and immunoblot analysis of the *fip37-4* mutant line were both performed to confirm the direct involvement of FIP37 in the integrity of the thylakoid membrane complexes as compared to the WT and the complemented line (FIPc). Also, the developmental changes, such as the bushy phenotype and the reduced apical dominance previously described were verified (Figure 12) (Růžička *et al.*, 2017).
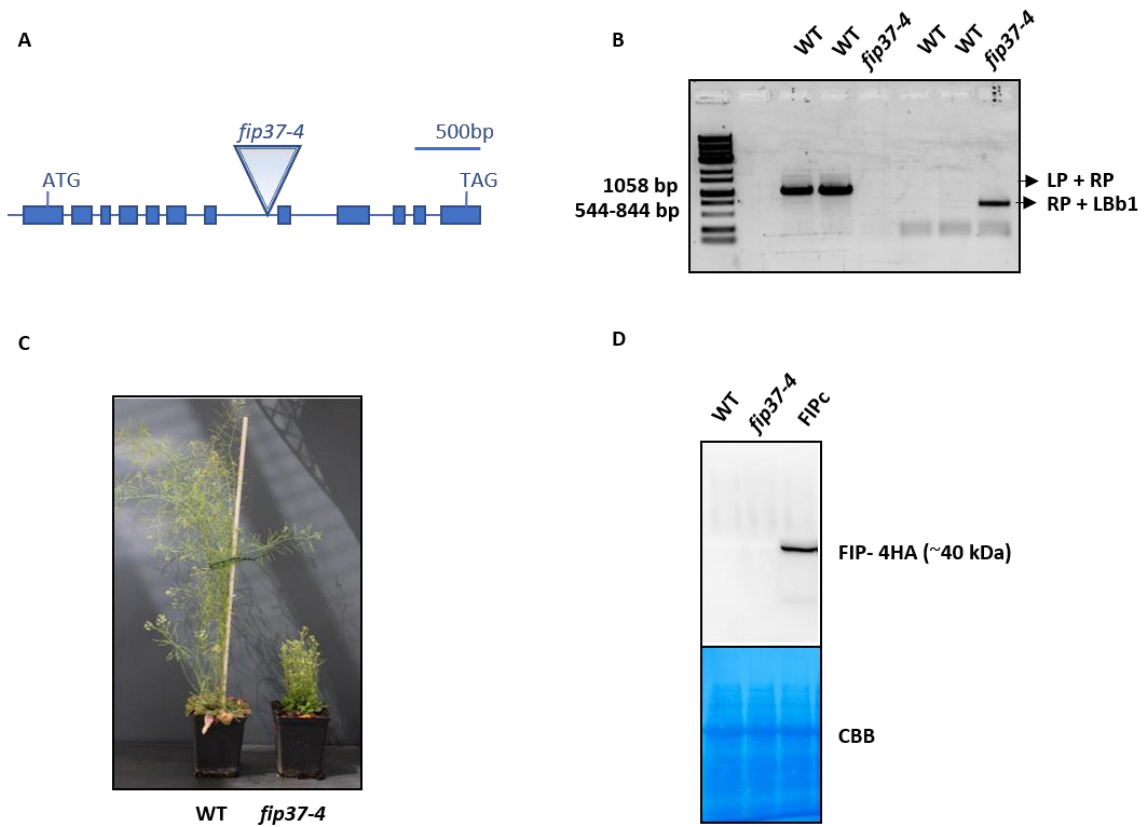
Figure 12: Characterization of the *fip37-4* line. (A) Schematic diagram of the T-DNA insertion in *fip37-4* (SALK_018636). Exons and introns are represented by blue boxes and lines, respectively. (B) PCR using genomic DNA extracted from WT and *fip37-4* with three primers (FIP4 LP, FIP4 RP, LBb1) shown in (Appendix Table 3) was performed in order to confirm the T-DNA line insertion. FIP4 LP and FIP4 RP yielded an amplicon of 1058 bp conforming to the expected size of the wild-type allele, while the combination of FIP4 RP and LBb1 amplified the mutated allele (544-844 bp). (C) 7-week-old *fip37-4* plants showing altered plant development including the previously described bushy phenotype and reduced apical dominance compared to WT (Růžička *et al.*, 2017). (D) Western blot analysis using anti-HA antibody showing the expected band of FIP37-4HA (42,0 kDa) in the complemented line (FIPc). No band, as expected, was present in WT and *fip37-4*. Coomassie brilliant blue (CBB) staining of the large subunit of RuBisCO served as the loading control.

Alterations in the effective PSII quantum yield Y(II) and non-photochemical quenching (NPQ) during light exposure were also investigated (Figure 13). Under control conditions, WT and FIPc lines showed a comparable increase of Y(II) over time and a decrease of NPQ after reaching its maximum triggered by the onset of illumination. Y(II) and NPQ were slightly decreased and increased in *fip37-4*, respectively. Under cold, however, notable changes in *fip37-4* were observed for all parameters tested. Not only a significant reduction of F_v/F_m but also a severe decrease in Y(II) and an increase in NPQ values were detected, indicating increased photosynthetic deficiencies in *fip37-4* during cold acclimation (Figure 13).

According to a previous study in WT plants, 90% of the metabolome perturbations under cold turned back to the initial state after de-acclimation within 4 days. Moreover, a change in the global transcript pattern was also found in the cold, in which the main acclimation state was fully reversed when plants were shifted back to the control condition (Garcia-Molina *et al.*, 2020).

Therefore, we also investigated *FIP37* expression and photosynthetic performance when plants were de-acclimated (Figure 14). Strikingly, both *FIP37* expression in the WT and photosynthetic parameters in *fip37-4* were entirely restored in de-acclimated samples.
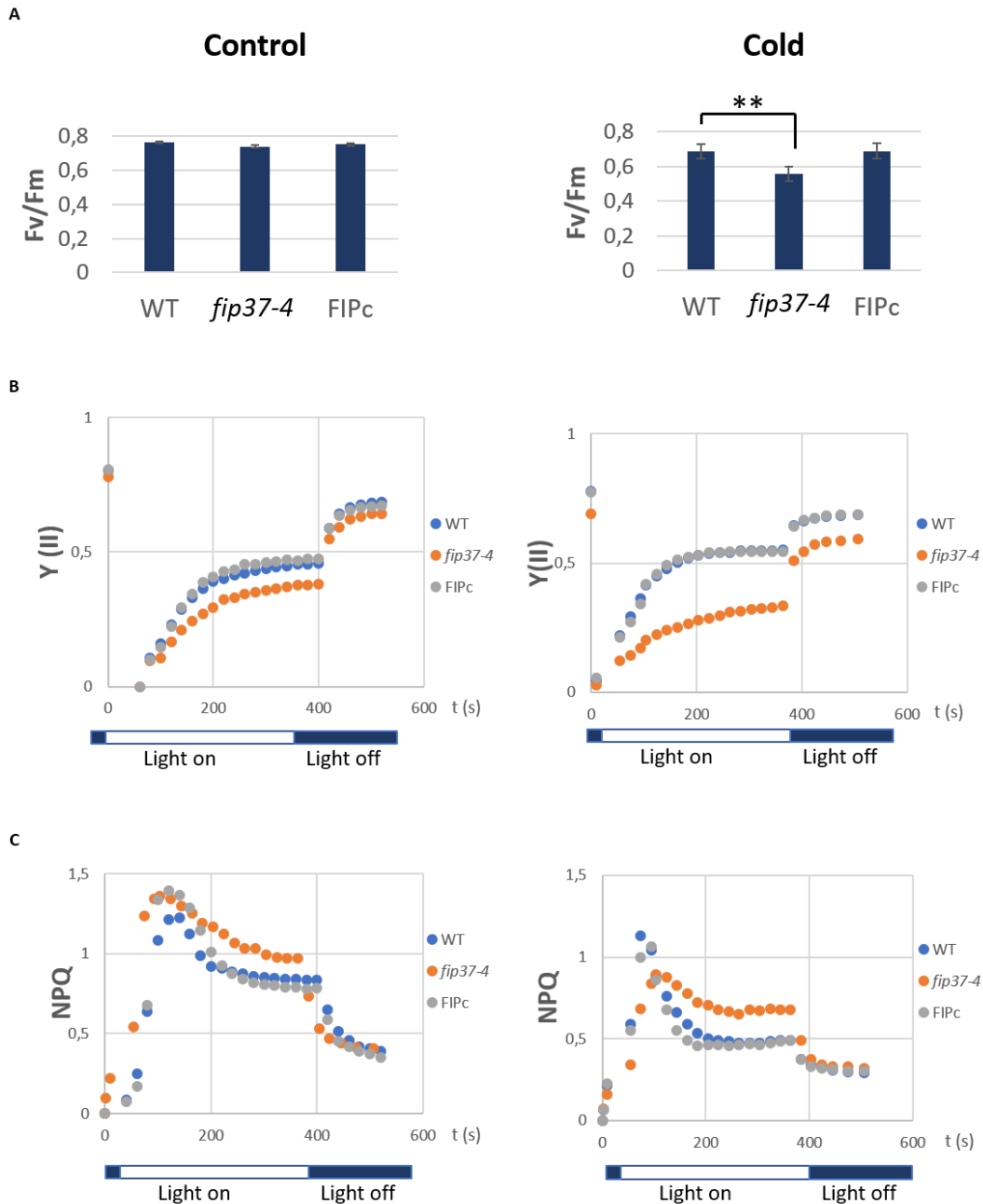
Figure 13: FIP37 influences Arabidopsis PSII photosynthetic performance under cold acclimation. (A) F_v/F_m values and (B and C) kinetics of the deviations in effective PSII quantum yield Y(II) and NPQ (non-photochemical quenching) during a transition from light (80 μmol photons $m^{-2}sec^{-1}$) to dark in WT, *fip37-4* and FIPc lines under standard conditions (22°C) and after 4 days of cold treatment. Plants were dark-adapted for 30 min before parameter determination. At least three replicates for each genotype were measured. Statistical significance was determined using Tukey HSD. ** corresponds to a p-value ≤ 0.01.

Overall, these outcomes suggest that FIP37 potentially plays a crucial role in cold acclimation in Arabidopsis and indicates a hitherto unexplored link to photosynthesis.
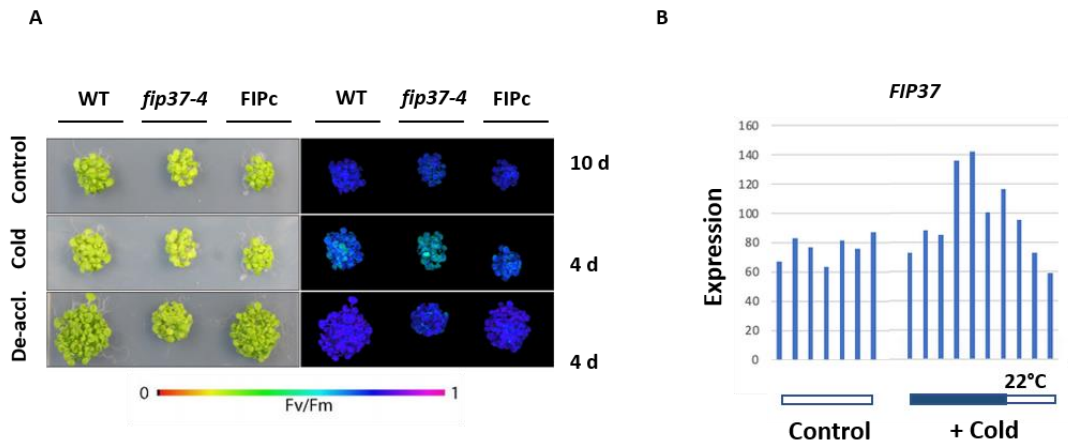
Figure 14: FIP37 influences Arabidopsis photosynthesis performance under cold de-acclimation. (A) PAM Chlorophyll Fluorescence Imaging of seedlings of WT, *fip37-4* and FIPc lines under standard conditions (10 days 22°C), cold (4 days at 4°C) and de-acclimation - when plants were shifted back to 22°C for 4 days. The left part of the picture shows the visible phenotype of the plant whereas on the right chlorophyll fluorescence images for Fv/Fm are shown in a false-color scale ranging from 0 to 1 with the bar as a scale shown underneath (see also Figure 13 for the values). Plants were dark-adapted for 30 min before parameters determination. At least five replicates for each genotype were measured. (B) Expression of *FIP37* in the wild-type (WT) plants before and after several time points of cold treatment. Data extracted from (Garcia-Molina *et al*., 2020).

3.4 FIP37 Influences PSI Activity Under Cold Acclimation

Our previous results demonstrated that the maximum quantum efficiency of PSII was impaired in *fip37-4*. To better understand these observations in photosynthetic performance, we also investigated the activity of PSI using the Dual-PAM measuring system (Walz, Effeltrich) for the assessment of P700 redox reactions. For this, the yield of PSI [Y(I)], the acceptor- and donor-site limitation of PSI [Y(NA)]) and [Y(ND)]) and the nonregulated energy dissipation in PSI [Y(NO)] were measured (Figure 15). The yield of Y(I) was slightly reduced under control conditions but strongly decreased *in fip37-4* under cold. The acceptor-site limitation of Y(NA) did not change under both control and cold conditions. On the other hand, Y(ND) showed an increase in *fip37-4* when compared to the WT and FIPc, especially under cold. Y(NO) also varies only under cold in *fip37-4*.

3.5 FIP37 Is Required for Accumulation of Specific Photosynthetic Proteins During Cold Acclimation

Recently we reported the potential role of different RNA methylations in plant cells with a particular focus on chloroplasts and photosynthesis (Manavski *et al.*, 2021). Indeed, the results strongly support our hypothesis that plant m^6A RNA modifications play essential roles in plant acclimation and photosynthetic performance. To better understand these results, we further investigated the expression of components of the photosynthetic machinery at the protein level. To this end, the accumulation of representative subunits of PSI, PSII, Cytb_6f complex, ATP synthase, subunits of light-harvesting proteins as well as CurT1 and components of the cyclic electron transport were analyzed by immunoblotting using total protein extracts of 10-day-old seedlings before and after 4 days of cold treatment (Figure 16A). With the exception of slightly downregulated proteins of PSI (PsaA, PsaD, Lhca3), the Cytb_6f complex (PetA) and the cyclic electron transport (PGRL1), *fip37-4* accumulated similar levels of all other tested photosynthetic proteins of PSII, LhcB3 and the ATP synthase (AtpB) under control conditions (Figure 16A). However, after 4 days cold treatment all tested subunits of PSI (PsaA, PsaD, PsaO, Lhca3), Cytb_6f complex (PetA, PetB), the cyclic electron transport (PGR5, NdhB) and the CurT1 protein, which is required for the curvature of the thylakoid membrane, are drastically downregulated below 50% as compared to the WT (Figure 16A). Again, subunits of PSII (PsbA, PsbD, PsbO, LhcB6) and the ATP synthase (AtpB) were not affected in *fip37-4*.
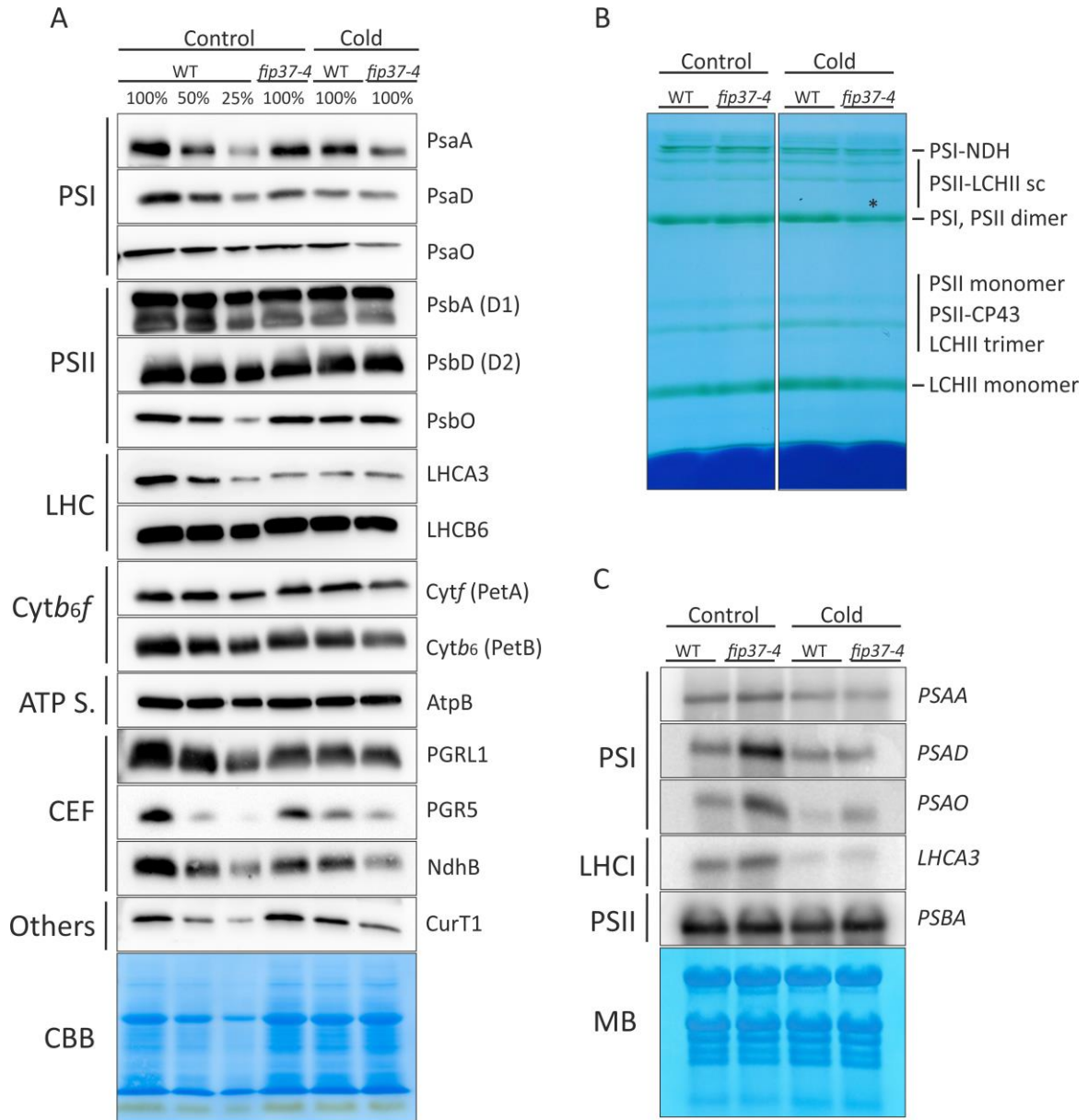
In addition to protein accumulation, photosynthetic complexes were analyzed by Blue Native (BN) gels from *fip37-4* mutant and WT lines (Figure 16B). No marked differences could be found between *fip37-4* and WT under control conditions. The band mainly corresponding to the PSI and to a lesser extent to the PSII dimer was reduced in *fip37-4* exclusively under cold treatment, which agrees with the lower accumulation of representative proteins associated with PSI shown in Figure 16A.
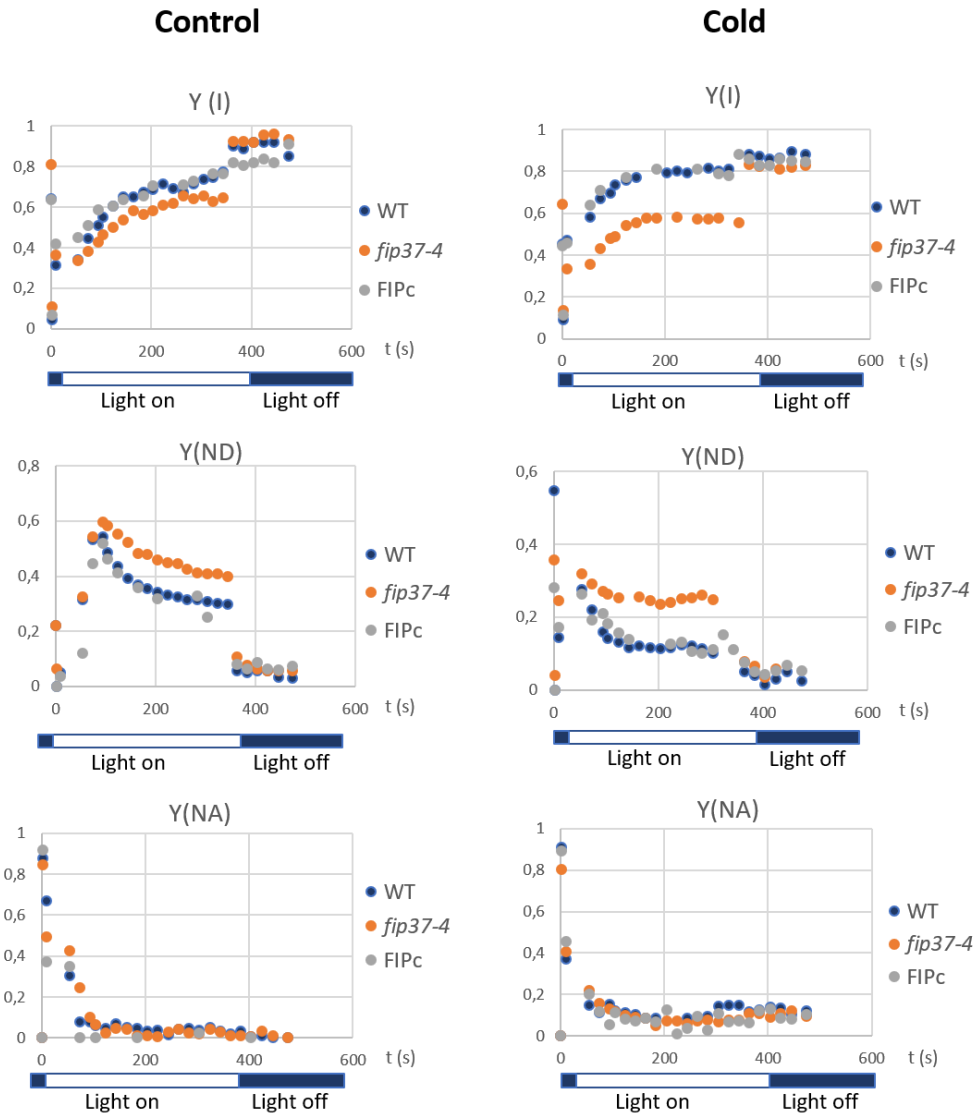
Figure 15: Steady-state of PSI photosynthetic parameters. The yield of PSI [Y(I)], the acceptor- and donor-site limitation of PSI [Y(NA)] and [Y(ND)] were measured after 380 s light induction at 80 μmol photons $m^{-2} s^{-1}$. Plants were dark-adapted for 30 min before parameters determination. At least five replicates for each genotype were measured.

We also examined the RNA levels of some representative genes from the PSI (*psaA, psaD, psaO, lhca3*), PsbA and LhcA3. To our surprise, under control, the levels of all tested nuclear-derived PSI transcripts were much higher in *fip37-4* as compared to the WT. The plastid *psaA* transcripts were only slightly upregulated in the mutant. No changes were observed for *psbA* transcripts. On the other hand, all tested nuclear-derived PSI transcript levels were reduced under cold exposure in the WT and reached levels comparable to those in the mutant, except for PSAO, which still showed an increased transcript level in *fip37-4*. These results indicate that FIP37-mediated RNA methylation is required for the

expression of nuclear-encoded PSI genes or the stability of PSI RNAs under cold acclimation. Slightly elevated transcript levels of the plastid *PSAA* transcripts could reflect a compensatory response to reduced PSI protein levels in the mutant.

Figure 16: Protein accumulation of photosynthetic proteins, analyses of photosynthetic complexes and gene expression in plants lacking FIP37. (A) Accumulation of representative subunits of photosynthetic complexes. Aliquots corresponding to 15 µg of total protein were separated by sodium dodecyl sulfate–polyacrylamide gel electrophoresis, blotted onto PVDF membranes and detected with specific antibodies (Appendix Table 4) for members of the PSI, PSII, LHCs, Cytochrome b_6f complex, ATP synthase (ATP), cyclic electron transport (CEF) and Curt1. Coomassie brilliant blue (CBB) staining served as a loading control. (B) Blue native (BN) analysis of thylakoid membranes. Thylakoid membranes were isolated and solubilized in 1% β-DM (n-dodecyl-beta-D-maltoside) and material equal to 25 µg chlorophyll content was separated on gradient BN gel (4-12%). * Corresponds to changes in PSI in *fip37-4* under cold. (C) RNA-gel-blot analysis of *PSAA*, *PSAD*, *PSAO, LHCA3* and *PSBA* genes in the wild type (WT) and *fip37-4* plants before and after 4 days of cold treatment. 8 µg of RNAs from Arabidopsis leaves were used. Methylene blue was used as a loading control (MB).

3.6 FIP37 Potentially Affects Thylakoid Organization Under Cold

Curt1 complexes are highly enriched in grana stacks and required for the curvature and thus the architecture of the thylakoid membrane (Armbruster *et al.*, 2013). Since levels of the Curt1 protein appeared to be severely reduced in cold-acclimated *fip37-4* mutants we attempted to probe into the ultrastructure of the chloroplast. For this, chloroplasts from 10-day-old seedlings before and after 4 days of cold treatment were analyzed by transmission electron microscopy. Under standard conditions, chloroplasts from both WT and *fip37-4* displayed intact plastid and thylakoid membranes, in addition to well-defined grana stacks, indicating that the lack of *fip37-4* has apparently no obvious effect on chloroplast ultrastructure at 22°C (Figure 17). However, under cold acclimation, *fip37-4* thylakoids were organized in a ''wave-like'' form and grana stacks consisted of fewer but broader layers of membranes, whereas WT retained a similar ultrastructure when compared to standard conditions (Figure 17). Reduced levels of Curt1 support the changed ultrastructure and strongly indicate that FIP37, beyond its association with photosynthesis and cold acclimation, can potentially be involved in a wide range of chloroplast functions, such as the thylakoid membrane organization.
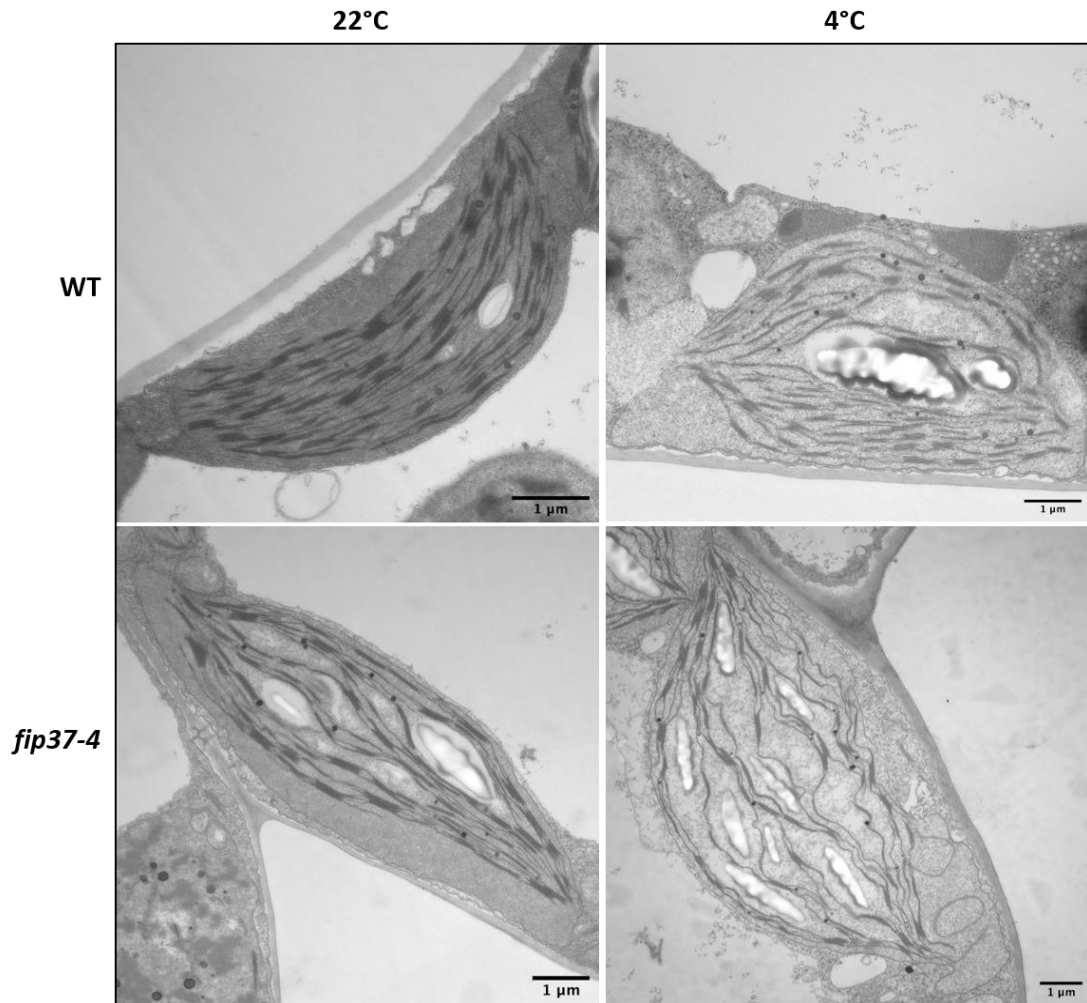
Figure 17: Effects of cold on chloroplast ultrastructure in wild-type (WT) and in *fip37-4* mutant seedlings. WT and *fip37-4* were cultivated on half-strength Murashige and Skoog (MS) medium and harvested before or after 4 days of cold treatment at 4°C. Chloroplasts were examined by transmission electron microscopy (TEM). Representative chloroplasts images are demonstrated. Scale bar: 1μm.

3.7 FIP37 Influences ROS Formation Under Cold Acclimation

Chloroplasts produce reactive oxygen species (ROS) under hostile environmental conditions via both photosystems (PSI and PSII) (Li and Kim, 2022). Thus, we decided to test ROS formation in cells lacking FIP37 under cold acclimation. WT and *fip37-4* plants were grown under standard and cold conditions for 4 days and ROS formation was examined before and after the cold treatment (Figure 18). NBT and DAB stainings were used to detect O_2^- and H_2O_2, respectively, and both showed no differences when comparing all lines under standard conditions at 22°C. Transfer of the plants to 4°C, on the other hand, resulted in more intense NBT and DAB staining of the *fip37-4* mutant compared to WT

(Figure 18A). The FIPc complementation lines showed always a comparable coloration to the wild type. In addition to the staining, gene expression of ROS-related genes was monitored by RT-qPCR. In the cold, a slight increase in the expression of the transcription factors *ZAT12* and *ZAT10* was detected in *fip37-4*. The transcript level of superoxide dismutase1 (*SOD1*) showed an increase in all tested lines under cold whereas no alterations in expression were seen for the ascorbate peroxidase1 (*APX1*) (Figure 18B). Altogether, these results indicate an increase in ROS formation in plants lacking FIP37, especially under cold.
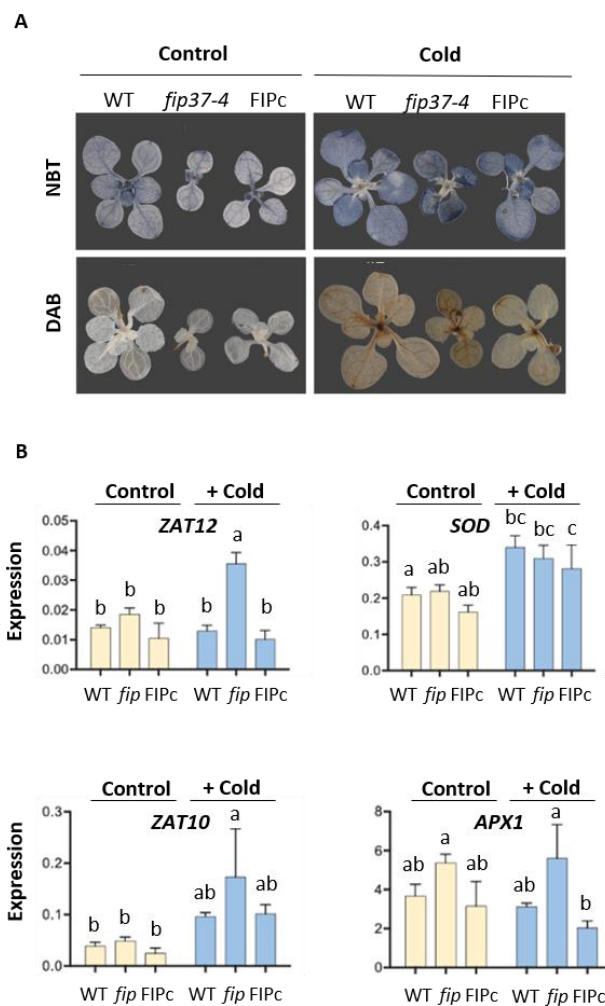
Figure 18: Cold treatment leads to an increased accumulation of reactive oxygen species (ROS) in *fip37-4.* (A) NBT and DAB staining of plants before or after 4 days of cold treatment (4°C). NBT staining is indicative of superoxide (O_2^-) and DAB staining is indicative of H_2O_2 production. (B) Expression of ROS-related genes (*ZAT12*, *ZAT10*, *SOD1* and *APX1*) by qRT-PCR. Bars denote the means of 3 independent biological replicates with the corresponding standard deviation. Different letters within individual titles represent significant differences between tested temperatures (22°C and 4°C) and genotypes (WT, *fip37-4* and FIPc) according to two-way ANOVA with post-hoc Tukey HSD ($p < 0.05$).

3.8 Impact of FIP37 on Plant Development Under Cold Acclimation

FIP37 is very conserved among several plant species (Shen *et al.*, 2016). To monitor the effects of cold acclimation on development in plants with reduced FIP37 levels, we first measured the fresh weight, leaf area and chlorophyll content of plants cultivated on MS medium grown horizontally under standard and cold conditions. Interestingly, all these parameters were already reduced in the mutant line at 22ºC (Figures 19A and 19B). To further address the impact of FIP37 on plant development, WT, *fip37-4* and FIPc lines were vertically grown at 22ºC and at 4ºC, the latter condition after 2 days of seed germination at 22ºC (Figure 19C).

Strikingly, the root growth was inhibited in *fip37-4* plants after 30 days and 60 days of cold incubation at 4°C. To reassess this cold phenotype, plants were grown under standard conditions at 22ºC. Indeed, the three lines presented similar root development (~ 8-9 cm) after 21 days of growth. *fip37-4* leaves were clearly paler under cold, while the WT and FIPc produced normal green leaves. In addition, secondary root formation was impaired in cells lacking FIP37 already at 22°C. Therefore, in agreement with a previous study (Růžička *et al.*, 2017), root and plant development is affected in *fip37-4* under standard conditions. However, a more prominent alteration is observed under cold acclimation (Figure 19). The fact that *fip37-4* produces less chlorophyll is consistent with our previous results showing that *fip37-4* was paler and affected photosynthetic performance and accumulation of thylakoid membrane complexes under cold acclimation. All these results demonstrate that the *fip37-4* knockdown line had effects on the growth and development of seedlings already under standard conditions but photosynthesis is particularly impaired only during cold acclimation.
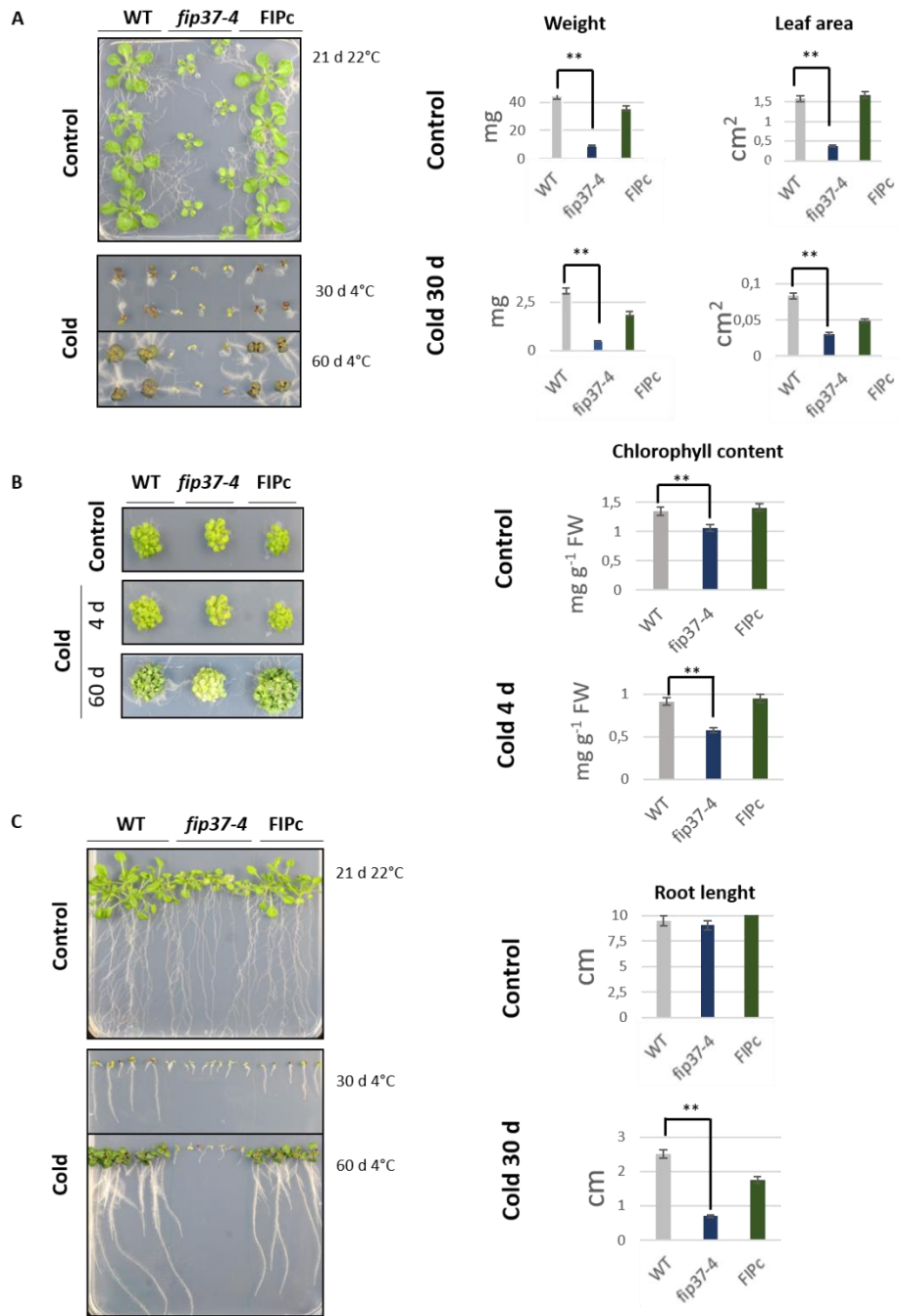
Figure 19: Impact of FIP37 on Arabidopsis plant development. (A) Growth phenotype of WT, *fip37-4* and FIPc growing horizontally on ½ MS medium at 22°C (for 21 days) and at 4°C (for 30 and 60 days). Graphs show fresh weight and leaf area of plants under control and after 30 days under cold. (B) Chlorophyll content in WT, *fip37-4* and FIPc under standard conditions at 22°C and after 4 days of cold treatment. (C) The cold-sensitive phenotype of the *fip37-4* growing vertically on ½ MS medium showing root growth at 22°C (for 21 days) and at 4°C (for 30 and 60 days) compared to WT and FIPc. Graphs show root lengths of plants under control and after 30 days under cold. At least 25 replicates for each genotype were measured. Statistical significance was determined using Tukey HSD. ** corresponds to a p-value ≤ 0.01.

## 3.9 FIP37 Influences Anthocyanin Production Under Cold Acclimation

Flavonoids are natural compounds present in flowers, leaves and seeds of many plant species. They can be divided into 3 different subgroups based on their chemical structures, including flavonols, proanthocyanidins and anthocyanins (Winkel-Shirley, 2001). Many functions were reported for these compounds such as fruit and flower pigmentation. However, the putative function of anthocyanins in plant defense against UV light and pathogens is still enigmatic. These pigments accumulate in response to abiotic stresses, cold and high light, for instance, playing a possible, still unknown role in plant tolerance to different environmental conditions (Winkel-Shirley, 2002). The purple leaf phenotype due to the accumulation of anthocyanins is clearly absent in *fip37-4* when compared to WT and FIPc under cold conditions at 4°C (Figure 20A). Indeed, anthocyanin content was drastically reduced in *fip37-4* (Figure 20B). Another function of anthocyanins was proposed to be related to photoprotection due to its accumulation under high light and during ROS formation (Renner and Zohner, 2019), which agrees with the increase in ROS formation in *fip37-4* previously demonstrated.
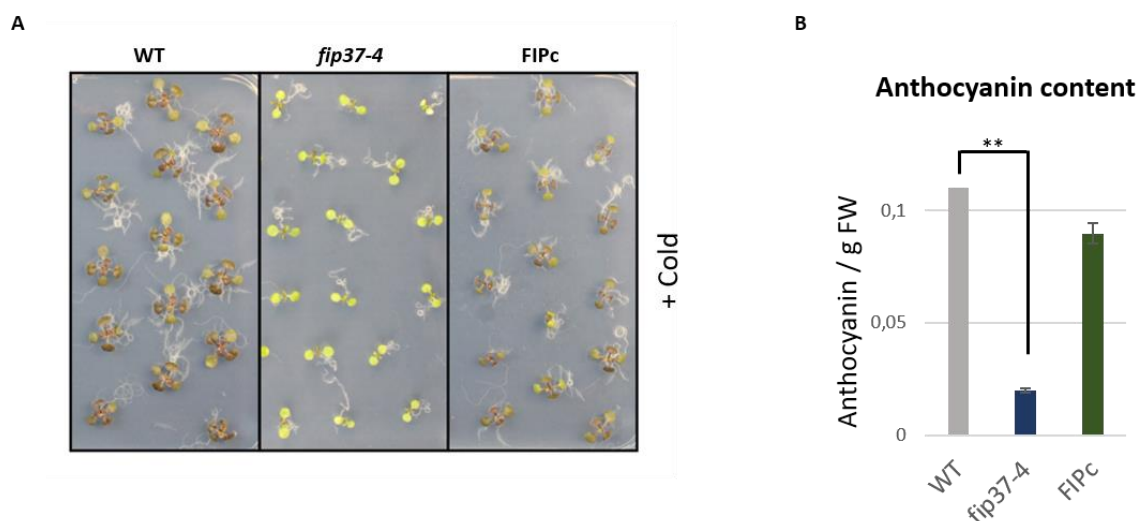
Figure 20: Impact of FIP37 on Arabidopsis anthocyanin production. (A) Growth phenotype of WT, *fip37-4* and FIPc growing horizontally on ½ MS medium at 22°C for 7 days followed by shifting to 4°C for 30 days. (B) Anthocyanin content in WT, *fip37-4* and FIPc under cold treatment. At least 15 replicates for each genotype were measured. Statistical significance was determined using Tukey HSD. ** corresponds to a p-value ≤ 0.01.

## 3.10 FIP37 Reduces Expression of Specific Cold-Shock Response Genes

We further tested the expression of known genes associated with cold shock response and cold acclimation in Arabidopsis. C-repeat-binding factors (CBFs) play important roles in plant acclimation (Liu *et al.*, 2019). These factors bind to the C-repeat responsive element motif found in promoters of cold-responsive (*COR*) genes, such as *COR15A* and *RD29A*. In addition, *CBF* genes can also be controlled by another set of transcription factors, including ICE1 (Inducer of CBF expression I), which regulate the transcription activation of *CBF*s under cold (Figure 21B) (Zhao *et al*., 2015). In the absence of FIP37, the expression of both *COR15A* and *RD29A* were reduced after 4 hours of cold treatment. Particularly for *COR15A*, a reduction in its expression was also observed after 24 hours at 4°C. No clear alteration in gene expression of *CBF2* was detected under the same conditions (Figure 21A). Therefore, these results indicate that FIP37 impacts the expression of essential genes related to the response and adaption to cold, particularly the expression of *COR* genes.
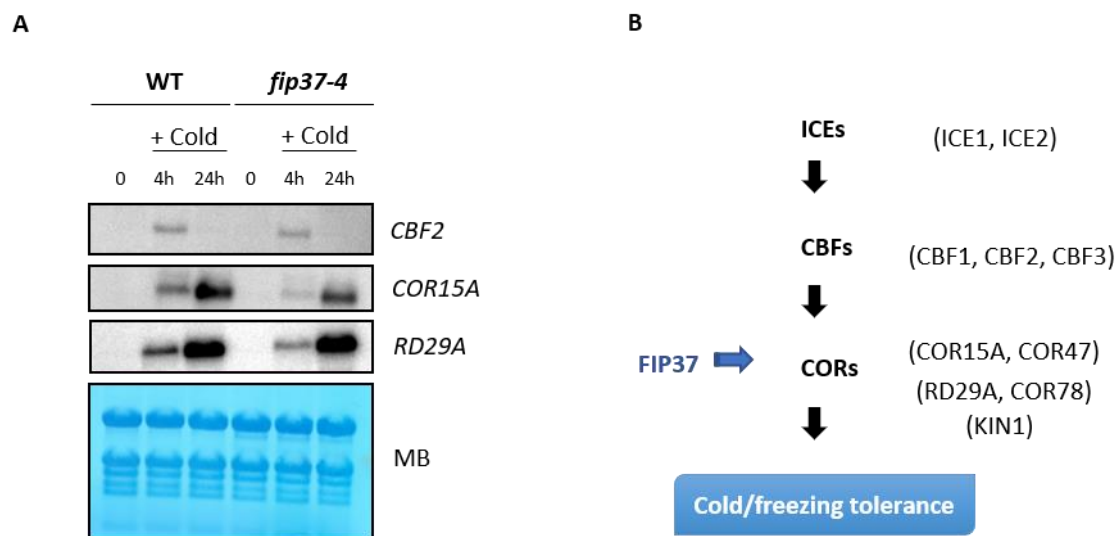
Figure 21: Impact of FIP37 in the expression of genes related to Arabidopsis cold acclimation. (A) RNA-gel-blot analysis of *CBF2*, *COR5A* and *RD29A* genes in the wild type (WT) and *fip37-4* plants before and after 4 and 24 hours of cold treatment at 4°C. 8 µg of RNAs from Arabidopsis leaves were used. Methylene blue was used as a loading control (MB). (B) Cascade of genes associated with cold acclimation in Arabidopsis.

3.11 Concluding Summary

Altogether, our results indicated that FIP37 has a pleiotropic effect and plays distinct roles in Arabidopsis (Figure 22). In the WT m^6A methylation occurs in several plant mRNAs under control and cold acclimation. This important RNA mark is capable of controlling the fate of these mRNAs throughout distinct processes, such as RNA stability, export, processing and/or translation. In *fip37-4*, however, the methylation status in the plant decreases to 10% (Růžička *et al.*, 2017) and many of these mRNAs are no longer methylated, leading to different effects in plants (Figure 22). Notably, we have shown that photosynthetic performance is strongly reduced under cold acclimation in *fip37-4*. As FIP37 is a nuclear-encoded protein, our hypothesis is that FIP37-mediated methylation of nucleus-derived mRNAs ensures efficient photosynthetic performance, plant development, ROS formation and thylakoid membrane organization during cold acclimation.
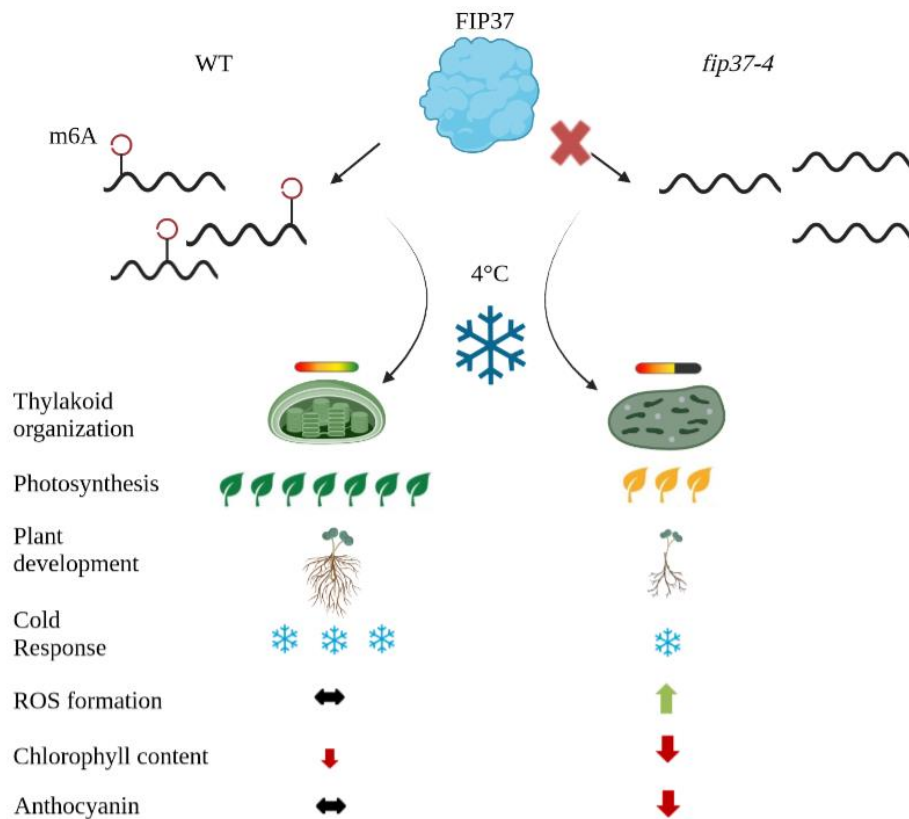
Figure 22: Schematic drawing of the proposed FIP37 functions. FIP37 influences plant development, thylakoid organization, photosynthetic performance, cold shock response, ROS formation and chlorophyll/anthocyanin production under cold acclimation in Arabidopsis. Green, red and black arrows indicate an increase, decrease or no changes, respectively, in ROS formation and chlorophyll/anthocyanin content. The picture was made using biorender.com.

4. Discussion

RNA methylation as well as the interpretation of these marks are becoming known as an essential post-transcriptional mechanism of gene regulation in the response of plants to (a)biotic stresses, as well as in plant cellular development. The potential role of erasers, writers and readers in plant stress response has been previously studied (Shao *et al.*, 2021). However, the function of these RNA modifiers in plant acclimation remained unknown so far. The results presented here demonstrate that several erasers, writers and readers show

altered expression patterns upon cold, heat and HL acclimation (Figure 9), which strongly indicates that these factors have important roles under these particular conditions. Here, we analyzed in detail the Arabidopsis m^{6}A writer protein FIP37 and we could demonstrate its important role in photosynthetic performance, thylakoid organization, protein and pigment accumulation, plant development and ROS formation during cold acclimation. All these alterations are reversible upon deacclimation.

4.1 m^{6}A Writers Are Essential Key Players in Photosynthetic Performance

Despite a slightly lower chlorophyll content, no marked difference in the photosynthetic performance was observed between the wild-type Col-0 and the *fip37-4* line under standard conditions. In contrast, under cold acclimation, the *fip37-4* knockdown line displayed a clear reduction of photosynthetic activity (Figure 11). These results suggest that FIP37 and, consequently, the m^{6}A marks it introduces positively influence photosynthesis under low temperatures. The first hint for a beneficial impact of RNA methylation on photosynthetic performance under stress conditions has been described only recently. When a watermelon m^{6}A methyltransferase (ClMTB) was overexpressed in tobacco, transgenic plants were more tolerant to drought, an improvement in photosynthesis was observed and stress-responsive gene expression was modulated as well (He *et al.*, 2021). When WT and the overexpression lines (OEMTB-15) were exposed to low-watered conditions for 10 days, the leaves of WT plants showed a severe dehydration phenotype and strong wilting symptoms, whereas OEMTB-15 plants remained healthy, turgid and their leaves fairly green. The plant survival rate after re-watering demonstrated a recovery of 76,6% for OEMTB-15 but only 6,67% for WT plants. Strikingly, the maximum photochemical quantum yield of PSII (F_v/F_m) was higher in OEMTB lines when compared to the WT plants (He *et al.*, 2021). Under our conditions, when a FIP37 knockdown line is used, we see exactly the opposite situation: down-regulation of one component of the nuclear methyltransferase complex reduced photosynthetic output only at cold, resulting in lower Fv/Fm. This supports the idea that m^{6}A could regulate the functionality and/or stability of several RNAs related to photosynthesis and plant cold response. Indeed, previous results using different m^{6}A RNA immunoprecipitation and sequencing techniques have shown that several RNAs associated with photosynthesis and chloroplast functions are commonly

methylated (Qin *et al.*, 2022, Shen *et al.*, 2016, Manavski *et al.*, 2021). For instance, differential m⁶A methylation among leaves, flowers and roots showed that green leaves have the highest extent of m⁶A methylation among these three organs. These transcripts were mainly related to photosynthesis, regulation of transcription, and stress response (Wan *et al.*, 2015). In addition, our recent review has summarized a list of chloroplast- and nucleus-encoded genes associated with photosynthesis found in m⁶A epitranscriptomes of different accessions of Arabidopsis (Appendix Table 2) (Manavski *et al.*, 2021).

The subcellular localization of FIP37 and its expression in different organs were previously demonstrated (Shen *et al.*, 2016). FIP37 is highly expressed in young Arabidopsis leaves and the protein is known to be nucleus localized, where it assists in adding the m⁶A modification to RNAs. Our results unequivocally indicate that FIP37 function supports photosynthesis, chloroplast ultrastructure and accumulation of thylakoid membrane complexes and pigments during cold treatment. The chloroplast genome of *A. thaliana* is composed of 154,478 base pairs, 129 genes and 85 protein-coding genes *(Dobrogojski et al.*, 2020). However, most of the chloroplast proteins are encoded by the nuclear genome, which may explain the effect of the introduction of m⁶A marks in nuclear RNAs on photosynthesis. Thus, regardless of the cell compartment in which RNA methylation occurs, these labels can directly or indirectly affect the proper functioning of other cell compartments and organelles within the plant cell. Indeed, many photosynthetic mRNAs that are nucleus-encoded and simultaneously contain m⁶A marks in their structures have been identified by a recently developed neural network called DENA (Deeplearning Explore Nanopore m⁶A), which quantifies m⁶A in *Arabidopsis thaliana* RNAs using nanopore sequencing (Qin *et al.*, 2022). DENA accomplishes a high accuracy of m⁶A detection (90%) in the m⁶A sites identified by miCLIP in Arabidopsis. The m⁶A profile of WT, *mtb* and *fip37-4* at single-nucleotide resolution was evaluated. Over 55,000 RRACH sites were found and m⁶A sites were commonly present near the stop codon and within the 3`UTR in mRNAs. In agreement with our results, Gene Ontology (GO) analysis of the m⁶A-altered genes clearly shows an overaccumulation of processes associated with abiotic stresses (salt, cold and light conditions). Most importantly, processes such as photosynthesis, electron transport chain and light reactions were highly enriched. A list of representative photosynthetic nucleus-encoded genes was published previously (Leister and Schneider, 2003). Of 59 nucleus-encoded photosynthetic transcripts shown in this publication, a total of 41 transcripts have m⁶A marks present in both WT and *fip37-4*

(Appendix Table 5). However, in *fip37-4*, a reduction in m^{6}A methylation marks of almost 50% of these representative transcripts was observed (Appendix Table 5, red label), whereas 22% of them showed an increase in m^{6}A levels (Appendix Table 5, green label). These results indicate a dynamic regulation of photosynthetic transcripts mediated by FIP37 already at 22°C. Our results showed a drastic reduction in photosynthetic performance in *fip37-4* under cold. Therefore, it is tempting to consider that these changes in m^{6}A may be even more dramatic in photosynthetic transcripts under cold acclimation. To confirm this, techniques such m^{6}A-RIPseq and nanopore sequencing using cold-treated Arabidopsis RNAs of WT and *fip37-4* mutant plants need to be applied in the future.

4.2 Roles of m^{6}A Writers, Readers and Erases on Stress Conditions

Notably, the enrichment of m^{6}A levels in poly(A) RNAs specifically under cold (Figure 10) agrees with the upregulation of *FIP37* and other genes encoding representative members of the major m^{6}A writer complex in the nucleus under the same conditions. In addition, m^{6}A demethylases, such as *ALKBH9B* (AT2G17970) and *ALKBH10B* (AT4G02940), were downregulated under cold conditions (Figure 9, shown in purple squares). These proteins have opposite roles to writer proteins and are, therefore, capable of removing RNA marks. The importance of an RNA demethylase (ALKBH6) under abiotic stresses was recently studied. The expression levels of ALKBH6, seed germination and seedling growth of *alkbh6* T-DNA knockdown mutants were accessed under different environmental conditions. The expression of *ALKBH6* was increased under salt stress (NaCl), while its level was decreased under cold (Huong *et al.*, 2020). These results agree with our expression analysis of m^{6}A erasers (Figure 9) and confirm the downregulation of another Arabidopsis m^{6}A demethylase at low temperatures. In addition, the germination rate of *alkbh6* mutants was improved compared to WT plants after salt, cold or ABA treatment, but not under dehydration stress (Huong *et al.*, 2020). Considering plant growth and development, no differences were observed in seedling and root growth under cold stress at 10ºC, which can be sensed by the plants as a moderate temperature compared to 4ºC used in our work. However, at 45ºC the *alkbh6* mutants grew slower and had a lower survival rate when compared to WT (Huong *et al.*, 2020).

Very recently, the involvement of m^{6}A RNA methylation marks under cold has been demonstrated in flowers in tomato plants (Yang *et al*., 2021). Low temperature directly affects m^{6}A methylation abundance on a set of transcripts related to anther growth. Under low temperature, anther m^{6}A quantification was decreased at both the tetrad and uninucleate stages of anther development. In agreement, the expression of all m^{6}A writer components (*SlMTA*, *SlMTC*, *SlMTD*, *SlFIP37* and *SlHAKAI*) was downregulated in anthers at the mature pollen stage (VI) upon cold. This result agrees with the positive correlation between the expression of genes encoding m^{6}A writer proteins and the m^{6}A levels we have shown. Whether this downregulation in the expression of the m^{6}A writers demonstrated in tomato anthers RNAs also happens in Arabidopsis anthers transcripts under cold is not known. Furthermore, the low-temperature stress resulted in pollen abortion in tomato plants. This phenotype was caused by impairment of the tapetum development and pollen formation, accompanied by a reduction of m^{6}A levels in tomato anthers. The m^{6}A epitranscriptome revealed that more than 3.837 m^{6}A peaks differed between control and cold anthers, suggesting a specific role of m^{6}A in tomato anthers at low temperatures. m^{6}A levels were lower for most of these transcripts and RNA-seq revealed an upregulation of these genes under low temperatures. These differentially m^{6}A enriched transcripts under low temperature were mainly associated with ATPase (adenosine triphosphatase) activity, and ATP-binding pathways and lipid metabolism (Yang *et al*., 2021). Noteworthy, other studies have already reported this inverse correlation between gene expression and m^{6}A levels in transcripts. It was found that the most highly expressed transcripts are generally less modified by m^{6}A and most of the transcripts with low expression are more modified by this RNA label (Wang *et al*., 2017). Here, under control conditions, the expression of representative photosynthetic genes encoding PSI components was drastically upregulated in *fip37-4* (Figure 16C). However, this upregulation was no longer observed under cold conditions for most of these genes tested, indicating either an increase in m^{6}A levels in photosynthetic transcripts or another level of control, such as RNA translation or stability, under cold acclimation when compared to control conditions.

As mentioned above, m^{6}A writers transfer a methyl group from SAM (S-adenosylmethionine) to the adenosine located at the sixth position in RNAs. The S-adenosylmethinine synthetase (SAMS), in turn, is an enzyme that uses ATP and methionine to catalyze the biosynthesis of SAM. Interestingly, the SAMS is known to play a role in cold resistance in transgenic lines when overexpressed (Choi *et al*., 2022). SAMS enzyme

activity as well as its gene expression increased under cold when compared to control conditions, demonstrating a correlation with the expression of the m^{6}A writer components (Figure 9). At low temperatures, SAMS overexpressing lines showed relatively lower ion leakage - approximately half of the values found in control conditions - suggesting that these genes are important for cold plant response and adaptation. Nonetheless, no correlation with methylation of RNAs or other molecules was evaluated, which would be an interesting area for research in the future. Altogether, these findings characterized m^{6}A marks as part of a complex layer in controlling gene expression and established a link between m^{6}A methylation and plant response to changing environmental conditions.

4.3 The Destiny of m^{6}A-modified mRNAs Has a Region-dependent Regulation

The exact location of m^{6}A marks in mRNAs plays a role in the fate of these RNAs. In apples, MdMTA-mediated m^{6}A modifications enhance drought tolerance by promoting mRNA stability and translation efficiency of genes related to lignin deposition and scavenging of reactive oxygen species (ROS) under drought conditions (Hou *et al.*, 2022). Transcriptome-wide m^{6}A methylome analysis in *MdMTA* RNAi plants revealed a significant reduction of m^{6}A peaks in 3´UTRs but an increase in CDS regions. Investigation of the m^{6}A levels and the expression of representative genes showed for both a downregulation of *MdLEA* (related to drought stress), *MdLAC4*, *Md4CL3* (lignin biosynthesis), *MdORM2*, *MdMYC4* and *MdMPV17* (H$_2$O$_2$ pathway) in *MdMTA* RNAi plants. Assays using actinomycin D revealed that the stability of *MdLEA*, *MdLAC4*, *MdORM2*, *MdMYC4* and *MdMPV17* mRNAs was lower in *MdMTA* RNAi lines upon drought. For *Md4CL3* mRNA, however, no difference in mRNA stability was observed. Particularly, in this case, the m^{6}A marks were located in the 5´ UTR. RNA modifications in this specific region have been shown to be associated with translation in a cap-independent manner (Meyer *et al.*, 2015). Indeed, the translation efficiency of the *Md4CL3* mRNA was impaired in *MdMTA* RNAi plants under drought stress. Thus, when apple plants are exposed to drought environments, *MdMTA* expression and m^{6}A levels are both induced to promote mRNA stability and translation efficiency of genes involved in lignin deposition and ROS scavenging (Hou *et al.*, 2022). In Arabidopsis, m^{6}A levels in photosynthetic transcripts are predominantly reduced in *fip37-4* at 22°C (Appendix Table 5). If the same

happens under cold and how it influences the RNA fate and, consequently, the synthesis of photosynthetic proteins is still unknown. However, a drastic downregulation in protein levels of PSI, cyclic electron transport and Cytb_6f complex is clearly observed in *fip37-4*, especially under cold (Figure 16A), and this downregulation pattern was not observed in the expression of PSI transcripts (Figure 16C). This suggests that under cold acclimation lower m^{6}A levels in photosynthetic transcripts are caused by the lack of FIP37. In case this is true, different mechanisms of regulation could explain the lower accumulation of photosynthetic proteins we observed here. As in apples, m^{6}A could function as a protecting mark from RNases, playing a role in RNA degradation under cold acclimation. Thus, in the absence of this mark in *fip37-4,* nucleus-encoded photosynthetic transcripts may serve as target of many RNases. Another possibility is that m^{6}A can form secondary structures in the RNAs that disrupt the binding of ribosomes, inhibiting translation under these conditions. To confirm this, techniques such as RNA stability and translation efficiency assays from cold-treated Arabidopsis need to be performed in the future.

4.4 FIP37 and its Role in Plant Growth and Development

In Arabidopsis, the complete loss of *FIP37* caused a sporophytic recessive, seed-lethal phenotype providing evidence for an essential function of FIP37 during endosperm development and embryogenesis (Vespa *et al.*, 2004). Knockdown lines of *FIP37* have also been shown to influence the overproliferation of shoot apical meristem (SAM) (Shen *et al.*, 2016). In rice, OsFIP is essential for male gametogenesis regulating the early degeneration of microspores (Zhang *et al.*, 2019). All these studies shed light on how FIP37 can influence different aspects of plant growth and development. In our study, plant growth measured by weight and leaf area was affected already under control conditions in *fip37-4*, but it became more drastic under cold as we showed additional impairments in chlorophyll content, chloroplast development and root lengths. In addition, the accumulation of CURT1 proteins responsible for thylakoid curvatures was downregulated specifically in *fip37-4* under cold. Interestingly, the nuclear-encoded CURT1 proteins are chloroplast-localized (Armbruster *et al.*, 2013) and the number of m^{6}A sites in *Curt1A*, *Curt1B*, *Curt1C* and *Curt1D* vary between WT and *fip37-4*, most of them being reduced in *fip37-4* under control conditions (Qin *et al.*, 2022). Therefore, as in photosynthetic transcripts, m^{6}A marks possibly have important functions in chloroplast development and thylakoid organization.

4.5 Outlook

Considering that photosynthesis, plant development and RNA methylation are very dynamic processes, especially under different environmental conditions, the molecular mechanisms of how m^6A methylation affects photosynthesis and chloroplast development need further investigation. Nonetheless, the characterization and the results presented here provide a fundamental source for the comprehension and determination of these regulatory mechanisms regarding m^6A marks in plant RNAs.

The current work expands the knowledge of the m^6A roles in Arabidopsis transcripts. So far, no studies have demonstrated that m^6A marks influence photosynthetic performance under plant acclimation. RNA modifications are regulated by the RNA modifiers (readers, writers and erasers). These factors usually form protein complexes and work in collaboration with each other depending on the environmental conditions. Therefore, it is not surprising that the control of many transcripts may be adjusted regarding the plant lines, plant age and external conditions. Although the present work demonstrates the influence of m^6A in photosynthesis and other chloroplast functions, the exact molecular mechanism of how m^6A regulates nuclear-encoded photosynthetic transcripts remains to be addressed. Nanopore sequencing using WT plants and *fip37-4* have been performed under control conditions (Qin *et al.*, 2022). Now, it would be interesting to identify specifically those transcripts which are methylated by FIP37 under cold acclimation through epitranscriptomic analysis. This would provide novel insights into the regulatory interplay between m^6A and plant development, photosynthesis and acclimation regarding specific transcripts carrying m^6A marks. Even though the exact mechanism is still not clear, this new characterization of *fip37-4* here presented will increase the interest and attention to the m^6A cellular epitranscriptome field. It is remarkable that already under control conditions many photosynthetic nucleus-encoded transcripts exhibited distinct levels of m^6A marks in *fip37-4* compared to the WT. Therefore, a more dramatic change in m^6A levels and/or its localization within the transcript may occur under cold acclimation. Under cold, the expression of representative genes of the photosynthetic apparatus does not vary or even increase when comparing WT and *fip37-4* lines. However, a drastic downregulation in protein levels were observed for instance for some specific candidates of PSI. These results

strongly indicate that this post-transcriptional mark possibly plays a role in RNA stability in photosynthetic transcripts. As sessile organisms, plants must develop different survival strategies to cope with nutrient, temperature and water limitations as well as excess of light. Here, FIP37 and other RNA modifiers are shown to be responsive to different acclimation conditions, suggesting important roles in these particular conditions. Recently, a CRISPR-based m^6A editing system was proposed, in which m^6A writers and erasers are fused to a dCas13 protein. This protein complex binds to RNA targets without mediating their cleavage and, as a consequence, the m^6A factors are no longer able to add or remove the m^6A marks at the target site in specific transcripts (Wilson *et al.*, 2020). Hence, editing m^6A modifications in key transcripts involved in plant development, photosynthesis and acclimation conditions through CRISPR technology may be an interesting method to improve crop productivity in the near future.

5. References

Al-Whaibi, M. H. (2011) 'Plant heat-shock proteins : A mini review', *Journal of King Saud University - Science*. 23, pp. 139–150. doi: 10.1016/j.jksus.2010.06.022.

Anderson, S.; Kramer, M.; Gosai, S.; Yu, X.; Vandivier, L.; Nelson, A.; Anderson, Z.; Beilstein, M.; Fray, R.; Lyons, E.; Gregory, B. (2018) 'N6-Methyladenosine Inhibits Local Ribonucleolytic Cleavage to Stabilize mRNAs in Arabidopsis', *Cell Reports*. 25, pp. 1146-1157.e3. doi: 10.1016/j.celrep.2018.10.020.

Armbruster, U.; Labs, M.; Pribil, M.; Viola, S.; Xu, W.; Scharfenberg, M.; Hertle, A.; Rojahn, U.; Jensen, P.; Rappaport, F.; Joliot, P.; Dörmann, P.; Wanner, G.; Leister, D. (2013) 'Arabidopsis CURVATURE THYLAKOID1 Proteins Modify Thylakoid Architecture by Inducing Membrane Curvature', *The Plant Cell*. 25, pp. 2661–2678. doi: 10.1105/tpc.113.113118.

Arribas-Hernández, L.; Bressendorff, S.; Hansen, M.; Poulsen, C.; Erdmann, S.; Brodersen, P. (2018) 'An m^{6}A-YTH Module Controls Developmental Timing and Morphogenesis in Arabidopsis', *The Plant Cell.* 30, pp. 952–967. doi: 10.1105/tpc.17.00833.

Balacco, D. L. and Soller, M. (2019) 'The m^{6}A Writer: Rise of a Machine for Growing Tasks', *Biochemistry*. 58, pp. 363−378 doi: 10.1021/acs.biochem.8b01166.

Barkan, A. and Goldschmidt-Clermont, M. (2000) 'Participation of nuclear genes in chloroplast gene expression', *Biochimie* 82 pp. 559−572. doi:10.1016/S0300-9084(00)00602-7.

Boccaletto, P.; Machnicka, M.; Purta, E.; Piatkowski, P.; Baginski, B.; Wirecki, T.; Lagard, V.; Ross, R.; Limbach, P.; Kotter, A.; Helm, M.; Bujnicki, J. (2018) 'Modomics: a database of RNA modification pathways', *Nucleic Acids Research*. 46, pp. 303–307. doi: 10.1093/nar/gkx1030.

Bodi, Z.; Zhong, S.; Mehra, S.; Song, J.; Graham, N.; Li, H.; May, S.; Fray, R. (2012) 'Adenosine methylation in Arabidopsis mRNA is associated with the 3 end and reduced levels cause developmental defects', *Frontiers in Plant Science*. 3, pp. 1–10. doi:

10.3389/fpls.2012.00048.

Börner, T.; Aleynikova, A.; Zubo, Y.; Kusnetsov, V. (2015) 'Chloroplast RNA polymerases : Role in chloroplast biogenesis', *BBA - Bioenergetics*. 1847, pp. 761–769. doi: 10.1016/j.bbabio.2015.02.004.

Buul, C and Knippenberg, P. (1985) 'Nucleotide sequence of the ksgA gene of Escherichia coli : comparison of methyitransferases effecting dimetylation of adenosine in ribosomal RNA', *Gene*. 38, pp. 65–72. doi: 10.1016/0378-1119(85)90204-5.

Choe, J.; Lin, S.; Zhang, W.; Liu, Q.; Wang, L.; Moya, J.; Du, P.; Kim, W.; Tang, S.; Sliz, P.; Santisteban, P.; George, R.; Gregory, R. (2018) 'mRNA circularization by METTL3–eIF3h enhances translation and promotes oncogenesis', *Nature*. 561, pp. 556-580. doi: 10.1038/s41586-018-0538-8.

Crosatti, C.; Rizza, F.; Badeck, F.; Mazzucotelli, E.; Cattivelli, L. (2013) 'Harden the chloroplast to protect the plant', *Physiologia Plantarum*. 50, pp. 55–63. doi: 10.1111/j.1399-3054.2012.01689.x.

Dobrogojsk, J.; Adamiec, M.; Luciński, R (2020) 'The chloroplast genome : a review National Center for Biotechnology Information', *Acta Physiologiae Plantarum*. Springer Berlin Heidelberg, 42, pp. 1–13. doi: 10.1007/s11738-020-03089-x.

Duan, H.; Wei, L.; Zhang, C.; Wang, Y.; Chen, L.; Lu, Z.; Chen, P.; He, C.; Jia, G. (2017) 'ALKBH10B is an RNA N6-methyladenosine demethylase affecting arabidopsis floral transition', *Plant Cell*, 29, pp. 2995–3011. doi: 10.1105/tpc.16.00912.

Espinoza-Corral, R.; Heinz, S.; Klingl, A.; Jahns, P.; Lehmann, M.; Meurer, J.; Nickelsen, J.; Soll, J.; Schwenkert, S. (2019) 'Plastoglobular protein 18 is involved in chloroplast function and thylakoid formation', Journal of Experimental Botany. 70, pp. 3981–3993. doi: 10.1093/jxb/erz177.

Faure, J.; Gingerich, D. and Howell, S. H. (1998) 'An Arabidopsis immunophilin, AtFKBP12, binds to AtFIP37 (FKBP interacting protein) in an interaction that is disrupted by FK506', *The Plant Journal*. 15, pp. 783–789. doi: 10.1046/j.1365-313x.1998.00248.x.

Feldmann, K. A. and David Marks, M. (1987) 'Agrobacterium-mediated transformation of

germinating seeds of *Arabidopsis thaliana*: A non-tissue culture approach', *MGG Molecular & General Genetics*. 208, pp. 1–9. doi: 10.1007/BF00330414.

Feng, P.; Guo, H.; Chi, W.; Chai, C.; Sun, X.; Xu, X.; Ma, J.; Rochaix, J.; Leister, D.; Wang, H.; Lu, C.; Zhang, L. (2016) 'Chloroplast retrograde signal regulates flowering', *Proceedings of the National Academy of Sciences of the United States of America*. 113, pp. 10708–10713. doi: 10.1073/pnas.1521599113.

Frye, M.; Harada, B.; Behm, M.; He, C. (2018) 'RNA modifications modulate gene expression during development', *Science*. 361, pp. 1346-1349. doi: 10.1126/science.aau1646.

Fryer, M.; Oxborough, K.; Mullineaux, P.; Baker, N. (2002) 'Imaging of photo-oxidative stress responses in leaves', *Journal of Experimental Botany*. 53, pp. 1249–1254. PMID: 11997373.

Garalde, D.; Snell, E.; Jachimowicz, D.; Sipos, B.; Lloyd, J.; Bruce, M.; Pantic, N.; Admassu, T.; James, P.; Warland, A.; Jordan, M.; Ciccone, J.; Serra, S.; Keenan, J.; Martin, S.; McNeill, L.; Wallace, J.; Jayasinghe, L.; Wright, C.; Turner, D. (2018) 'Highly parallel direct RNA sequencing on an array of nanopores', *Nature Methods*. 15, pp. 201–206. doi: 10.1038/nmeth.4577.

Garcia-Campos, M.; Edelheit, S.; Toth, U.; Safra, M.; Shachar, R.; Viukov, S.; Winkler, R.; Nir, R.; Lasman, L.; Brandis, A.; Hanna, J.; Rossmanith, W.; Schwartz, S. (2019) 'Deciphering the "m^{6}A Code" via Antibody-Independent Quantitative Profiling', *Cell*. Elsevier Inc., 178, pp. 731-747.e16. doi: 10.1016/j.cell.2019.06.013.

Garcia-Molina, A.; Kleine, T.; Schneider, K.; Mühlhaus, T.; Lehmann, M.; Leister, D. (2020) 'Translational Components Contribute to Acclimation Responses to High Light, Heat, and Cold in Arabidopsis to Acclimation Responses'. *iScience*. 23, 10133. doi: 10.1016/j.isci.2020.101331.

Geula, S.; Moshkovitz, S.; Dominissini, D.; Novershtern, N.; Rechavi, G.; Hanna, J. (2015) 'm^{6}A mRNA methylation facilitates resolution of naïve pluripotency toward differentiation', *Science*. 347, pp. 1002-1006. doi: 10.1126/science.1261417.

Grozhik, A.; Linder, B.; George, A.; Jaffrey, S. (2017) 'Mapping m^{6}A at individual-

nucleotide resolution using crosslinking and immunoprecipitation (miCLIP)', *Methods Mol Biol.* 1562, pp. 55–78. doi: 10.1007/978-1-4939-6807-7.

He, Y.; Li, Y.; Yao, Y.; Zhang, H.; Wang, Y.; Gao, J.; Fan, M. (2021) 'Plant Physiology and Biochemistry Overexpression of watermelon m6A methyltransferase ClMTB enhances drought tolerance in tobacco by mitigating oxidative stress and photosynthesis inhibition and modulating stress-responsive gene expression', *Plant Physiology and Biochemistry.* 168, pp. 340–352. doi: 10.1016/j.plaphy.2021.10.007.

Hornyik, C.; Terzi, L. C. and Simpson, G. G. (2010) 'Article The Spen Family Protein FPA Controls Alternative Cleavage and Polyadenylation of RNA', *Developmental Cell.* 18, pp. 203–213. doi: 10.1016/j.devcel.2009.12.009.

Hou, N.; Li, C.; He, J.; Liu, Y.; Yu, S.; Malnoy, M.; Tahir, M.; Xu, L.; Ma, F.; Guan, Q. (2022) 'MdMTA-mediated m^{6}A modification enhances drought tolerance by promoting mRNA stability and translation efficiency of genes involved in lignin deposition and oxidative stress', *New Phytologist.* 234, pp. 1294–1314. doi: 10.1111/nph.18069.

Hu, J.; Cai, J.; Park, S.; Lee, K.; Li, Y.; Chen, Y.; Yun, J.; Xu, T.; Kang, H. (2021) 'N6-Methyladenosine mRNA methylation is important for salt stress tolerance in Arabidopsis', *The Plant Journal.* 106, pp. 1759-1775. doi: 10.1111/tpj.15270.

Huang, J.; Dong, X.; Gong, Z.; Qin, L.; Yang, S.; Zhu, Y.; Wang, X.; Zhang, D.; Zou, T.; Yin, P.; Tang, C. (2019) 'Solution structure of the RNA recognition domain of METTL3-METTL14 N 6 -methyladenosine methyltransferase', *Protein & Cell.* 10, pp. 272–284. doi: 10.1007/s13238-018-0518-7.

Huong, T.; Ngoc, L.; Kang, H. (2020) 'Functional Characterization of a Putative RNA Demethylase ALKBH6 in Arabidopsis Growth and Abiotic Stress Responses', *International Journal of Molecular Science.* 21, pp. 1–14. doi: 10.3390/ijms21186707.

Hüner, N.; Bode, R.; Dahal, K.; Hollis, L.; Rosso, D.; Krol, M.; Ivanov, A. (2006) 'Photostasis and cold acclimation : sensing low temperature through photosynthesis', *Physiologia Plantarum.* 126, pp. 28–44. doi: 10.1111/j.1399-3054.2005.00627.x.

Johnson, M. P. (2016) 'Photosynthesis: An overview of photosynthesis', *Essays in Biochemistry.* 60, pp. 255–273. doi: 10.1042/EBC20160016.

Kleine, T.; Nägele, T.; Neuhaus, E.; Linneweber, C.; Fernie, A.; Geigenberger, P.; Grimm, B.; Kaufmann, K.; Klipp, E.; Meurer, J.; Möhlmann, T.; Mühlhaus, T.; Naranjo, B.; Nickelsen, J.; Richter, A.; Ruwe, H.; Schroda, M.; Schwenkert, S.; Trentmann, O.; Willmund, F.; Zoschke, R.; Leister, D. (2021) 'Acclimation in plants – the Green Hub consortium', The Plant Journal. 106, pp. 23–40. doi: 10.1111/tpj.15144.

Krämer, U. (2015) 'Planting molecular functions in an ecological context with *Arabidopsis thaliana*', *Elife*. 4, pp. 1–13. doi: 10.7554/eLife.06100.

Kreps, J.; Wu, Y.; Chang, H.; Zhu, T.; Wang, X.; Harper, J. (2002) 'Transcriptome Changes for Arabidopsis in Response to Salt, Osmotic, and Cold Stress', *Plant Physiology*. 130, pp. 2129–2141. doi: 10.1104/pp.008532.

Ku, C.; Sathi, S.; Roettger, M.; Garg, S.; Covo, E.; Martin, W. (2015) 'Endosymbiotic gene transfer from prokaryotic pangenomes : Inherited chimerism in eukaryotes', *PNAS*. 112, pp. 10139–10146. doi: 10.1073/pnas.1421385112.

Lamers, J.; Der Meer, T. Van and Testerink, C. (2020) 'How plants sense and respond to stressful environments', *Plant Physiology*. 182, pp. 1624–1635. doi: 10.1104/PP.19.01464.

Leister, D. and Schneider, A. (2003) 'From Genes to Photosynthesis in *Arabidopsis thaliana*', *International Review of Cytology*. 228, pp. 31–83. doi: 10.1016/s0074-7696(03)28002-5.

Lence, T.; Paolantoni, C.; Worpenberg, L.; Roignant, Y. (2019) 'Mechanistic insights into m^6A RNA enzymes', *Biochimica et Biophysica Acta - Gene Regulatory Mechanisms*. Elsevier, 1862(3), pp. 222–229. doi: 10.1016/j.bbagrm.2018.10.014.

Lesnyak, D.; Osipiuk, J.; Skarina, T.; Sergiev, P.; Bogdanov, A.; Edwards, A.; Savchenko, A.; Joachimiak, A.; Dontsova, O. (2007) 'Methyltransferase That Modifies Guanine 966 of the 16 S rRNA Functional Identification and Tertiary Structure*', *Journal of Biological Chemistry*. 282, pp. 5880–5887. doi: 10.1074/jbc.M608214200.

Li, M. and Kim, C. (2022) 'Chloroplast ROS and stress signaling', *Plant Communications*. 3, p. 100264. doi: 10.1016/j.xplc.2021.100264.

Linder, B.; Grozhik, A.; George, A.; Meydan, C.; Mason, C.; Jaffrey, S. (2015) 'Single-

nucleotide-resolution mapping of m^{6}A and m^{6}Am throughout the transcriptome'. *Nature Methods*, 12, pp. 767–772. doi: 10.1038/nmeth.3453.

Liu, H.; Begik, O.; Lucas, M.; Ramirez, J.; Mason, C.; Wiener, D.; Schwartz, S.; Mattick, J.; Smith, M.; Novoa, E. (2019) 'Accurate detection of m^{6}A RNA modifications in native RNA sequences', *Nature Communications*. 10, pp. 1–9. doi: 10.1038/s41467-019-11713-9.

Liu, J.; Yue, Y.; Han, D.; Wang, X.; Fu, Y.; Zhang, L.; Jia, G.; Yu, M.; Lu, Z.; Deng, X.; Dai, Q.; Chen, W.; He, C. (2014) 'A METTL3 – METTL14 complex mediates mammalian nuclear RNA N6-adenosine methylation'. 10, pp. 2013–2015. doi: 10.1038/nchembio.1432.

Liu, N.; Dai, Q.; Zheng, G.; He, C.; Parisien, M.; Pan, T. (2015) 'N6-methyladenosine-dependent RNA structural switches regulate RNA-protein interactions', *Nature*. 518, pp. 560–564. doi: 10.1038/nature14234.

Liu, N. and Pan, T. (2016) 'N6-methyladenosine - encoded epitranscriptomics', *Nature structural & Molecular biology*. 23, pp. 98-102 doi: 10.1038/nsmb.3162.

Liu, Y.; Dang, P.; Liu, L.; He, C. (2019) 'Cold acclimation by the CBF – COR pathway in a changing climate : Lessons from *Arabidopsis thaliana*', *Plant Cell Reports*. 38, pp. 511–519. doi: 10.1007/s00299-019-02376-3.

Luo, G.; MacQueen, A.; Zheng, G.; Duan, H.; Dore, L.; Lu, Z.; Liu, J.; Chen, K.; Jia, G.; Bergelson, J.; He, C. (2014) 'Unique features of the m^{6}A methylome in *Arabidopsis thaliana*', *Nature Communications*. 5, pp. 1–8. doi: 10.1038/ncomms6630.

Manavski, N.; Torabi, S.; Lezhneva, L.; Arif, M.; Frank, W.; Meurer, J. (2015) 'HIGH CHLOROPHYLL FLUORESCENCE145 Binds to and Stabilizes the psaA 5`UTR via a Newly Defined Repeat Motif in Embryophyta', *Plant Cell*. 27, pp. 2600–2615. doi: 10.1105/tpc.15.00234.

Manavski, N.; Vicente, A.; Chi, W.; Meurer, J. (2021) 'The Chloroplast Epitranscriptome: Factors, Sites, Regulation, and Detection Methods', *Genes (Basel)*. 12,1121, pp. 1-22. doi: 10.3390/genes12081121.

Margulis, L. (1993) 'Origins of species : acquired genomes and individuality', *BloSystems*. 31, pp. 121–125. doi: 10.1016/0303-2647(93)90039-f.

McIntyre, A.; Gokhale, N.; Cerchietti, L.; Jaffrey, S.; Horner, S.; Mason, C. (2020) 'Limits in the detection of m^{6}A changes using MeRIP/m^{6}A-seq', *Scientific Reports*. 10, pp. 1–15. doi: 10.1038/s41598-020-63355-3.

Melo, Y.; Kılıç, M.; Aro, E.; Gollan, P. (2021) 'Photosystem I Inhibition , Protection and Signalling : Knowns and Unknowns'. 12 , pp. 1–11. doi: 10.3389/fpls.2021.791124.

Meyer, K.; Saletore, Y.; Zumbo, P.; Elemento, O.; Mason, C.; Jaffrey, S. (2012) 'Comprehensive analysis of mRNA methylation reveals enrichment in 3′ UTRs and near stop codons', *Cell*. 149, pp. 1635–1646. doi: 10.1016/j.cell.2012.05.003.

Meyer, K.; Patil, D.; Zhou, J.; Zinoviev, A.; Skabkin, M.; Elemento, O.; Pestova, T.; Qian, S.; Jaffrey, S. (2015) '5`UTR m^{6}A Promotes Cap-Independent Translation', *Cell*. 163, pp. 999–1010. doi: 10.1016/j.cell.2015.10.012.

Meyer, K. D. (2019) 'DART-seq: an antibody-free method for global m^{6}A detection', *Nature Methods*. 16, pp. 1275–1280. doi: 10.1038/s41592-019-0570-0.

Mielecki, D.; Zugaj, D.; Muszewska, A.; Piwowarski, J.; Chojnacka, A.; Mielecki, M.; Nieminuszczy, J.; Grynberg, M.; Grzesiuk, E (2012) 'Novel AlkB Dioxygenases - Alternative Models for In Silico and In Vivo Studies', *Plos One*. 7:e30588, pp. 1-11. doi: 10.1371/journal.pone.0030588.

Mitchell-Olds, T. and Schmitt, J. (2006) 'Genetic mechanisms and evolutionary significance of natural variation in Arabidopsis', *Nature*. 441, pp. 947–952. doi: 10.1038/nature04878.

Morales, D. and Reyes, J. (2021) 'A birds'-eye view of the activity and specificity of the mRNA m^{6}A methyltransferase complex', *WIRES*. 12:e1618, pp. 1–15. doi: 10.1002/wrna.1618.

Mower, J. P. and Vickrey, T. L. (2018) 'Structural Diversity Among Plastid Genomes of Land Plants', *Plastid Genome Evolution*. 85, pp. 263-292. doi: 10.1016/bs.abr.2017.11.013.

Neff, M. M. and Chory, J. (1998) 'Genetic interactions between phytochrome A,

phytochrome B, and cryptochrome 1 during Arabidopsis development', Plant Physiology. 118, pp. 27–36. doi: 10.1104/pp.118.1.27.

Ngoc, L.; Park, S.; Cai, J.; Huong, T.; Lee, K.; Kang, H. (2021) 'RsmD , a Chloroplast rRNA m2G Methyltransferase, Plays a Role in Cold Stress Tolerance by Possibly Affecting Chloroplast Translation in Arabidopsis', Plant Cell Physiology. 62, pp. 948–958. doi: 10.1093/pcp/pcab060.

Nichols, J. L. (1979) 'N6-methyladenosine in maize poly(a)-containing rna', *Plant Science Letters*. 15, pp. 357–361.

Nichols, J. L. and Welder, L. (1981) 'Nucleotides adjacent to N6-methyladenosine in maize poly(a)-containing RNA', *Plant Science Letters*. 21, pp. 75–81. doi.org/10.1016/0304-4211(81)90071-7.

Niyogi, K. K. (1999) 'Photoprotection Revisited: Genetic and Molecular Approaches', *Annual Reviews in Plant Physiology*. 50, pp. 333-359. doi: 10.1146/annurev.arplant.50.1.333.

Parker, M.; Knop, K.; Sherwood, A.; Schurch, N.; Mackinnon, K.; Gould, P.; Hall, A.; Barton, G.; Simpson, G. (2020) 'Nanopore direct RNA sequencing maps the complexity of arabidopsis mRNA processing and m^{6}A modification', *eLife*. 9, pp. 1–35. doi: 10.7554/eLife.49658.

Pérez, M.; Aparicio, F.; Gresa, M.; Bellés, J.; Navarro, J.; Pallás, V. (2017) 'Arabidopsis m^{6}A demethylase activity modulates viral infection of a plant virus and the m^{6}A abundance in its genomic RNAs', *PNAS*. 114, pp. 10755–10760. doi: 10.1073/pnas.1703139114.

Porra, R.; Thompson, W.; Kriedemann, P (1989) 'Determination of accurate extinction coefficients and simultaneous equations for assaying chlorophylls a and b extracted with four different solvents : verification of the concentration of chlorophyll standards by atomic absorption spectroscopy', *BBA - Bioenergetics*. 975, pp. 384–394. doi.org/10.1016/S0005-2728(89)80347-0.

Qin, H.; Ou, L.; Gao, J.; Chen, L.; Wang, J.; Hao, P.; Li, X. (2022) 'DENA : training an authentic neural network model using Nanopore sequencing data of Arabidopsis transcripts for detection and quantification of N6-methyladenosine on RNA', *Genome Biology*.

23(1):25, pp. 1–23. doi:10.1186/s13059-021-02598-3

Renner, S. and Zohner, C. (2019) 'The occurrence of red and yellow autumn leaves explained by regional differences in insolation and temperature', *New Phytologist*. 224, pp.1464-1471 doi: 10.1111/nph.15900.

Růžička, K.; Zhang, Mi.; Campilho, A.; Bodi, Z.; Kashif, M.; Saleh, M.; Eeckhout, D.; Showk, S.; Li, H.; Zhong, S.; Jaeger, G.; Mongan, N.; Hejátko, J.; Helariutta, Y.; Fray, R. (2017) 'Identification of factors required for m^{6}A mRNA methylation in Arabidopsis reveals a role for the conserved E3 ubiquitin ligase HAKAI', *New Phytologist*, 215, pp. 157–172. doi: 10.1111/nph.14586.

Schägger, H.; Aquila, H.; Jagow, G. (1988) 'Coomassie Blue-Sodium Dodecyl Sulfate-Polyacrylamide Electrophoresis for Direct Visualization of Polypeptides during Electrophoresis', *Analytical Biochemistry*. 205, pp. 3–7. doi: 10.1016/0003-2697(88)90179-0.

Schindelin, J.; Carreras, I.; Preibisch, S.; Rueden, C.; Saalfeld, S.; Hartenstein, V.; Eliceiri, K.; Tomancak, P.; Cardona, A. (2012) 'Fiji : an open-source platform for biological-image analysis', *Nature Methods*. 9, pp. 676-682. doi: 10.1038/nmeth.2019.

Schwartz, S.; Mumbach, M.; Jovanovic, M.; Wang, T.; Maciag, K.; Bushkin, G.; Mertins, P.; Ovanesyan, D.; Lander, E.; Regev, A. (2014) 'Perturbation of m^{6}A Writers Reveals Two Distinct Classes of mRNA Methylation at Internal and 5` Sites', *CellReports*. 8, pp. 284–296. doi: 10.1016/j.celrep.2014.05.048.

Schwenkert, S.; Fernie, A.; Geigenberger, P.; Leister, D.; Möhlmann, T.; Naranjo, B.; Neuhaus, E. (2021) 'Plant Science Chloroplasts are key players to cope with light and temperature stress', *Trends in Plant Science*. 27, pp. 577-587. doi: 10.1016/j.tplants.2021.12.004.

Scutenaire, J.; Deragon, J.; Jean, V.; Benhamed, M.; Raynaud, C.; Favory, J.; Merret, R.; Antonelli, C. (2018) 'The YTH domain protein ECT2 is an m^{6}A reader required for normal trichome branching in arabidopsis', *Plant Cell*. 30, pp. 986–1005. doi: 10.1105/tpc.17.00854.

Shao, Y.; Wong, C.; Shen, L.; Yu, H. (2021) 'ScienceDirect Plant Biology N6-

methyladenosine modification underlies messenger RNA metabolism and plant development', *Current Opinion in Plant Biology*. 63, p. 102047. doi: 10.1016/j.pbi.2021.102047.

Shen, L.; Liang, Z.; Gu, X.; Chen, Y.; Teo, Z.; Hou, X.; Cai, W.; Dedon, P.; Liu, L.; Yu, H. (2016) 'Article N6-Methyladenosine RNA Modification Regulates Shoot Stem Cell Fate in Arabidopsis Article N6-Methyladenosine RNA Modification Regulates Shoot Stem Cell Fate in Arabidopsis', *Developmental Cell*. 38, pp. 186–200. doi: 10.1016/j.devcel.2016.06.008.

Somerville, C. and Koornneef, M. (2002) 'A fortunate choice: the history of Arabidopsis as a model plant', *Nature Reviews*. 3, pp. 883-9. doi: 10.1038/nrg927.

Tang, Y.; Chen, K.; Song, B.; Ma, J.; Wu, X.; Xu, Q.; Wei, Z.; Su, J.; Liu, G.; Rong; R.; Lu, Z.; Magalhães, J.; Rigden, D.; Meng, J. (2021) 'm6A-Atlas: a comprehensive knowledgebase for unraveling the N6-methyladenosine (m6A) epitranscriptome', *Nucleic acids research*, 49, pp. 134–143. doi: 10.1093/nar/gkaa692.

The Arabidopsis Genome Initiative (2000) 'Analysis of the genome sequence of the flowering plant *Arabidopsis thaliana*', *Nature*. 61, pp. 796–815. doi: 10.1134/S1022795411020074.

Theocharis, A.; Clément, C.; Barka, E. (2012) 'Physiological and molecular changes in plants grown at low temperatures', *Planta*. 235, pp. 1091–1105. doi:10.1007/s00425-012-1641-y.

Tiwari, B.; Habermann, K.; Arif, M.; Weil, H.; Molina, A.; Kleine, T.; Mühlhaus, T.; Frank, W. (2020) 'Identification of small RNAs during cold acclimation in *Arabidopsis thaliana*', *BMC Plant Biology*, 20(1):298, pp. 1–25. doi:10.1186/s12870-020-02511-3.

Tokuhisa, J.; Vijayan, P.; Feldmann, K.; Browse, J. (1998) 'Chloroplast development at low temperatures requires a homolog of DIM1, a yeast gene encoding the 18S rRNA dimethylase', *Plant Cell*, 10, pp. 699–711. doi: 10.1105/tpc.10.5.699.

Tzafrir, I.; Muralla, R.; Dickerman, A.; Berg, M.; Rogers, R.; Hutchens, S.; Sweeney, T.; McElver, J.; Aux, G.; Patton, D.; Meinke, D. (2004) 'Identification of Genes Required for Embryo Development in Arabidopsis', Plant Physiology. 135, pp. 1206–1220. doi:

10.1104/pp.104.045179.published.

Vespa, L.; Vachon, G.; Berger, F.; Perazza, D.; Faure, J.; Herzog, M. (2004) 'The Immunophilin-Interacting Protein AtFIP37 from Arabidopsis Is Essential for Plant Development and Is Involved in Trichome Endoreduplication', 134, pp. 1283–1292. doi: 10.1104/pp.103.028050.lian.

Wan, Y.; Tang, K.; Zhang, D.; Xie, S.; Zhu, X.; Wang, Z.; Lang, Z. (2015) 'Transcriptome-wide high-throughput deep m^{6}A-seq reveals unique differential m^{6}A methylation patterns between three organs in *Arabidopsis thaliana*'. *Genome Biology*. 272, pp. 1–26. doi: 10.1186/s13059-015-0839-2.

Wang, Z.; Tang, K.; Zhang, D.; Wan, Y.; Wen, Y.; Lu, Q.; Wang, L. (2017) 'High-throughput m^{6}A-seq reveals RNA m^{6}A methylation patterns in the chloroplast and mitochondria transcriptomes of *Arabidopsis thaliana*', *PLoS ONE*. 12, pp. 1–24. doi: 10.1371/journal.pone.0185612.

Watson, S. J.; Sowden, R. G. and Jarvis, P. (2018) 'Abiotic stress-induced chloroplast proteome remodelling : a mechanistic overview', *Journal of Experimental Botany*. 69, pp. 2773–2781. doi: 10.1093/jxb/ery053.

Wei, L.; Song, P.; Wang, Y.; Lu, Z.; Tang, Q.; Yu, Q.; Xiao, Y.; Zhang, X.; Duan, H.; Jia, G. (2018) 'The m^{6}A reader ECT2 controls trichome morphology by affecting mRNA stability in arabidopsis', *Plant Cell*. 30, pp. 968–985. doi: 10.1105/tpc.17.00934.

Wilson, C.; Chen, P.; Miao, Z.; Liu, D. (2020) 'Programmable m^{6}A modification of cellular RNAs with a Cas13-directed methyltransferase', *Nature Biotechnology*. 38, pp. 1431-1440. doi: 10.1038/s41587-020-0572-6.

Winkel-Shirley, B. (2002) 'Biosynthesis of flavonoids and effects of stress', *Current Opinion in Plant Biology*. 5, pp. 218–223. doi: 10.1016/s1369-5266(02)00256-x.

Winkel-Shirley, B. (2001) 'Flavonoid Biosynthesis. A Colorful Model for Genetics, Biochemistry, Cell Biology, and Biotechnology', *Plant Physiology*. 126, pp. 485–493. doi: 10.1104/pp.126.2.485.

Wohlgemuth, H.; Mittelstrass, K.; Kschieschan, S.; Bender, J.; Weigel, H.-J.; Overmeyer,

K.; Kangasjäarvi, J.; Sandermann, H.; Langebartels, C. (2002) 'Activation of an oxidative burst is a general feature of sensitive plants exposed to the air pollutant ozone', *Plant, Cell and Environment*. 25, pp. 717–726.doi: 10.1046/j.1365-3040.2002.00859.x

Woodson, J. D. and Chory, J. (2008) 'Coordination of gene expression between organellar and nuclear genomes', Nature Reviews. 9, pp. 383-95. doi: 10.1038/nrg2348.

Yamamoto, H Shikanai, T. (2019) 'PGR5-Dependent Cyclic Electron Flow Protects Photosystem I under Fluctuating Light at Donor and Acceptor Sides', *Plant Physiology*. 179, pp. 588-600. doi: 10.1104/pp.18.01343.

Yang, D.; Xu, H.; Liu, Y.; Li, M.; Ali, M.; Xu, X.; Lu, G. (2021) 'RNA N6-Methyladenosine Responds to Low-Temperature Stress in Tomato Anthers', *Frontiers in Plant Science*. 12, pp. 1–17. doi: 10.3389/fpls.2021.687826.

Yang, Y. and Guo, Y. (2018) 'Unraveling salt stress signaling in plants', *Journal of Integrative Plant Biology*. 60, pp. 796–804. doi: 10.1111/jipb.12689.

Yu, J.; Chen, M.; Huang, H.; Zhu, J.; Song, H.; Zhu, J.; Park, J.; Ji, S. (2018) 'Dynamic m^6A modification regulates local translation of mRNA in axons'. Nucleic Acids Research. 46, pp. 1412–1423. doi: 10.1093/nar/gkx1182.

Yue, H.; Nie, X.; Yan, Z.; Weining, S. (2019) 'N6-methyladenosine regulatory machinery in plants: composition, function and evolution', *Plant Biotechnology Journal*. 17, pp. 1194–1208. doi: 10.1111/pbi.13149.

Zhang, F.; Zhang, Y.; Liao, J.; Yu, Y.; Zhou, Y.; Feng, Y.; Yang, Y.; Lei, M.; Bai, M.; Wu, H.; Chen, Y. (2019) 'The subunit of RNA N6-methyladenosine methyltransferase OsFIP regulates early degeneration of microspores in rice', *PLoS Genetics*. 15, pp. 1–19. doi: 10.1371/journal.pgen.1008120.

Zhang, Z.; Theler, D.; Kaminska, K.; Hiller, M.; Grange, P.; Pudimat, R.; Rafalska, I.; Heinrich, B.; Bujnicki, J.; Allain, F.; Stamm, S. (2010) 'The YTH domain is a novel RNA binding domain', *The Journal of Biological Chemistry*. 285, pp. 14701–14710. doi: 10.1074/jbc.M110.104711.

Zhao, C.; Lang, Z. and Zhu, J. (2015) 'Cold responsive gene transcription becomes more

complex', *Trends in Plant Science*. 20, pp. 466–468. doi: 10.1016/j.tplants.2015.06.001.

Zhong, S.; Li, H.; Bodi, Z.; Button, J.; Vespa, L.; Herzog, M.; Fray, R.. (2008) 'MTA is an Arabidopsis messenger RNA adenosine methylase and interacts with a homolog of a sex-specific splicing factor', *Plant Cell*, 20, pp. 1278–1288. doi: 10.1105/tpc.108.058883.

Zhu, J. K. (2016) 'Abiotic Stress Signaling and Responses in Plants', *Cell*. Elsevier, 167, pp. 313–324. doi: 10.1016/j.cell.2016.08.029.

Zou, M.; Mu, Y.; Chai, X.; Ouyang, M.; Yu, L-J.; Zhang, L.; Meurer, J.; Chi, W. (2020) 'The critical function of the plastid rRNA methyltransferase, CMAL, in ribosome biogenesis and plant development', *Nucleic Acids Research*. 48, pp. 3195–3210. doi: 10.1093/nar/gkaa129.

I Appendix Tables

Table 2: Summary of chloroplast- and nucleus-encoded genes found in m⁶A epitrancriptomes of different accessions of *Arabidopsis*. The information of this table was extracted from data of three published epitranscriptomes and the 'm⁶A-Atlas' tool was used to predict updated numbers of methylation sites (www.xjtlu.edu.cn/biologicalsciences/atlas) (Tang *et al.*, 2021). Extracted from (Manavski *et al.*, 2021).

GENE(S)	NAME(S)	GENE ONTOLOGY	ACCESSION(S)	M⁶A-ATLAS	REFERENCE(S)
AT1G24490	ALB4	chloroplast organization	Con-0	1	
AT5G45390	CLPP4	chloroplast organization	Con-0	4	
AT3G19720	ARC5	chloroplast organization	Con-0	3	
AT5G35220	EGY1	chloroplast organization	Con-0	0	
AT3G48870	HSP93-III	chloroplast organization	Con-0	2	
AT2G48120	PAC	chloroplast organization	Con-0	0	
AT1G24490	ALB4	Plastid organization	Hen-16	1	
AT5G10490	MSL2	Plastid organization	Hen-16	0	
AT3G17040	HCF107	Plastid organization	Hen-16	4	
AT1G63900	DAL1	Plastid organization	Hen-16	5	
AT5G02250	EMB2730	Plastid organization	Hen-16	3	
AT2G06520	PSBX	photosynthesis	Con-0	0	
AT3G16140	PSAH-1	photosynthesis	Con-0	0	(Luo *et al.*, 2014)
AT1G70760	CRR23	photosynthesis	Con-0	1	
AT4G28660	PSB28	photosynthesis	Con-0	0	
AT1G06680	PSBP-1	photosynthesis	Con-0	1	
AT1G74470	CHLP	photosynthesis	Con-0	0	
AT5G35220	EGY1	photosynthesis	Con-0	0	
AT3G61470	LHCA2	photosynthesis	Con-0	1	
AT5G66570	PSBO1	photosynthesis	Con-0	7	
AT4G28750	PSAE-1	photosynthesis	Con-0	5	
AT5G16440	IPP1	photosynthesis	Con-0	6	
AT3G16250	NDF4	photosynthesis	Con-0	9	
AT2G05100	LHCB2.1	photosynthesis	Con-0	1	
AT1G32060	PRK	photosynthesis	Con-0	4	
AT1G55670	PSAG	photosynthesis	Col-0	0	
AT2G05100	LHCB2	photosynthesis	Col-0	1	
AT3G08940	LHCB4	photosynthesis	Col-0	4	
AT3G21055	PSBTN	photosynthesis	Col-0	0	
AT1G67740	PSBY	photosynthesis	Col-0	5	(Wan *et al.*, 2015b)
AT1G03130	PSAD-2	photosynthesis	Col-0	12	
AT2G34420	LHB1B2	photosynthesis	Col-0	1	
AT1G15820	LHCB6	photosynthesis	Col-0	0	
AT4G10340	LHCB5	photosynthesis	Col-0	5	

AT1G61520	LHCA3	photosynthesis	Col-0	3	
AT2G06520	PSBX	photosynthesis	Col-0	0	
AT3G27690	DEG13	photosynthesis	Col-0	0	
AT3G15190	PRPS20	photosynthesis	Col-0	0	
ATCG01160	RRN5S	Chloroplast rRNA	Col-0	0	
ATCG00970	RRN5S	Chloroplast rRNA	Col-0	0	
ATCG01210	RRN16S	Chloroplast rRNA	Col-0	0	
ATCG01180	RRN23S	Chloroplast rRNA	Col-0	0	
ATCG00950	RNA23S	Chloroplast rRNA	Col-0	5	
ATCG00920	RRN16S	Chloroplast rRNA	Col-0	0	
ATCG00640	RPL33	ribosomal proteins	Col-0	0	
ATCG00650	RPS18	ribosomal proteins	Col-0	0	
ATCG00400	tRNA-Leu	tRNA	Col-0	2	
ATCG00550	PSBJ	photosystem reaction proteins	Col-0	0	(Wang *et al.*, 2017)
ATCG00510	PSAI	photosystem reaction proteins	Col-0	0	
ATCG00140	ATPH	ATP synthase subunit C	Col-0	0	
ATCG01130	TIC214	Ycf1 protein	Col-0	5	
ATCG01010	NDHF	NADH-Ubiquinone oxidoreductase	Col-0	3	
ATCG01040	YCF5	Cytochrome C assembly protein	Col-0	0	
ATCG00660	RPL20	ribosomal proteins	Col-0	0	

Table 3: List of oligonucleotides used in this study. Sequences are given in 5' →3' direction.

NAME	SEQUENCE	PURPOSE
ACTIN_FWD	CTTGCACCAAGCAGCATGAA	qRT PCR
ACTIN_REV	CCGATCCAGACACTGTACTTCCTT	qRT PCR
ZAT12_FWD	AAGAAGCCTAACAACGACGC	qRT PCR
ZAT12_REV	AACAAAGCGCGTGTAACCAA	qRT PCR
ZAT10_FWD	CACAAGGCAAGCCACCGTAAG	qRT PCR
ZAT10_REV	TTGTCGCCGACGAGGTTGAATG	qRT PCR
SOD1_FWD	CTGGTCCACATTTCAACCCC	qRT PCR
SOD1_REV	CTTTCCGAGGTCATCAGGGT	qRT PCR
APX1_FWD	TAGGTCTGGCTTCGAAGGTG	qRT PCR
APX1_REV	CAGCAGCGTATTTCTCGACC	qRT PCR
FIP4 LP	ATCGCAAAGAGAAAAGAAGCG	Genotyping
FIP4 RP	GTTCTGCACTTTGCCATAAGC	Genotyping
LBB1	GCGTGGACCGCTTGCTGCAACT	Genotyping
CBF2_FWD	GGCTCCGATTACGAGTCTC	Probe for RNA gel blot
CBF2_REV	GCTCCATAAGGACACGTCATC	Probe for RNA gel blot
RD29A_FWD	CACACCAGCAGCACCCA	Probe for RNA gel blot
RD29A _REV	CCGAGAACAGAGTCAAAGTCC	Probe for RNA gel blot
COR15A_FWD	GGCGATGTCTTTCTCAGGAG	Probe for RNA gel blot
COR15A _REV	GTGGCATCCTTAGCCTCTC	Probe for RNA gel blot
MTA RNAPROBE_FWD	ATGGAAACTGAATCTGATGACGC	Probe for RNA gel blot
MTA RNAPROBE_REV	CTCTTTGCTATGGTTGAGCC	Probe for RNA gel blot
MTB RNAPROBE_FWD	GAGCATCAAGATCGTGATTCC	Probe for RNA gel blot
MTB RNAPROBE_REV	CCAGGAGGTCCACCACC	Probe for RNA gel blot
FIP37 RNAPROBE_FWD	ATGGAGTTTTCATCACAAGACG	Probe for RNA gel blot
FIP37 RNAPROBE_REV	CACCAGCAATTTCTTCTTTTGC	Probe for RNA gel blot
HAKAI RNAPROBE_FWD	GAGGGATTCCCCGACGG	Probe for RNA gel blot
HAKAI RNAPROBE_REV	GACCGTCTCTACCCCGG	Probe for RNA gel blot
PSAA_ FWD	AGCGAGCACCAGTTTGACTT	Probe for RNA gel blot
PSAA_ REV	TGCCCATAAGAAATCGCGGA	Probe for RNA gel blot
PSAD_ FWD	CCCAAATCCCTCTCCTTCAC	Probe for RNA gel blot
PSAD_ REV	CCTTCTCTTCCTGGATTCGC	Probe for RNA gel blot
PSAO_ FWD	GGCAGCAACATTTGCAACACC	Probe for RNA gel blot
PSAO_ REV	CAGTCCTGCCCTTGAATCC	Probe for RNA gel blot
LHCA3_ FWD	GGCAGCACAAGCACTTGTG	Probe for RNA gel blot
LHCA3_ REV	CCAGTCCTGTAACCTCCGG	Probe for RNA gel blot
PSBA_ FWD	TATACAACGGCGGTCCTTATG	Probe for RNA gel blot
PSBA_ REV	CGGCCAAAATAACCGTGAG	Probe for RNA gel blot

Table 4: Primary and secondary antibodies used for immunoblot analysis. Specific antibodies, dilutions and expected size bands (in kDa) are listed.

PRIMARY ANTIBODY	DILUTION	SECONDARY	DILUTION	SIZE EXPECTED
LHCA3	1:5000	rabbit	1:50000	26 kDa
LHCB6	1:5000	rabbit	1:50000	24 kDa
PSAA	1:5000	rabbit	1:50000	55-60 kDa
PSAD	1:1000	rabbit	1:50000	17,9 kDa
PSAO	1:5000	rabbit	1:50000	10,1 kDa
PSBA	1:10000	rabbit	1:50000	28-30 kDa
PSBD	1:5000	rabbit	1:50000	28-30 kDa
PSBO	1:5000	rabbit	1:50000	33 kDa
CYTF (*PETA*)	1:5000	rabbit	1:50000	31-32 kDa
CYTB6 (*PETB*)	1:5000	rabbit	1:50000	24 kDa
ATP-B	1:5000	rabbit	1:50000	54 kDa
PGRL1	1:2500	rabbit	1:50000	9 kDa
PGR5	1:1250	rabbit	1:50000	9,8 kDa
NDHB	1:1000	rabbit	1:50000	35 kDa
CURT1A-C	1:2000	rabbit	1:50000	~18 kDa

Table 5: List of photosynthetic nucleus-encoded genes obtained from nanopore sequencing data of Arabidopsis transcripts containing m⁶A sites in Col-0 and *fip37-4* grown at 22 °C. Table extracted from (Qin *et al.*, 2022). Green, red and grays colors indicate that m⁶A sites increase, decrease or does not change in *fip37-4* when compared to the WT.

	Genes	m^{6}A sites	
		WT	*fip37-4*
1	*PSBO1*	1	2
2	*PSBO2*	4	4
3	*PSBP1*	15	10
4	*PSBQ1*	10	11
5	*PSBQ2*	2	1
6	*PSBR*	3	1
7	*PSBS*	18	14
8	*PSBW*	4	2
9	*PSBX*	3	3
10	*PSBY*	1	0
11	*LHCB4.1*	2	1
12	*LHCB4.2*	4	4
13	*LHCB4.3*	4	0
14	*LHCB5*	5	5
15	*LHCB6*	2	4
16	*PSAD1*	8	8
17	*PSAD2*	6	6
18	*PSAE1*	3	1
19	*PSAE2*	4	4
20	*PSAF*	1	0
21	*PSAG*	2	1
22	*PSAH1*	2	2
23	*PSAH2*	3	2
24	*PSAK*	2	2
25	*PSAL*	7	6
26	*PSAN*	6	7
27	*PSAO*	2	3
28	*PETC*	8	7
29	*PETE1*	4	2
30	*ATPC*	6	5
31	*ATPC1*	7	7
32	*ATPD*	4	3
33	*LHCA1*	6	6
34	*LHCA3*	9	8
35	*LHCA5*	8	9

36	*LHCA6*	5	4
37	*LHCB1.1*	3	4
38	*LHCB1.3*	1	2
39	*LHCB2.2*	3	3
40	*LHCB2.1*	3	3
41	*LHCB3*	4	6

II List of Abbreviations

°C	Degree Celsius	mM	Millimolar
µg	Microgram	mRNA	Messenger ribonucleic acid
µl	Microlitre	MTD	Methyltransferase Domain
µm	Micrometre	NADPH	Nicotinamide adenine dinucleotide phosphate
ATP	Adenosine triphosphate	OD	Optical density
A	Adenosine	PAGE	Polyacrylamide gel electrophoresis
ANOVA	Analysis of variance	PAM	Pulse-Amplitude-Modulation
ATP	Adenosine triphosphate	PCR	Polymerase chain reaction
bp	Base pair	RBP	RNA-binding protein
cm	Centimeter	RIP- Seq	RNA-immunoprecipitation coupled with deep sequencing
cDNA	Complementary DNA	RNA	Ribonucleic acid
Da	Dalton	RNase	Ribonuclease
DNA	Deoxyribonucleic acid	rpm	rounds per minute
EMSA	Electrophoretic Mobility Shift Assay	rRNA	Ribosomal ribonucleic acid
FC	Fold change	tRNA	Transfer ribonucleic acid
GFP	Green fluorescent protein	s	Seconds
g	Grams	SAM	S-adenosylmethionine; Shoot apical meristem
h	Hour	SDS	Sodium dodecyl sulfate
IP	Immunoprecipitation	t	Time
LC/MS	Liquid Chromatography/ Mass Spectrometry	UTR	Untranslated region
M	Molar	w/v	Weight per volume
mg	Milligram	WT	Wild type
min	Minutes		
mL	Milliliter		

III List of Figures

IV List of Tables and Appendix Tables

V Acknowledgements